

Introducing tolerance to foreign and partly foreign proteins by erythrocyte binding and artificial glycosylations

THÈSE N° 8190 (2018)

PRÉSENTÉE LE 9 FÉVRIER 2018

À LA FACULTÉ DES SCIENCES DE LA VIE

UNITÉ DU PROF. LUTOLF

PROGRAMME DOCTORAL EN BIOTECHNOLOGIE ET GÉNIE BIOLOGIQUE

ÉCOLE POLYTECHNIQUE FÉDÉRALE DE LAUSANNE

POUR L'OBTENTION DU GRADE DE DOCTEUR ÈS SCIENCES

PAR

Kym Lorenz BRÜNGGEL

acceptée sur proposition du jury:

Prof. A. Radenovic, présidente du jury
Prof. M. Lütolf, Prof. J. A. Hubbell, directeurs de thèse
Prof. D. Neri, rapporteur
Prof. C. M. Jewell, rapporteur
Prof. C. Heinis, rapporteur



ÉCOLE POLYTECHNIQUE
FÉDÉRALE DE LAUSANNE

Suisse
2018

Wir müssen Wissen -

We must know

Wir werden Wissen

We will know

— David Hilbert

Acknowledgements

Jeffrey A. Hubbell: I would like to thank you for giving me the opportunity to pursue my PhD in your lab. I think you have created a truly amazing lab, where one can come up with an idea of a new material, produce and investigate that material in the lab and then evaluate it *in vivo*. I would further like to thank you for how you handled the move from Lausanne to Chicago, you were very accommodating allowing myself and Fiona a smooth transition.

My thesis Jury Members: I would like to thank you for making your time available for reviewing my thesis.

Xavier Quaglia-Thermes, Giacomo Diaceri and Ani Solaniki: Thank you for your help with most of my animal experiments. Your support was outstanding, I learned a lot from you and it was a pleasure to work with you guys.

Hubbell and Swartz Lab Lausanne: Thanks for your help and all the good moments we shared. Special thanks to Alizee, Priscilla and Scott.

Hubbell and Swartz Lab Chicago: I really enjoy working alongside you guys. You made the transition to Chicago very easy and my stay in the US a great pleasure.

My friends from High school: You guys know who you are, you are truly amazing friends and every time we manage to meet up is just great fun. Special thanks to Renato, who managed to lose every squash game we played in Lausanne, and Simon who helped me with printing this document!

My family: Who has always supported me and actively encouraged me to get a great education.

Fiona: When I found out that Jeff's lab is moving to Chicago you immediately started searching a Job which allowed you to transfer to the US. You sacrificed a lot to come with me and I'm very grateful to have you. The support I get from you is amazing and we had many unforgettable moments during my time in Jeff's lab.

Chicago, 20 September 2017

Kym

Abstract

Over the last few years, protein drugs have steadily gained importance in the clinic. Compared to small molecule drugs, protein drugs are taken up by antigen presenting cells, which degrade the proteins into peptides that are then presented on major histocompatibility complex I and II to CD8+ respectively CD4+ T-cells. CD4+ T-cells are then able to activate B-cells, which upon activation will produce anti-drug antibodies. While anti-drug antibodies have mostly been viewed as a safety risk leading to drug injection related side effects, they have recently been proven to diminish the efficacy of the treatment. High antibody titers against Humira, a clinically approved monoclonal antibody used to treat rheumatoid arthritis, have been associated with low serum drug concentration and high disease activity score, ultimately leading to treatment failure.

Two approaches to induce tolerance were recently developed in the Hubbell lab. One approach utilizes protein variants that are designed to bind to circulating erythrocytes. As 1 % of erythrocytes undergo apoptosis each day and are taken up by antigen presenting cells, along with the bound protein, they are presented to the immune system in a non-inflammatory tolerogenic fashion. Immunological tolerance is thereby induced against the apoptotic erythrocyte debris and the associated bound protein. The second approach uses synthetic glucose, galactose or mannose polymers conjugated to the target protein. The polymers target C-type lectins, which are known to clear apoptotic debris, leading to presentation of the protein by hepatic antigen presenting cells in a tolerogenic liver microenvironment.

This thesis investigates the potential of these approaches to induce tolerance towards protein drugs. Arylsulfatase B was used as a model protein to investigate the potential of tolerance induction by targeting circulating erythrocytes, as 97% of patients receiving arylsulfatase B develop anti-drug antibodies. An erythrocyte binding variant of arylsulfatase B was created by chemically conjugating the erythrocyte binding peptide ERY1 to arylsulfatase B. In mice receiving two doses of ERY1-arylsulfatase B one week apart followed by weekly doses of arylsulfatase B a significant delay of four weeks in the production of anti-drug antibodies was found when compared to mice receiving weekly doses of only arylsulfatase B.

To investigate the ability of synthetic glyco-polymers to induce tolerance towards protein drugs we used asparaginase as model protein. Between 37.5% to 75% of patients treated with asparaginase develop anti-drug antibodies. Administering three intravenous injections of asparaginase-conjugated to glucose polymers before eight weeks of treatment with asparaginase significantly reduced anti-drug antibody titers by a factor of 125 when compared to animals only receiving eight weeks of treatment with asparaginase. Three pre-injections with

Abstract

asparaginase conjugated to the galactose or mannose polymer led to a reduction in anti-drug antibody titers by a factor of 12 respectively 400 after 5 weeks of treatment with asparaginase when compared to mice receiving only asparaginase for 5 weeks.

These results indicates that synthetic glyco polymers, especially mannose and glucose based ones, are able to induce long term tolerance towards asparaginase. Synthetic glucose and mannose polymers therefore represent an excellent molecular approach to induce tolerance towards protein drugs.

Key words: Tolerance induction, Immune tolerance, Erythrocyte, Synthetic glyco polymers, Arylsulfatase B, Asparaginase, Anti-drug Antibodies

Zusammenfassung

Protein Arzneimittel haben über die letzten Jahre stetig an klinischer Bedeutung gewonnen. Im Vergleich zu niedermolekularen Arzneimitteln können Protein basierte Arzneimittel von Antigen präsentierenden Zellen aufgenommen und in Peptide degradiert. Diese können auf dem Haupthistokompatibilitätskomplex I und II CD8+ respektive CD4+ T-Zellen präsentiert werden. Folglich können CD4+ T-Zellen B-Zellen aktivieren, welche Antikörper gegen das Protein Arzneimittel produzieren. Lange Zeit wurden anti-Arzneimittel Antikörper nur als Sicherheitsrisiko betrachtet. Kürzlich wurde jedoch gezeigt, dass anti-Arzneimittel Antikörper auch die Wirksamkeit einer Therapie herabsetzen können. Hohe Antikörper Titer gegen Humira, ein klinisch zugelassener monoklonaler Antikörper, wurden mit tiefer Serum Konzentration des Arzneimittels und hoher Krankheitsaktivität assoziiert und führten schlussendlich zum Scheitern der Therapie.

Zwei Ansätze um Toleranz zu induzieren wurden kürzlich im Hubbell Labor entwickelt. Einer dieser Ansätze verwendet eine Arzneimittelvariante die zu Erythrozyten im Blut bindet. 1% der Erythrozyten werden jeden Tag apoptotisch und werden von Antigen präsentierenden Zellen aufgenommen und dem Immunsystem in nicht entzündlicher und tolerogener Art präsentiert. Immunologische Toleranz wird dadurch gegen die apoptotischen Rückstände der Erythrozyten und dem daran gebundenen Protein induziert. Die zweite Methode benutzt synthetische Glukose, Galaktose oder Mannose Polymere die zum Zielprotein konjugiert werden. Diese Polymere zielen auf C-Typ Lektine, welche apoptotischen Schutt in der Leber aufnehmen, wodurch das Protein von hepatischen Antigen präsentierenden Zellen in einer tolerogenen Leber Mikroumgebung präsentiert wird.

Diese Dissertation untersucht das Potential dieser Methoden zur Toleranzinduktion für auf Proteinen basierte Arzneimittel. Um das Potential der Toleranzinduktion durch Erythrozytenbindung zu untersuchen wurde Arylsulfatase B als Modell benutzt, da 97% der Patienten Antikörper gegen Arylsulfatase B entwickeln. Das Erythrozyten bindende Peptid ERY1 wurde chemisch an Arylsulfatase B konjugiert. Mäuse die zwei Injektionen ERY1-Arylsulfatase B erhielten gefolgt von einmal wöchentlichen Arylsulfatase B Injektionen entwickelten vier Wochen später Antikörper verglichen mit Mäusen die nur Arylsulfatase B erhielten.

Um die Fähigkeit Toleranz zu induzieren von synthetischen Zucker Polymeren zu untersuchen wurde Asparaginase als Modellarzneimittel gewählt. Bis zu 75% der Patienten entwickeln Antikörper gegen Asparaginase. 3 Injektionen von Asparaginase konjugiert zu einem Glukose Polymer gefolgt von acht wöchentlichen Behandlung mit Asparaginase reduzierte Antikörper gegen das Arzneimittel signifikant. Verglichen mit Mäusen die nur 8 Wochen Asparaginase Be-

Zusammenfassung

handlung erhielten waren die anti-Arzneimittel Antikörper 125 Mal tiefer. Drei Pre-injektionen mit Asparaginase konjugiert zu Galaktose oder Mannose polymer führte zu einer Reduktion in anti-Arzneimittel Antikörper um ein 12- respektive 400-faches nach 5 Wochen Asparaginasebehandlung verglichen mit Mäusen welche nur 5 Wochen Asparaginasebehandlung erhielten.

Dieses Resultat zeigt das synthetische Zucker Polymere, besonders auf Mannose und Glukose basierte, die Fähigkeit haben Langzeittoleranz gegenüber Asparaginase zu induzieren. Synthetische Glukose und Mannose Polymere sind deshalb ein ausgezeichneter molekularer Ansatz um Toleranz gegenüber Arzneimitteln zu induzieren.

Stichwörter: Toleranz Induktion, Immuntoleranz, Erythrozyten, Synthethische Zucker Ploy-
mere, Arylsulfatase B, Asparaginase, anit-Arzneimittel Antikörper

Contents

Acknowledgements	i
Abstract (English/Deutsch)	iii
List of figures	xi
List of tables	xv
Motivation	1
State of the art	5
When the Induction of Immunological Tolerance is Needed	5
Antigen Targeting to Dendritic Cells	6
Antigen Specific T Cell Tolerance Induction with Soluble Peptides	6
Antigen Specific T Cell Tolerance Induction by Antigen Coupled Apoptotic Cells . . .	7
Nanoparticle Platforms for Tolerance Induction	8
Regulatory T Cell Immunotherapy	9
Antigen-Specific B Cell Deletion	9
1 Tolerance Induction by Erythrocyte Binding	11
1.1 Introduction	11
1.1.1 Mucopolysaccharidosis VI	11
1.1.2 Tolerance Induction by Engineered Erythrocyte Binding	13
1.1.3 Tolerance Induction towards Asparaginase	17
1.2 Materials and Methods	19
1.2.1 Animals	19
1.2.2 Cloning	19
1.2.3 Protein Expression	19
1.2.4 Protein Purification	19
1.2.5 LPS detection with HEK Blue-mTLR4 cells	22
1.2.6 ERY1 Conjugation with SMCC and Sulfo-SMCC	22
1.2.7 ERY1 Conjugation with BMPH	23
1.2.8 Conjugation of NHS-ester Dyes	23
1.2.9 Erythrocyte Binding by Flow Cytometry	24
1.3 Results	25

Contents

1.3.1	Immunogenicity of Ovalbumin, TER119-Ovalbumin and ERY1-Ovalbumin	25
1.3.2	Production and Characterization of Arylsulfatase B	26
1.3.3	Immunogenicity of Arylsulfatase B	28
1.3.4	Immunogenicity of ERY1-Arylsulfatase B and TER119-Arylsulfatase B . .	29
1.3.5	Tolerance Induction with ERY1-Arylsulfatase B	32
1.3.6	Tolerance Induction with deglycosylated ERY1-Arylsulfatase B	33
1.3.7	Tolerance Induction with ERY1-BMPH-Arylsulfatase B	35
1.4	Discussion	38
2	Searching new Binders to Erythrocytes by Phage Display	41
2.1	Introduction	41
2.1.1	Motivation to Search for new Erythrocyte Binders	41
2.1.2	Phage Display Technology, the Human Domain Antibody Library	41
2.2	Materials and Methods	43
2.2.1	Glycophorin A Isolation	43
2.2.2	Biotin Conjugation and Binding to Magnetic Beads	43
2.2.3	Phage Display	43
2.2.4	Erythrocyte Binding by Flow Cytometry	44
2.3	Results	45
2.3.1	Screening against Mouse and Human Glycophorin A	45
2.3.2	Screening against Mouse and Human Erythrocytes after Glycophorin A Screen	46
2.3.3	Screening against Mouse, Monkey and Human Erythrocytes	47
2.4	Discussion	49
3	Tolerance Induction by Antigens Bearing Synthetic Glycosylations	51
3.1	Introduction	51
3.1.1	Liver Targeting for Tolerance Induction by Synthetic Antigen Glycosylation	51
3.1.2	Antigen Specific Tolerance Induction in CD4+ and CD8+ T-cells by Syn- thetic Glycosylated Ovalbumin	52
3.2	Materials and Methods	55
3.2.1	Chemical Synthesis	55
3.2.2	Protein Conjugation to Synthetic Polymeric <i>N</i> - Acetylglucosamine, <i>N</i> - Acetylgalactosamine and <i>N</i> - Acetylmannosamine	61
3.3	Results	62
3.3.1	Synthetic Polymeric <i>N</i> -Acetylglucosamine for Tolerance Induction to- wards Asparaginase	62
3.3.2	Synthetic Polymeric <i>N</i> - Acetylgalactosamine and <i>N</i> - Acetylmannosamine for Tolerance Induction towards Asparaginase	66
3.4	Discussion	68
A	Appendix	71

Bibliography	98
Curriculum Vitae	99

List of Figures

I	Novel FDA approvals since 1993	1
II	Anti drug antibodies can reduce the efficiency of drugs	3
III	Proposed mechanisms for tolerance induction by peptides or antigen-coupled cells	7
1.1	Engineering Antigens for Erythrocyte Binding	13
1.2	Erythrocyte-targeted antigens induce CD8+ T cell tolerance and resistance to antigen challenge	14
1.3	Treatment with erythrocyte-targeted antigen prevents T cell- induced type 1 diabetes.	15
1.4	Memory of tolerance can be induced by exclusively endogenous T cell populations	17
1.5	Erythrocyte-binding ASNase is nonimmunogenic and acts as a tolerogen that enables follow-on treatment with WT enzyme	18
1.6	Cu ²⁺ arylsulfatase B purification step	20
1.7	Blue Sepharose arylsulfatase B purification step	20
1.8	Hydrophobic interaction chromatography of arylsulfatase B purification	21
1.9	Cation exchange chromatography of arylsulfatase B purification	22
1.10	Immunogenicity of 150 pmol, 30 pmol and 6 pmol of Ovalbumin, TER119-Ovalbumin and ERY1-Ovalbumin	25
1.11	Production, purification and HPLC profile and activity of Arylsulfatase B	26
1.12	<i>In vitro</i> uptake and <i>in vivo</i> clearance of ARSB	27
1.13	Arylsulfatase B immunogenicity in different mouse strains	28
1.14	TER119-Arylsulfatase B and ERY1-Arylsulfatase B characterization by SDS-PAGE, flow cytometry and MALDI-TOF	30
1.15	Immunogenicity of ERY1-ARSB and TER119-ARSB in C57/BL6 mice	31
1.16	ERY1-ARSB pretolerization in FVB mice	32
1.17	Deglycosylated ERY1-ARSB characterization and erythrocyte binding of sulfo-SMCC ERY1-FITC-ARSB and sulfo-SMCC ERY1-FITC-OVA	34
1.18	ERY1-ARSB conjugated with sulfo-SMCC and deglycosylated ERY1-ARSB pretolerization in FVB mice	35
1.19	Characterization of ERY1-ARSB conjugation with BMPH	36
1.20	ERY1-ARSB-BMPH significantly delays the development of anti ARSB antibodies	37

List of Figures

2.1	Isolated mouse glycoporphin A and phage titers for screens against mouse and human glycoporphin A followed by screens against mouse and human erythrocytes.	45
2.2	Phage titers for phage display against human, mouse and monkey erythrocytes and binding curves for two isolated human domain antibodies against monkey erythrocytes	48
3.1	Structure and Liver Uptake of pGlu-Ovalbumin and pGal-Ovalbumin compared to Ovalbumin	52
3.2	pGlu- and pGal-ovalbumine induce CD4+ and CD8+ T-cell tolerance in a OTI and OTII model	53
3.3	pGlu-ovalbumin induces endogenous regulatory T-cells which are essential to maintain tolerance upon restimulation	54
3.4	Pretolerization with pGlu-asparaginase is able to induce and maintain tolerance towards asparaginase	63
3.5	Tolerization with pGlu-asparaginase leads to different anti-asparaginase IgG subtypes compared to non tolerized mice	64
3.6	Conjugation of pGlu is essential for tolerance induction towards Asparaginase .	65
3.7	Pretolerization with pMan-asparaginase is able to induce and maintain tolerance towards asparaginase	67
A.1	Reported immunogenicity for FDA approved antibody therapeutics	72
A.2	Reported immunogenicity for FDA non antibody biologics	73
A.3	Immune responses to replacement lysosomal enzymes	73
A.4	Uptake of arylsulfatase B from serum after i.v. injection in every mouse	74
A.5	Repaet experiment of Arylsulfatse B immunogenicity in FVB mice	74
A.6	Weekly and every second week injected TER119-ARSB compared by Injection .	74
A.7	Percentage of mice not showing detectable levels against ARSB, ERY1-ARSB, deglycosylated ERY1-ARSB pretolerized and ERY1-ARSB pretolerized	75
A.8	Complete Sequencing results from third Round of Phage Display against Human Erythrocytes	77
A.9	Complete Sequencing results from fourth Round of Phage Display against Human Erythrocytes	78
A.10	Complete Sequencing results from second Round of Phage Display against Mouse Erythrocytes	80
A.11	Complete Sequencing results from third Round of Phage Display against Mouse Erythrocytes	81
A.12	Complete Sequencing results from first Round of Phage Display against Monkey Erythrocytes	82
A.13	Complete Sequencing results from second Round of Phage Display against Monkey Erythrocytes	83
A.14	Binding of four human domain antibodies identified by phage display against monkey blood towards monkey blood on a phage level	84
A.15	Size exclusion chromatogram of asparaginase and pGlu-asparaginase	84

A.16 pGlu-asparaginase unreduced and reduced on an SDS-PAGE gel	85
A.17 pGal-asparaginase and pMan-asparaginase unreduced and reduced on an SDS-PAGE gel	85

List of Tables

2.1	Complementarity determining regions of the domain Antibodies found more than once in a given round of screening against human or mouse glycoprophin A	46
2.2	Complementarity determining regions of the domain Antibodies found more than once in a given round of screening against human or mouse erythrocytes after two rounds of screening against human or mouse glycoprophin A	46
2.3	Complementarity determining regions of the domain Antibodies found more than once in a given round of screening against human, mouse or monkey erythrocytes	47

Motivation

For a long time small molecules have been dominating new molecular entity (NMEs) approvals, but since the FDA approval of insulin as the first drug produced with recombinant DNA technology in 1982 [55], protein drugs have consistently gained more importance. This is reflected in the increase of biologics license approvals (BLAs) by the FDA in the last 23 years [87] (a protein drug needs a new molecular entity approval and a biologics license approval). Figure I shows the approvals for new molecular entities and biologics license approvals from 1993 to 2016. In the last 5 years biologics have made up 30% of the newly approved molecular entities, while from 1993 to 1997 it was only 9%. Furthermore 8 of the top 10 selling drugs in 2016 have been biologics (IMSHealth).

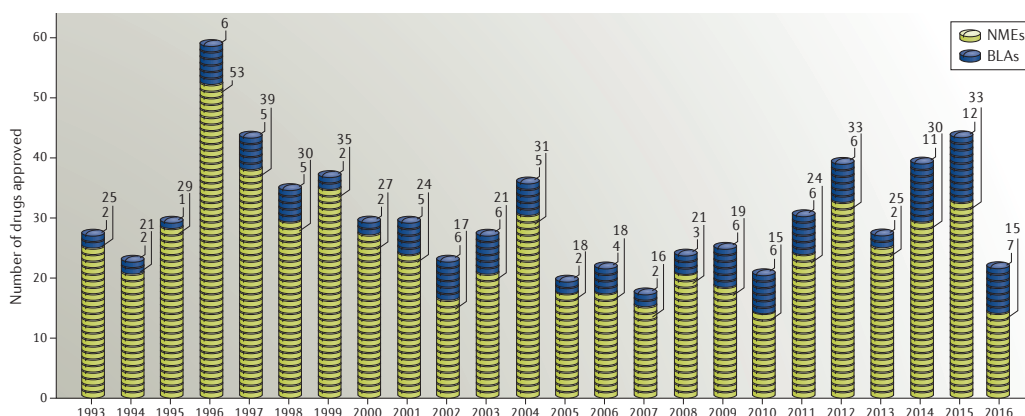


Figure I – New molecular entities and biologics licence applications approved by the Center for Drug Evaluation and Research (CDER) since 1993. Data are from Drugs@FDA. Figure adapted from [87].

One main difference between a small molecule drug and a protein drug lies in the ability of antigen presenting cells to take up proteins, process them and present them as peptides on the major histocompatibility complex (MHC) class I and II to the immune system. Protein drugs are expressed and purified to be free of any pathogen-associated molecular patterns (PAMPs) and danger associated molecules (DAMPs). This means that they are presented to T-cells without any co-stimulation, a process which is known to lead to T-cell clonal anergy or adaptive tolerance [106]. This process has shown to be essential in maintaining tolerance

Motivation

against self, as self-reactive T-cells escape negative selection in the thymus and must be held in check by a peripheral tolerance mechanism [85, 91, 115].

However, this seems not to be the case in reality, as most biologics have a significant portion of patients developing antibodies against the protein drug (anti-drug antibodies). For example, the chimeric anti-CD20 antibody Rituximab (Roche) used for the treatment of non-Hodgkin lymphoma has a reported immunogenicity of 11% [6]. The humanized anti-IL2R antibody Daclizumab (Zenapax, Roche) has an immunogenicity of 14-34% [6]. Most surprisingly even the fully human anti-TNF α antibody Adalimumab has an immunogenicity ranging from 2.6% to 26% based on the indication it is used to treat [6]. This is even more surprising considering that recombinantly expressed IgG in CHO cells [118] and their glycosylation patterns are found in human blood serum, as one of many different IgG glycosylation patterns present in human blood serum [6, 51].

If we move away from IgG and consider protein drugs which are investigated to a much lesser degree, there is usually not much to no information present comparing the glycosylation of the recombinant protein to the human one. For example, recombinantly expressed human Factor VIII (Kogenate FS, Bayer Schering Pharma) used to treat Hemophilia A has an immunogenicity of 15% [119]. Some of the highest immunogenicities can be observed in drugs used for enzyme replacement therapy for lysosomal storage diseases. In these diseases the patient has no or an impaired catalytic activity of an enzyme. This enzyme is then recombinantly expressed and injected into the patient on a regular basis to deliver and maintain its catalytic activity. For example, arylsulfatase B (*N*-acetylgalactosamine-4-sulfatase, Naglazyme) used to treat Mucopolysaccharidosis VI has an immunogenicity of 97% and Iduronate-2-sulfatase (ElaPrase, Shire) used to treat Hunter's disease has a 51% immunogenicity [119]. Both proteins are heavily glycosylated [29]. A comprehensive listing of protein drugs and their immunity can be found in appendix A.1 to A.3

For the clinical approval process, anti-drug antibodies have not been considered particularly important up to this point as long as overall safety of the drug could be shown. Furthermore only neutralizing antibodies were considered to have an influence on efficacy. If a patient has developed antibodies, it is determined if they are considered neutralizing antibodies by an *in vitro* assays, where the activity of the protein is measured in presence of the patients blood serum [29, 120]. Let's consider, as it is the case for arylsulfatase B, that only antibodies lowering the catalytic activity of the drug are considered neutralizing and having an effect on the efficacy [29, 38]. This means antibodies that hinder the uptake of the protein by the targeted pathway are not considered as neutralizing antibodies in this case, and neither are antibodies that are binding to the protein and then removed from circulation by active uptake by the FcR α [120]. These antibodies will influence the pharmacokinetics of the drug and are very likely to reduce the drug's efficacy. The different types of anti-drug antibodies are shown in Figure II A.

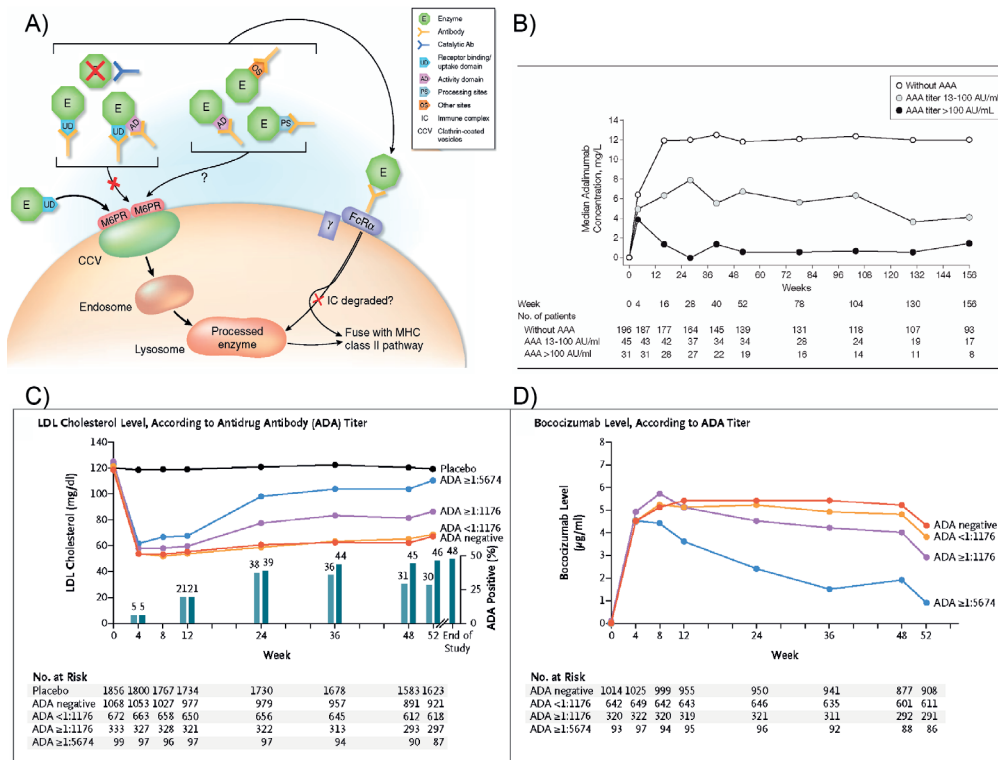


Figure II – A.) Binding of antibodies to enzyme may redirect the enzyme to FcR-expressing cells, such as macrophages and B cells. Enzyme–antibody complexes internalized through FcRs may prevent proper translocation of functional enzymes to the lysosome. Binding of antibody to other domains of the enzyme may change pharmacokinetics or redirect the enzyme to FcR-expressing cells. Figure adapted from [120] B.) Median adalimumab serum concentrations shown for patients without anti-adalimumab antibodies (AAA), with low AAA (13-100 AU/mL), and high anti-adalimumab titers (100 AU/mL). Patients who were AAA-negative had significantly higher adalimumab concentrations compared with patients with low AAA (P .001) and high antibody titers (P .001). Figure adapted from [7] C.) Shows the effect of anti-drug antibodies on LDL cholesterol levels among the patients who received placebo and among those who received bococizumab, according to whether the patients were ADA-negative throughout the trial, had ADA titers in the lowest two thirds of maximum titers (<1:1176) during follow-up, had ADA titers in the highest third of titers (>1:1176) during follow-up, or were in the subgroup with ADA titers in the top 10% (>1:5674). D) Plasma bococizumab levels according to the ADA titer. Figures C and D adapted from [100].

The importance of anti drug-antibodies and their effect on drug efficiency is becoming more and more clear. Development of anti-Humira (Adalimumab) antibodies is associated with higher disease activity and treatment failure in rheumatoid arthritis patients [7]. Patients with anti-drug antibodies have lower serum drug concentrations and were more likely to discontinue the treatment (fig. II B). It also showed a significant association between the presence or absence of anti-drug antibodies and disease activity score. While this was found after FDA approval of the drug, another study showed that a clinical phase 3 trial failed to show

Motivation

high enough efficacy of Bococizumab (Pfizer) in lipid reduction to file for approval because of anti-drug antibodies [100]. The multinational lipid-lowering trial conducted in 4300 patients showed that high anti-drug antibodies were correlated with high cholesterol levels and low Bococizumab levels (fig. II C, D). The cholesterol level in patients with the highest anti-drug antibody titers was almost at the level of the placebo group at the end of the study.

These examples show that the immunogenicity of the drug and the resulting anti-drug antibodies can revert the effect of the therapy for certain patients or even render a new approach to treat a disease inefficient, highlighting the need to develop a platform that allows us to induce tolerance to foreign and partly foreign proteins.

If we think about an ideal way to introduce tolerance towards proteins it would be similar to a vaccine. In a vaccine, you have the antigen and then molecules that activate the immune system. An ideal tolerogenic drug would therefore consist of an antigen and a tolerance inducing component. The tolerance inducing component can be a chemical conjugated entity, part of a fusion protein, nanoparticles or even cells that are pulsed with the antigen. Approaches using cells have regulatory and logistic hurdles and are very expensive. Ideally a tolerance-inducing drug is based on the drug it tries to tolerize against and can easily be modified. Therefore this thesis focuses on exploring molecular approaches to induce tolerance towards therapeutic proteins.

State of the Art

When Induction of Immunological Tolerance is Needed

The introduction of tolerance is needed as a treatment in two different settings: i) The immune system fails to correctly recognize self and develops immunity against a self protein. This leads to the development of allergies and autoimmune disease. ii) The immune system recognizes a foreign or partly foreign protein introduced in a therapy setting and develops immunity against it. In protein therapeutics this leads to injection related side effects and reduced effectiveness of the treatment while in transplantation it can lead to rejection of the transplant. While the same tolerizing platforms can be used in both settings, there are some fundamental differences to consider. The major concern in immunity against protein therapeutics are anti-drug antibodies, while a reduction in CD8+ T-cells only can be very beneficial in autoimmune diseases even when the antibody titres are not changed. Most autoimmune diseases are recognized at a stage when T-cell and B-cell responses are present. This means that antigen based approaches for tolerization in developed autoimmune diseases have a targeting and delivery problem as there are antibodies present that can recognize the treatment and interfere with it's delivery. For protein drugs and transplants we have the chance to educate a naive immune system before it is exposed to the antigen for the first time.

Current immune tolerization approaches usually target the pathways of immune activation or directly deplete T- and B-cells. For example, the anti-CD-20 antibody Rituximab systematically depletes B-cells. It is used in new onset diabetes 1 patients, where it can induce a delay of onset of the disease [95] and off label in organ transplantation. The same approach is used in T-cells to protect β -cells in diabetes type 1 by the T-cell depleting anti-CD3 antibody Teplizumab [62]. However the phase 3 clinical trial for Teplizumab ended disappointing, as the primary endpoint was not achieved [107]. Another strategy to target T-cells is to remove co-stimulatory receptors, as antigen presentation without co-stimulation leads to anergy or adaptive tolerance in T-cells [106]. This is used by the drug Abatacept, a fusion protein of the extracellular domain of CTLA-4 and the IgG 1 Fc region. The CTLA-4 component binds to CD80 and CD86 thereby inhibiting co-stimulation by preventing interaction with CD28 [86]. Abatacept is used to treat rheumatoid arthritis and it's second generation drug successor, Belatacept is used in transplantation to provide extended graft survival [117].

Neither of these approaches is antigen specific and they rely on suppressing important parts

of the immune system leading to serious side effects. The use of Rituximab has led to the reduction of immune defenses, which have become a serious clinical problem in patients treated with it [58]. In the following section, approaches which have the potential to induce antigen-specific tolerance are reviewed.

Antigen Targeting to Dendritic Cells

This approach focuses on delivering antigen directly to dendritic cells in a non-activated state. These dendritic cells will then process and present the antigen in a non-inflammatory fashion. One example of how to deliver antigens in this fashion is by using a fusion protein of the antigen and an antibody targeting the desired dendritic cell. CD8+, CD205+ dendritic cells are one subset that have been demonstrated to induce regulatory T-cells [124]. Targeting these cells has demonstrated effective tolerance induction in mouse models of type-1 diabetes and experimental autoimmune encephalomyelitis (EAE) [97, 111]. Another strategy uses the same antibody-antigen fusion approach but targets dendritic cells expressing the asialoglycoprotein receptor. This approach has been successfully used in mouse and macaque models to induce IL-10 expressing CD4+ T-cells which have the capability to suppress immune responses in an antigen-specific fashion [73].

Antigen-Specific T Cell Tolerance Induction with Soluble Peptides

One approach to delete antigen-specific T-cells is to inject peptides or altered peptide ligands in high doses. The reasoning behind this approach is that the presentation of antigen on MHC class II and recognition by the TCR without co-stimulatory molecules leads to activation-induced cell death or anergy of CD4+ T cells. In contrast, if the peptide is presented together with co-stimulatory molecules (CD80/86 and CD40) this will lead to activation of CD4+ T cells. The costimulatory molecules are up-regulated by cytokines related to inflammation. Therefore, the presence of antigen without inflammation should lead to antigen specific T-cell deletion. While soluble peptides are routinely used in clinic for allergy desensitization [110], their usage for autoimmune diseases has not been successful yet.

Soluble peptides have been shown to work in non-obese diabetic (NOD) mice. BDC2.5 TCR-transgenic NOD mice express rearranged α - and β -TCR genes of a diabetogenic T-cell clone. By activating the splenocytes of BDC2.5 TCR-transgenic NOD mice *in-vitro* with an antigen library followed by adoptively transferring them into NOD mice, elevated glucose levels were measured within one week [56]. Compared to the *in-vitro* activation, *in-vivo* immunization of BDC2.5 TCR-transgenic NOD mice with the antigen library lead to activation and apoptosis of the BDC2.5 T-cells. By injecting the same peptide library directly after the adoptive transfer of highly activated BDC2.5 T-cells, the animals were protected from onset of the diseases [57].

In a mouse model for multiple sclerosis (experimental autoimmune encephalomyelitis), treatment with the soluble myelin peptide has resulted in anaphylaxis [108]. This has also

been observed in clinics where an altered peptide ligand of myelin basic protein was used in MS patients to induce tolerance. The phase II clinical trial of this myelin peptide was suspended by the safety board because of hypersensitivity reactions in 9% of the patients [59]. However, in 2015 a clinical phase I trial was successfully conducted in MS patients by using trimmed MHC class II epitopes with an engineered MHC-II affinity (Clinical Trial identifier NCT01097668). The patients received escalating doses of the peptide for nine injections. The dose escalating schedule was first shown to be safe and efficient in mice [14].

Antigen-Specific T Cell Tolerance Induction by Antigen-Coupled Apoptotic Cells

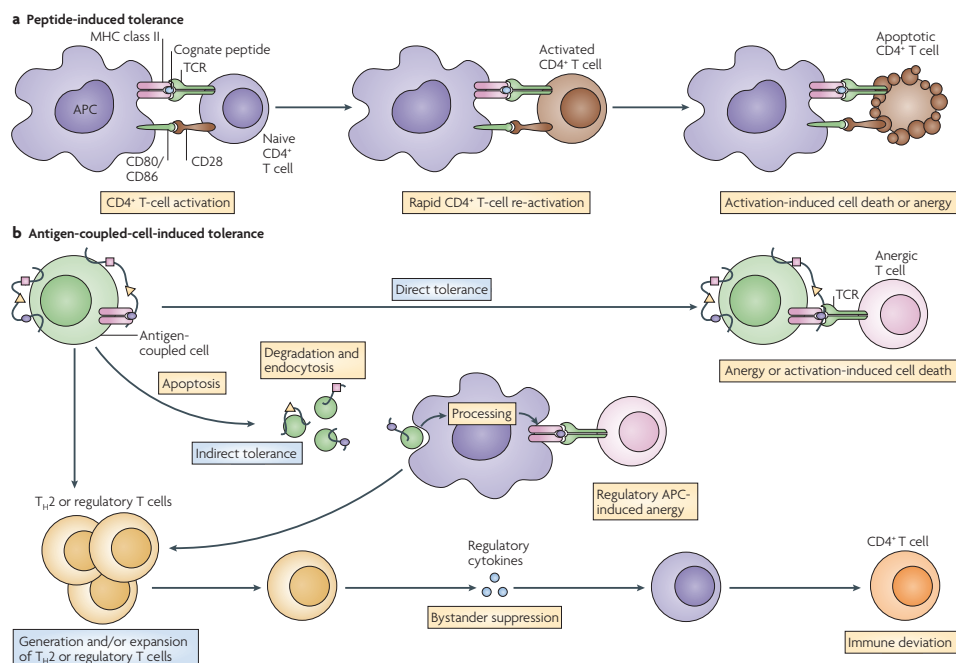


Figure III – A) In tolerance induced by soluble peptide and/or DNA vaccination, the presence of excess antigenic peptide is thought to induce an initial proliferative burst of the autoreactive CD4⁺ T cells, but the subsequent re-activation of the proliferating CD4⁺ T cells is inhibited due to activation-induced cell death (AICD) or anergy. B) In antigen-coupled-cell-induced tolerance, first, antigen-coupled cells induce direct tolerance following interaction of the T-cell receptor (TCR) on the host, antigen-specific CD4⁺ T cells with the antigen-coupled cells, leading to the induction of anergy through TCR stimulation in the absence of co-stimulation. Second, antigen-coupled cells induce indirect or cross-tolerance through the re-presentation of the apoptotic antigen coupled cells by ‘tolerogenic’ host antigen-presenting cells (APCs) leading to T-cell anergy. Third, antigen-coupled cells directly or indirectly activate regulatory T cells and/or T helper 2 (TH2) cells, and this results in bystander suppression of autoreactive CD4⁺ T cells through the action of regulatory cytokines, such as transforming growth factor- (TGF), interleukin-10 (IL-10) and/or IL-4. Figure adapted from [85].

In this approach, peripheral blood or splenic lymphocytes are surface cross-linked with antigen by using 1-ethyl-3-(3-dimethylaminopropyl) carbodiimide. These apoptotic antigen-coupled cells are then injected. They are recognized as self and presented in a tolerogenic fashion. They can induce tolerance in three ways: i) Activation-induced cell death or anergy is induced directly by presentation of the antigen, lack of inflammation and presence of self. ii) The antigen coupled cells are taken up by host cells and are cross-presented. Antigen presentation and the expression of PD-L1 and IL-10 by marginal zone antigen presenting macrophages leads to antigen specific anergy of T cells and iii.) induction of regulatory T cells (fig. III) [33, 85].

Antigen-coupled apoptotic lymphocytes have been shown to be an effective treatment in experimental autoimmune thyroiditis [13], uveitis [22], neuritis [35] and in the NOD mouse model of type 1 diabetes [28]. Antigen coupled peripheral blood lymphocytes showed prevention as well as arrest of progression in the experimental autoimmune encephalomyelitis multiple sclerosis model [85].

A phase I clinical trial has been carried out in multiple sclerosis patients to assess safety, feasibility and tolerability. The study showed good tolerability and safety for autologous peptide-coupled cells in multiple sclerosis patients [79]. This approach is technically demanding, since the cells need to be harvested from the patient, coupled to the antigen in sterile conditions and re-injected into the patient. In an enzyme replacement therapy setting, where multiple injections per year could be required to maintain tolerance, this approach seems very impractical.

Nanoparticle Platforms for Tolerance Induction

Nanoparticles have been modified with the goal to mimic the physiochemical properties of apoptotic cells. One such implementation uses 500 nm carboxylated polystyrene microparticles and conjugates them with peptide antigens. These microparticles are preferentially taken up by marginal zone macrophages expressing the MARCO and SIGN-R1 scavenger receptors. Both these receptors are implicated in the clearance of apoptotic cell debris. These particles are able to prime T-cells to a non-productive proliferative response when conjugated with the myelin antigen PLP₁₃₉₋₁₅₁ in a PLP₁₃₉₋₁₅₁-induced model of experimental autoimmune encephalomyelitis in mice [32].

A different approach uses nanoparticles as delivery vehicles for small molecules to antigen presenting cells to induce tolerogenic programming. One such approach encapsulates rapamycin to inhibit the mTOR (mechanistic target of rapamycin) pathway and thereby induce tolerogenic or regulatory T-cells, by delivery to dendritic cells. By using a 200 nm biodegradable poly(lactid-co-glycolide) nanoparticle, which co-encapsulates rapamycin and the model protein ovalbumin, reduced CD4⁺ T-cell proliferation and increased population of FoxP3⁺ regulatory T-cells in an adoptive OT-II T-cell transfer model [81]. These same nanoparticles encapsulated with PLP₁₃₉₋₁₅₁ and rapamycin were able to induce prophylactic and therapeutic

tolerance. Further, prophylactic use of those nanoparticles could reduce anti-Ovalbumin antibodies about 100 fold in mice and anti Factor VII antibodies in hemophilia-A mice 5 fold. However rapamycin is tolerogenic by itself and proof for the need of co-delivery by nanoparticle has not been shown. The approach has further not been shown to affect the targeted cells in an antigen specific fashion.

Regulatory T Cell Immunotherapy

Regulatory T cells are crucial for the establishment and maintenance of immune tolerance, exemplified by the fact that a single mutation in the gene encoding for the master regulatory transcription factor, FoxP3, causes severe autoimmunity in humans [67]. Whereas many of the above mentioned approaches rely on inducing development of FoxP3+ CD4+ T-cells *in vivo*, this approach relies on expanding and educating CD4+ T-cells *ex vivo* and then transferring them into the patient. This approach has been effective in preserving and restoring tolerance in mouse models of type 1 diabetes [112], lupus [105] and autoimmune hepatitis [71].

Regulatory T-cell immunotherapy has been tested in the clinic in phase I trials (ISRCTN number 06128462) for the treatment of children recently diagnosed with diabetes type 1. After one year, 8 of the 12 treated children were in remission and 2 patients no longer needed insulin therapy - the study did therefore not only show safety of the approach but also efficiency in the treatment of the disease. However, the protective effect diminished over time and a second infusion of *ex vivo* expanded and educated regulatory T-cells was far less effective than the first dose [82].

Antigen Specific B Cell Deletion

In autoimmune diseases [89] and enzyme replacement therapy, a B-cell response can be induced in a direct fashion without the help of CD4+ T-cells. Currently, the only solution against ongoing B-cell responses is the treatment with immunosuppressants. It would be preferable to eliminate B cells in an antigen specific manner. This can be achieved in two ways, either by targeting the B-cells through their B-cell receptor or by affecting APCs and CD4+ T-cells as they have the potential to suppress B-cells.

B cell depletion has been shown to lower the incidence of arthritis in a collagen-induced arthritis model [84]. To deplete B-cells, peptide tetramers containing the pathogenic epitope of mouse type II collagen were conjugated with toxins. Mice were immunized with type II collagen and treated with the toxin conjugated tetramer on day 10 and 20.

A protein based approach fused the extracellular domain of human myelin oligodendrocyte glycoprotein (MOG) to the CH2 and CH3 domains of the human IgG1 heavy chain. The dimerized protein was able to reduce the number of MOG specific B-cells in an anti-MOG Ig heavy chain knock-in mouse model [125].

State of the Art

An alternative approach exploits the natural mechanism to suppress B-cell activation. B-cells express inhibitory B-cell receptor coreceptors, for example CD22 and SIGLEC-G [52]. To be able to suppress B-cells, CD22 has to be brought in close proximity with the BCR. This approach has been used by creating nanoparticles which display antigen as well as a CD22 ligand [80]. These nanoparticles were able to reduce the titers against OVA and Factor VIII, which is used as an enzyme replacement therapy to treat Hemophilia A.

This approach has the advantage of not including toxic drug cargo. It leads to B-cell anergy or deletion by signalling and is thus a safer treatment. In addition, anergic B-cells have been shown to suppress the activation of humoral immunity [5]. Hence, an approach which can induce B-cell anergy might be much more powerful than one which simply depletes B-cells [48].

1 Tolerance Induction by Erythrocyte Binding

1.1 Introduction

1.1.1 Mucopolysaccharidosis VI

Mucopolysaccharidosis VI is a lysosomal storage disease, which results from a loss-of-function mutation in the gene coding for arylsulfatase B (Synonyms: *N*-acetylgalactosamine 4-sulfatase, Galsulfase, Naglazyme). There are more than 100 known mutations which lead to Mucopolysaccharidosis VI of different severity grades [31, 60, 61]. While the most common type of mutations are missense mutations, there are also nonsense mutations, deletions, insertions and splice site mutations. This high variety of mutations leads to different severities of the disease. The deficiency in arylsulfatase B leads to accumulation of its substrate, dermatan sulfate, in the lysosome, leading to an incomplete metabolism and enrichment of glycosaminoglycans. Persons who recessively inherited the deficiency genes for arylsulfatase B show severe skeletal abnormalities such as epiphyseal dysplasia, dwarfism, and facial dysmorphism, as well as widespread soft tissue pathology such as heart valve thickening, corneal clouding, joint stiffness, and carpal tunnel syndrome [2, 90].

Patients suffering from Mucopolysaccharidosis VI (MPS VI) show no signs of neurological disorder and have normal intelligence. Thus, there is no obvious requirement for the therapeutic protein to pass the blood brain barrier which made Mucopolysaccharidosis VI a candidate for enzyme replacement therapy. The gene for arylsulfatase B has been identified as a 533 amino acid sequence with a 36 amino acid N-terminal signalling peptide in 1990 [76, 96]. In 1992, a recombinant version without the N-terminal signaling peptide of arylsulfatase B was expressed in chinese hamster ovary (CHO) cells and shown to reverse glycosaminoglycan accumulation in fibroblasts from human MPS VI patients *in-vitro* [2]. The crystal structure of this recombinant protein (without signalling sequence) was determined in 1996 and highlighted the necessity of a post-translational modification of Cys91 to an oxo-alanine for enzymatic activity [12]. The recombinantly expressed arylsulfatase B without the signaling peptide is marketed as Naglazyme.

Chapter 1. Tolerance Induction by Erythrocyte Binding

Naglazyme was tested in a cat model of MPS VI [54] at doses of 0.2, 1 and 5 mg/kg once a week from birth [18]. Dose responsiveness was shown, as cats with 1 and 5 mg/kg showed greatly reduced or no spinal cord compression, and almost normal urinary glycosaminoglycan levels. There was near normalization of lysosomal storage in heart valve, aorta, skin, dura, liver, and brain perivascular cells, and skeletal pathology was reduced. No difference could be observed from 1 to 5 mg/kg while 0.2 mg/kg showed no apparent benefits [19]. It was noted that some cats developed antibodies against the drug, but it remained unclear if this affected distribution and uptake into the tissue.

Encouraged from the results in the cat model, a phase I/II randomized, two-dose, double-blind study was conducted to assess the safety and efficacy of Naglazyme in 2004. No serious drug-related adverse events were observed in this study. A dose dependent reduction of urinary glycosaminoglycan could be shown with a dose of 1 mg/kg showing more rapid and larger relative reduction compared to 0.2 mg/kg. Drug concentration in the blood showed rapid clearance of the drug after approximately five hours. Patients showed improvements in a 6-minute walk test, shoulder range of movement and joint pain [40].

A phase II open label clinical study was performed in 2005 with a dose of 1 mg/kg. Patients showed an increase of 155 m (98%) in the 12 minute walk test and a gain of 48 (110%) climbed stairs in the 3-minute stair climb test after 24 weeks of treatment. Improvement of the patients well-being could be shown and reduction of the mean urinary glycosaminoglycan levels by 76% showed a satisfactory biochemical response. 8 out of 10 patients were reported to developed antibodies in the first 6 weeks. There were no adverse side effects reported linked to the antibody development [39]. Evaluation of the impact of antibodies during these two studies at a later point showed undetectable Naglazyme concentrations in one patient with high antibody levels [37].

These studies were followed up by a phase III clinical trial including 121 patients. The improvements in the conditions of the patients as well as the biochemical response could be repeated. All but one of the 38 patients receiving the drug developed IgG antibodies to Naglazyme. Infusion associated reactions could be correlated with high antibody levels. In five patients, a correlation between rising antibody levels and rising urinary glycosaminoglycan concentrations was found [38]. Naglazyme received FDA approval in May 2005 and was approved in the EU in January 2006.

The combination of a high rate of antibody development in MPS VI patients, the fact that in some patients these antibodies lead to inversion of the beneficial effects [120] and the monomeric structure make Naglazyme an ideal candidate for immune-tolerance inducing treatments.

1.1.2 Tolerance Induction by Engineered Erythrocyte Binding

A new approach to induce tolerance towards protein antigens is to use erythrocytes as a vehicle for the antigen. Human erythrocytes have a half-life of about 120 days and therefore about 1% of human erythrocyte (4% in mice) undergo eryptosis, an apoptosis-like programmed cell death each day [10]. Eryptosis is similar to apoptosis in nucleated cells in phosphatidylserine asymmetry, membrane heterogeneity and annexin-V binding [70]. Cells undergoing apoptosis are taken up by antigen presenting cells and are presented in a tolerogenic fashion as a way to maintain tolerance towards self antigens. By binding antigens to erythrocytes we can target this innate tolerogenic pathways.

In order to omit any *ex vivo* manipulation of red blood cells, this approach relies on protein engineering to create protein variants that bind to red blood cells. Two methods have been developed to achieve this (fig. 1.1). i) Chemically conjugate a peptide to the antigen. ii) Create a fusion protein of the antigen with an antibody, an anti-body fragment or a single-chain variable fragment (scFv).

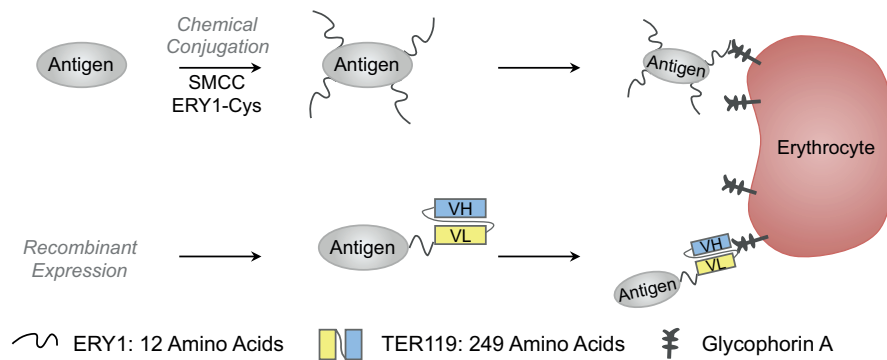


Figure 1.1 – Shows the two approaches to create erythrocyte binding. i) (Top) Conjugation of ERY1 to the antigen with SMCC leads to the erythrocyte binding ERY1-Antigen conjugate. ii) (Bottom) Fusion of the antigen and an erythrocyte binding antibody, antibody fragment or single chain antibody fragment by cloning leads to a recombinantly expressed fusion protein.

For the first approach a synthetic 12-amino acid peptide, termed ERY1, was discovered by phage display [68] and was shown to bind to the erythrocyte specific membrane protein glycophorin A (GYPA). The 12-amino acid binding sequence of ERY1 is extended with a linker which includes an activated cysteine that is available for conjugation leading to the full amino acid-sequence H_2N - WMVLPWLPGLDGGSGCRG- $CONH_2$. By using a linker like sulfo succinimidyl-4-(*N*- maleimidomethyl) cyclohexane-1-carboxylate (SMCC), the NHS-ester on SMCC will be bound to the protein and the cysteine of ERY1 will be bound to the maleimide of the linker. ERY1 needs a free N-terminus for binding, therefore conjugation can only be done at the C-terminus and multiple copies of ERY1 are required for strong binding to erythrocytes. This makes ERY1 unsuitable to deliver peptides, as they can not contain a sufficient number of amines.

Chapter 1. Tolerance Induction by Erythrocyte Binding

For the second strategy the scFv of the rat antibody TER119 was used, which recognizes a molecule associated with GYPA and is commonly used to stain erythrocytes [63]. TER119 can be fused to either the N- or C- terminus of a protein with a (GGGS)₄ linker. Further, TER119 is more suitable for usage with peptides or short proteins as it does not require a tertiary amine for conjugation and does not require multiple copies to reach its optimal K_d.

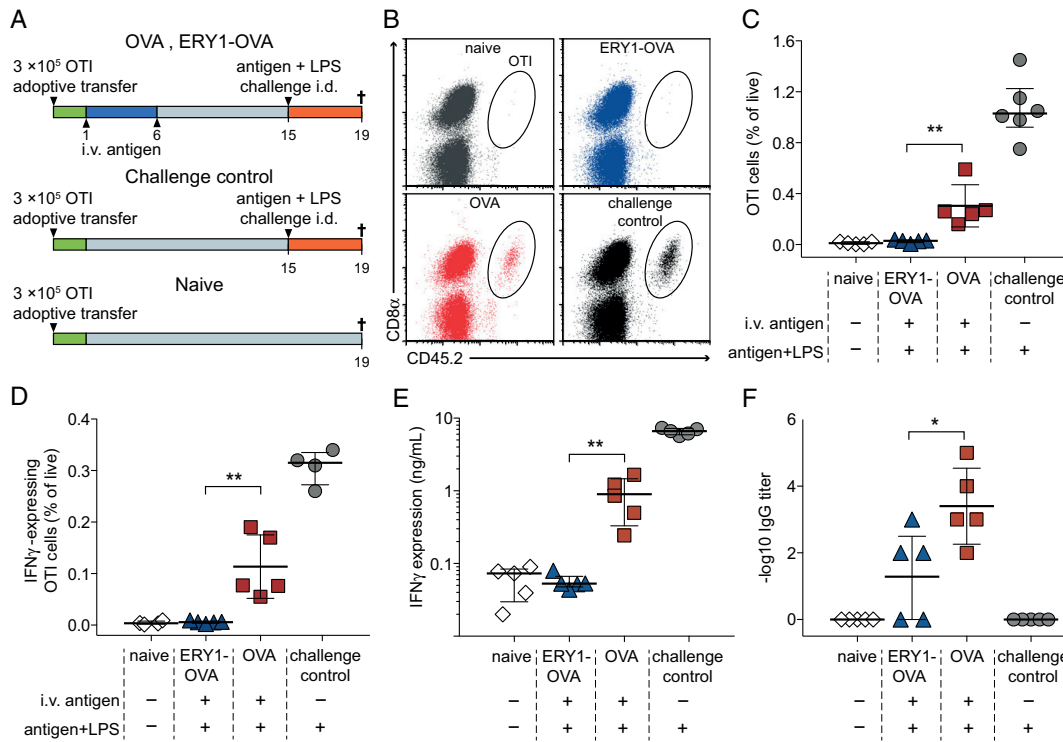


Figure 1.2 – (A) OTI CD8⁺ T-cell adoptive transfer tolerance model displays experimental protocol for experimental as well as challenge and naive control groups (n = 5). i.d., intradermal. (B) Flow cytometric detection of OTI CD8⁺ T-cell populations (CD3e⁺ CD8⁺ CD45.2⁺). (C) OTI CD8⁺ T-cell population quantification in the draining lymph nodes (inguinal and popliteal) 4 d following antigen challenge in CD45.1⁺ mice. **P < 0.01. (D) IFN- γ -expressing OTI CD8⁺ T cells in the draining lymph nodes 4 d following antigen challenge and restimulation with SIINFEKL peptide. **P < 0.01. (E) IFN- γ concentrations in lymph node cell culture media 4 d following restimulation with SIINFEKL peptide, determined by ELISA. **P < 0.01. (F) OVA-specific serum IgG titers at day 19. *P < 0.05. Data represent mean \pm SE. Figure adapted from [69].

The potential of inducing T-cell deletion was shown by deleting transgenic CD8⁺ T-cells with a TCR specific for the MHC I peptide of ovalbumin (OTI cells) with ERY1-ovalbumin. Mice were treated intra venous (i.v.) with ERY1-ovalbumin or ovalbumin (OVA) one day after OTI CD8⁺ T-cells were adoptively transferred. After 15 days the mice were challenged with OVA and lipopolysaccharide (LPS) injected intra dermal (i.d). The mice were sacrificed 4 days later and the OTI CD8⁺ T-cells from the draining lymph nodes were analyzed by FACS for

proliferation and IFN- γ expression. The amount of CD8+ T-cells in lymph nodes of mice treated with ERY1-ovalbumin was as low as the one in naive mice, whereas the amount in ovalbumin treated mice was significantly higher than the one treated with ERY1-ovalbumin ($p < 0.01$). Further, the percentage of CD8+ T-cells expressing IFN- γ was significantly higher in mice treated with ovalbumin compared to mice treated with ERY1-Ovalbumin ($p < 0.01$) (fig. 1.2 A-D). The secretion of IFN- γ was evaluated after 4 days of *in vitro* restimulation with the immunodominant SIINFEKL peptide. The lymphocytes of ovalbumin treated mice were found to secrete significantly higher levels of IFN- γ than mice treated with ERY1-ovalbumin (fig. 1.2 E). Further there is a trend that animals treated with ERY1-ovalbumin had lower antibody titers against ovalbumin than the mice treated with ovalbumin (fig. 1.2 F).

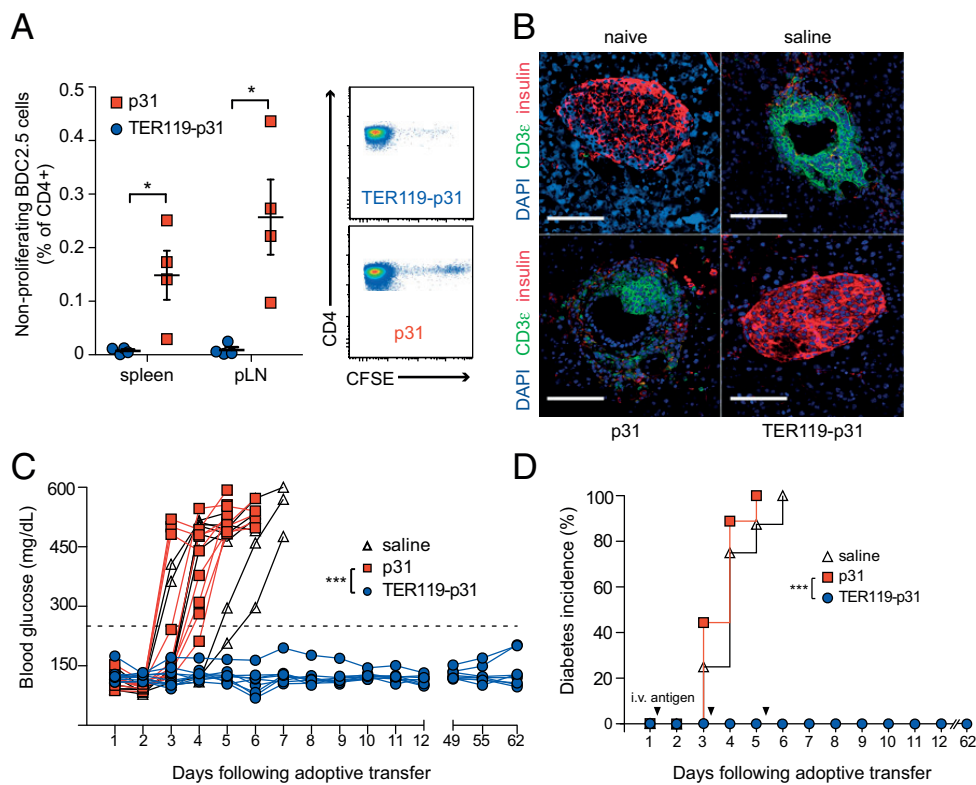


Figure 1.3 – (A) Increased proliferation and deletion of adoptively transferred diabetogenic BDC2.5 CD4+ T cells in the spleen and pancreatic lymph nodes 4 d following administration of TER119-p31 compared with p31, as determined by dilution of CFSE fluorescence via flow cytometry ($n = 4$). $*P < 0.01$. (B) Microscopy images of pancreatic islets stained for insulin (red), CD3e (green), and DAPI nuclear staining (blue), demonstrating marked T-cell infiltration and islet destruction of saline- and p31-treated mice but not of TER119-p31-treated mice. (Scale bar = 100 μ m.) (C) Glycemia monitoring as measured by daily blood glucose measurements following adoptive transfer of diabetogenic BDC2.5 CD4+ T cells and a tolerogenic treatment regimen of either saline, p31, or TER119-p31 ($n = 8$, $n = 9$, and $n = 9$, respectively). $***P < 0.0001$. (D) Diabetes incidence rate quantified by measurements in C; arrows indicate antigen administration time points. $***P < 0.0001$. Figure adapted from [69].

Chapter 1. Tolerance Induction by Erythrocyte Binding

To show the ability to delete and induce of tolerance to CD4⁺ T cells the BDC2.5 adoptive transfer model was used [44, 57] to induce type 1 diabetes. In this model transgenic diabetogenic CD4⁺ T cells are activated with the peptide p31 (YVRPLWVRME). These activated cells were then adoptively transferred and induced a rapid diabetes onset.

These mice were either injected with 10 μ g of TER119-p31 or with the equimolar dose of p31 8 hours after the transfer. Mice were sacrificed 4 days later and the proliferation of the BDC2.5 T-cells was analyzed in the spleen and pancreatic lymph node. TER119-p31 successfully represses the proliferation of the BDC2.5 CD4⁺ T-cells. They further show no T-cell infiltration of pancreatic islets for TER119-p31 treated animals whereas the saline and p31-treated mice show clear destruction and infiltration of the islets (fig.1.3 A, B). An analogous, yet longer, study was performed, where the mice were injected with 3 doses 3 days apart each of TER119-p31, p31 and saline. Hyperglycemia was found in mice treated with p31 and saline as early as 3 days after adoptive transfer with all the mice developing diabetes by day 6 (fig.1.3 C, D). No mice injected with TER119-p31 showed any signs of hyperglycemia or developing diabetes for the following 62 days.

To study if tolerization by ERY1-OVA is also efficient if only the endogenous T-cell repertoire is present, a study was conducted by Grimm et al. where one group received the first adoptive transfer and the other did not. After 30 days another adoptive transfer took place where OTI and OTII (transgenic CD4⁺ T cells with a TCR specific for the MHC I or II peptide of Ovalbumin) T-cells were transferred and challenged with OVA-LPS. The experimental scheme is shown in figure 1.4 A.

There was no significant difference found in proliferation of splenic OTI CD8⁺ T-cells or OTII CD4⁺ T-cells between the groups tolerized with ERY1-OVA whether they received the first adaptive transfer of OTI CD8⁺ T-cells or not (fig.1.4 B, C). Cells were restimulated with SIINFEKL for 6 hours in vitro. IFN- γ ⁺ OTI T-cells were analyzed by FACS, no significant difference was found between the tolerized groups regardless of receiving the first adoptive transfer or not (fig.1.4 E).

These results show the ability of antigens engineered to bind to erythrocyte to delete CD8⁺ and CD4⁺ T-cells and maintain tolerance upon restimulation with antigen. They further show that the endogenous reservoir of T-cells is enough to induce and maintain tolerance and no adoptive transfer is needed. This platform is ideal to study the induction of tolerance to foreign or partly foreign proteins, as B-cell responses are usually CD4⁺ T-cell help dependent [8] and the erythrocyte technology has been shown to effectively delete CD8⁺ T-cells and CD4⁺ T-cells in an antigen specific matter. Further it has been shown that CD4⁺ CD25⁺ Foxp3⁺ regulatory T-cells can actively suppress B cells [8, 74], those regulatory T-cells are present in a higher percentage in ovalbumin specific T-cells after treatment with ERY1-ovalbumin.

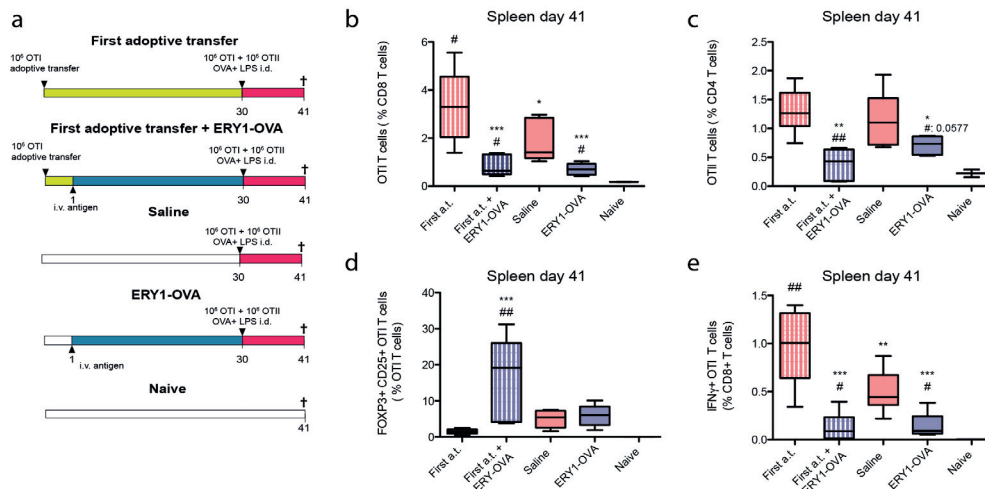


Figure 1.4 – (A) (a) 10^6 OTI CD8+ T cells (CD45.1+) were adoptively transferred into C57BL/6 mice (CD45.2+). The next day, mice were treated i.v. with ERY1-OVA to induce proliferation and deletion of OTI T cells. One month later, adoptive transfer of OTI and OTII T cells, with OVA+LPS i.d. challenge rather than additional molecular tolerization, was performed to assess long-term memory of tolerance. (b) OTI CD8+ T cell, (c) OTII CD4+ T cell and (d) CD25+FOXP3+ OTI T cell populations in the spleen on day 41. (e) IFN- γ + OTI T cells after 6 hours in vitro restimulation with SIINFEKL. Data represent mean \pm SD of n=5. 1 way ANOVA *: respective to first a.t. group, # respective to Saline group. *, #: < 0.05, **, #: < 0.01, ***, #: < 0.001. Figure adapted from [36].

1.1.3 Tolerance Induction towards Asparaginase

The enzyme asparaginase (ASNase) converts the non-essential amino acid asparagine into ammonia and aspartate. However, many leukemic cells don't have the ability to produce asparagine by biosynthesis and it therefore becomes an essential amino acid for survival of these cells. In an attempt to starve these leukemic cells, l-asparaginase is used as a drug to deplete the asparagine available to those cells. Asparaginase is used in acute lymphoblastic leukemia, Hodgkin's disease, acute myelocytic leukemia, acute myelomonocytic leukemia, chronic lymphocytic leukemia, lymphosarcoma, reiculosarcom and melanosarcoma [9]. Asparaginase is an important chemotherapeutic agent that is used in combination with other drugs; for example it is used in combination with vincristine and dexamethasone to treat acute lymphoblastic cancer. The first variant of asparaginase was approved by the FDA in 1978, today it is on the list of the World Health Organization of Essential Medicines, which consists of the most efficient and safe drugs needed in a healthcare system [122]. The variants of asparaginase expressed in *Escherichia coli* and *Erwinia chrysanthemi* turned out to be the most efficient in use against cancer [9]. Both variants are approved by the FDA as Elspar and Erwinaze respectively.

Chapter 1. Tolerance Induction by Erythrocyte Binding

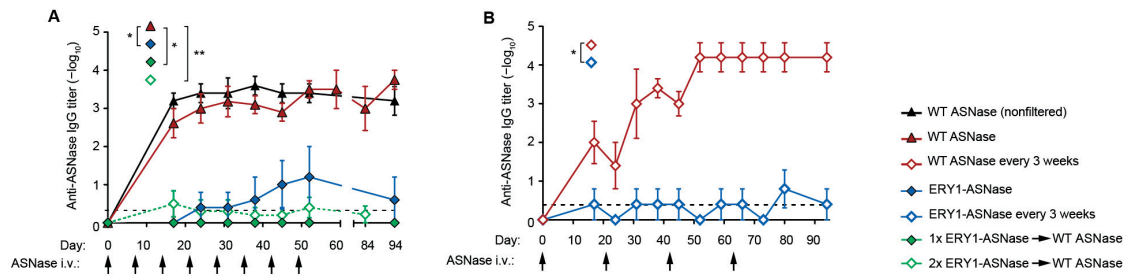


Figure 1.5 – A) Time course of anti-ASNase IgG antibody development in plasma of mice administered with eight weekly 15-mg doses of either WT ASNase or ERY1-ASNase or with one or two tolerogenic doses of ERY1-ASNase followed by WT ASNase for the remaining doses (end-point IgG titers, Mann-Whitney U test: *P 0.05, **P 0.01, ***P 0.001). (B) Time course of anti-ASNase IgG antibody development in plasma of mice administered a dose-sparing regimen of 15 mg of either WT ASNase or ERY1-ASNase every 3 weeks for a total of four doses (end-point IgG titers, Mann-Whitney U test: *P 0.05, **P 0.01, ***P 0.001). Figure adapted from [77].

Between 32.5% and 75% of patients develop anti-drug antibodies against the variant expressed in *Escherichia coli* [26] and higher level of antibodies have been correlated with a decrease in asparaginase activity. By conjugating asparaginase with ERY1, a variant of the drug could be made that has a high affinity to erythrocytes (about 4 nM [77]). This variant was found to be non-immunogenic in BALB/c mice and further was shown to induce tolerance, which allowed the switch from the erythrocyte-binding variant to the non-functionalized drug variant while maintaining tolerance whereas the drug variant on its own is highly immunogenic (fig. 1.5).

1.2 Materials and Methods

1.2.1 Animals

The Swiss Veterinary Authority and the EPFL Centre d'Application du Vivant previously approved all animal procedures. Female C57/BL6 (Harlan laboratories), BALB/c (Charles River Laboratories) and FVB mice (Charles River Laboratory) were used. First injections of the antigens took place between 8-10 weeks of age.

1.2.2 Cloning

Sequence encoding for human arylsulfatase B was synthesized by Genscript. The sequence was cloned into pSecTagA by Gibson assembly [34] with the coding sequence starting immediately after the Ig κ sequence. The coding sequence of arylsulfatase B was directly followed by the amber codon. For the TER119 fusion protein a (GGGS)₄ linker was inserted between arylsulfatase B and TER119. N- and C-terminal fusions were created by Gibson Assembly. For the N-terminal fusion TER119-(GGGS)₄ was inserted after the Ig κ sequence and followed by the arylsulfatase B sequence, for the C-terminal fusion (GGGS)₄- TER119 was inserted after the arylsulfatase B sequence and followed by the amber codon.

1.2.3 Protein Expression

The day before transfection CHO DG44 cells were passed by resuspension in ProCHO5 medium (Lonza AG) with 13.6 mg/L hypoxanthine (H), 3.84 mg/L thymidine (T), and 4mM glutamine (SAFC Biosciences) at a density of 2×10^6 cells/ml. Cells were maintained in common glass storage bottles with agitation on an orbital shaker at 110 rpm and a rotational diameter of 5 cm [88]. On the day of transfection, 5×10^9 cells were centrifuged and resuspended in 1 L of ProCHO5 medium with 4 mM glutamine and 13.6 mg/L hypoxanthine (H), 3.84 mg/L thymidine (T), and 4mM glutamine (SAFC Biosciences) at a density of 5×10^6 cells/ml. For a transfection of 1 L in a 5 L glass bottle, 3.0 mg DNA and 15 mg of polyethyleneimine (linear 25 kDa PEI [Polysciences] at 1 mg/ml in water, pH 7.0) was added to the culture. The bottle was incubated at 31°C with agitation of 110-120 rpm on an orbital shaker in an incubator with 5% CO₂ [99] for two hours, cells were then centrifuged and resuspended in JRH302Excell Media supplied with 4 mg/L of folic acid, 50 mg/l of serine and 80 mg/L of arginine. They were then incubated at 37°C with agitation of 110-120 rpm on an orbital shaker in an incubator with 5% CO₂ for up to 9 days. Viability of the cells was monitored and expression was stopped when the viability fell below 50.

1.2.4 Protein Purification

GE Healthcare life sciences ÄKTA pure and explorer 25 L systems were used for all purification steps. All buffers are 0.22 μ m filtered before use. All columns were cleaned in place after a

Chapter 1. Tolerance Induction by Erythrocyte Binding

purification run with the most stringent possible protocol according to the manual of the manufacturer. Columns were stored in 20% Ethanol between runs.

The supernatant from the protein expression was brought to 0.1 M NaAc, 0.5M NaCl, 10% glycerol and pH 6 by adding sterile glycerol, 1M NaAc at pH 5.5, NaCl as salt, pH was adjusted and the solution was 0.22 μm filtered. 3 5 ml HisTrap Hp columns (Gelifsciences) in series for a total column volume (CV) of 15 ml were stripped with 0.1 M EDTA, 0.5 M NaCl at pH 8, and then loaded with copper (0.1 M CuSulfate). For Cu^{2+} purification the following sepharose buffers were used: Buffer A: 20 mM NaAc pH 6, 0.5 M NaCl, 10% glycerol. Buffer B: 20mM Na_2PO_4 pH 7, 0.5 M NaCl, 10% glycerol, 0.5 M Imidazole. Columns were washed with 10 CVs of buffer A at 4 ml/min, sample was loaded at 4 ml/min. A maximal volume of 1000 ml of sample was loaded per run. If more then one run was needed, the columns were stripped and reloaded with Cu^{2+} between the runs. After sample loading the columns were washed for 10 CV's with Buffer A at 4 ml/min. Step elution was executed at 100 % buffer B for 8 CVs at 2 ml/minute. 5 ml fractions were collected. A typical chromatogram and a Coomassie blue stained SDS-PAGE gel of the eluates can be found in figure 1.6.

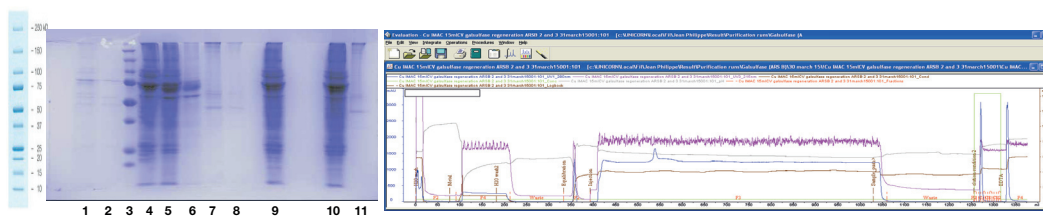


Figure 1.6 – Typical coomassie blue stained SDS-PAGE gel and chromatogram of Cu^{2+} arylsulfatase B purification step. 1 starting material, 2 flow through, 3 Molecular weight ladder 4-8 all fractions from an elution peak. 9-11 elution peaks of different runs.

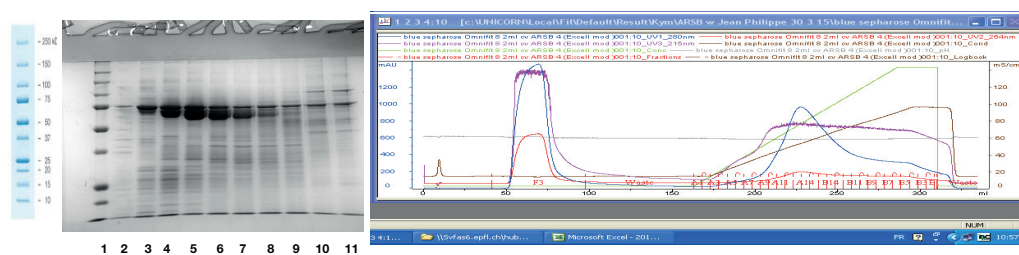


Figure 1.7 – Typical coomassie blue stained SDS-PAGE gel and chromatogram of Blue Sepharose arylsulfatase B purification step. 1 Molecular weight ladder, 2-11 fractions during the elution, 1 corresponds to fraction A8 on the chromatogram, 2 to A10, 3 to A12, 4 to A14, 5 to B15, 6 to B13, 7 to B11, 8 to B10, 9 to B5, 10 to B2.

All the elution fractions were pooled and extensively dialysed overnight in 0.1 M NaCl and 20 mM NaAc pH 5.5. The dialysed protein solution was 22 μm filtered. For the next purification a omnifit column was packed with Blue Sepharose resin (Gelifsciences) to a column volume

1.2. Materials and Methods

of 8 ml. The following buffers were used: Buffer A: 20 mM NaAc pH 5.5, Buffer B: 20 mM NaAc pH5.5, 1 M NaCl. The column was equilibrate with 90% Buffer A, 10% Buffer B for 5 CVs at 5 ml/min. The protein solution was then loaded onto the column at 5 ml/min followed by a wash with 90% Buffer A, 10% Buffer B for 5 CVs at 5 ml/min. Elution was done with a gradient over 15 CVs from 10% buffer B to 100% buffer B. During the elution 5 ml fractions were collected. A typical chromatogram and a Coomassie blue stained SDS-PAGE gel of the elution can be found in figure 1.7.

The eluate of the Blue Sepharose purification containing the protein was pooled. The NaCl concentration was estimated based on the conductivity at which the protein eluted. The pooled protein solution was brought to 3 M NaCl, 20 mM NaAc pH 4.5 by adding 5 M NaCl and 20 mM NaAc pH 4.5. pH was adjusted to 4.5 and the solution was 22 μ m filtered. For this step a hydrophobic interaction chromatography was performed. A HiTrap Phenyl HP 5ml column (Gelifsciences) was used. The following buffers were used: Buffer A: 20 mM NaAc pH 4.5 3 M NaCl, Buffer B: 20 mM NaAc pH 4.5. The column was equilibrated with 5 CVs of Buffer A at 1.2 ml/min. The protein was loaded at 1 ml/min and the column was then washed for 10 CVs with Buffer A at 1.2 ml/min. Elution was done by a linear gradient over 20 CVs form 0% buffer B to 100% at 1 ml/min. 4 ml fractions were collected during the run, a typical chromatogram and a Coomassie blue stained SDS-PAGE gel of the elution can be found in figure 1.8.

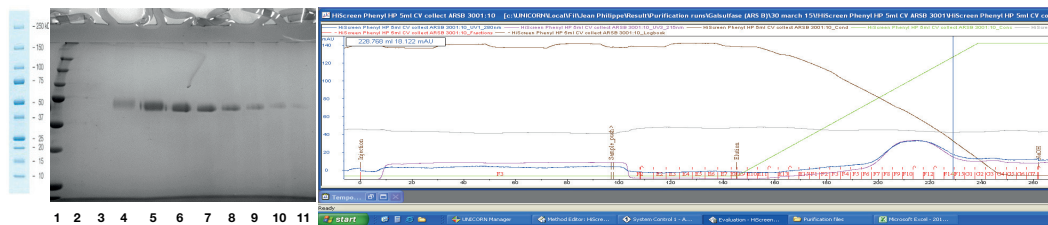


Figure 1.8 – Typical coomassie blue stained SDS-PAGE gel and chromatogram of hydrophobic interaction chromatography arylsulfatase B purification step. 1 Molecular weight ladder, 2-11 fractions during the elution, 1 corresponds to fraction F4 on the chromatogram, 3 to F7, 4 to F11, 5 to F13 6 to F14, 7 to F15, 8 to G2, 9 to G4, 10 to G6, 11 to G10.

The pooled fractions containing the protein were dialysed against 20 mM NaAc pH 4.5. A 4.7 ml HiScreen SP HP column (Gelifsciences) was used for this cation exchange chromatography. Buffer A was 20 mM NaAc, pH 4.5, Buffer B 20 mM NaAc at pH 4.5, 1 M NaCl. Column was equilibrated with 5 CVs of buffer A at 1 ml/min. The dialysed protein was loaded at 1 ml/min followed by a wash with 8 CVs of Buffer A. Elution was done by a linear gradient over 20 CVs form 0% buffer B to 100% at 1 ml/min and 2.5 ml fractions were collected. A typical chromatogram and a Coomassie blue stained SDS-PAGE gel of the elution can be found in figure 1.9.

Chapter 1. Tolerance Induction by Erythrocyte Binding

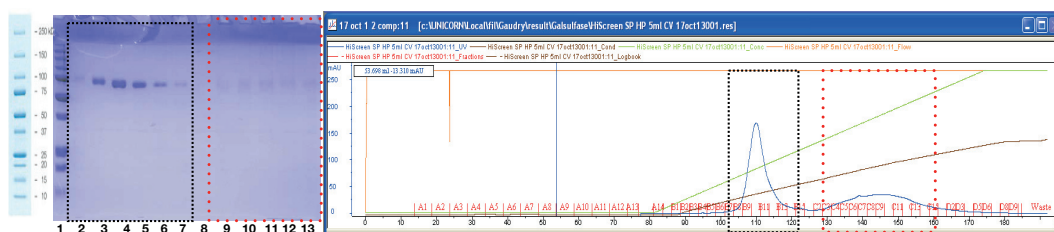


Figure 1.9 – Typical coomassie blue stained SDS-PAGE gel and chromatogram of cation exchange chromatography arylsulfatase B purification step. 1 Molecular weight ladder, 2-13 fractions during the elution, 1 corresponds to fraction F4 on the chromatogram, 2 to B8, 3 to B9, 4 to B10, 5 to B11 6 to B12, 7 to B13, 8 to C3, 9 to C5, 10 to C7, 11 to C9, 12 to C11, 13 to C13.

The clean arylsulfatase B was pooled and dialyzed against PBS concentrated with spin columns to about 1.5 mg/ml measured by nanodrop that was calibrated with a protein standard. Before the concentration was determined the protein was 0.22 μ m filtered. The protein was aliquoted and frozen at -80°C. Proteins were never freeze thawed. Any protein modification was done directly after purification before freezing.

1.2.5 LPS detection with HEK Blue-mTLR4 cells

Cells used for this assay were passed less than 30 times and had a confluence of 50-80% in culture after at least 48 hours. Cell cultures showing signs of suffering, characterized by the presence of adherent or floating round cells were not be used for the test. To culture cells DMEM high glucose media supplied with 10% FBS (Gelifsiences) was used. To perform the assay the medium was removed by aspiration and the monolayer of cells was washed with PBS. PBS was removed by aspiration and cells were detached by trypsin-EDTA. The cell suspension was homogenized by gentle pipetting and cells were counted. The cell were then seeded in a 48 wells plate at 15000 cells/well/400 μ l of culture medium 3 days before the test or at 30000 cells/well/400 μ l 2 days before the test. For the test dilutions of the LPS (Sigma, 5mg ultra pure *E.coli* 0111:B4 LPS) were prepared in 300 μ l in DMEM high glucose media supplied with 2% FBS (Gelifesiences). Protein samples were prepared in the same volume and medium. Cell culture medium was removed from the cells by aspiration and replaced with the prepared LPS standard or the protein sample. the samples were incubated at 37°C overnight (12-24 hours). 20 μ l of the supernatant was transferred per well into a 96 well plate and add 200 μ l of QuantiBlue (Invivogen) per well. Incubate at 37°C for 1 hour. Read plate at 620 and 650 nm.

1.2.6 ERY1 Conjugation with SMCC and Sulfo-SMCC

The erythrocyte-binding ERY1 peptide (19) (H₂N-WMVLPWLPGLDGGSGCRG-CONH₂) was custom-synthesized from Genscript. Ten molar equivalents (of the amount of protein used for conjugation) of SMCC (ThermoFischer Scientific) dissolved in sterile dimethylformamide or

for Sulfo-SMCC in sterile nuclease free water and was added to the target protein (arylsulfatase B). The reaction was carried out with gentle agitation for 1 hour at room temperature and desalted by two passes through Zeba Desalt spin columns (ThermoFischer Scientific). 10 equivalents of ERY1 were dissolved in 3 M guanidine hydrochloride and then added to the protein-SMCC conjugate. The following reaction was carried out for another hour at room temperature with gentle agitation. The buffer was then changed by passing the ERY1-SMCC-Protein conjugate twice through a Zeba Desalt spin column (ThermoFischer Scientific).

ERY1(FITC) ($\text{H}_2\text{N-WMVLPWLPGLDGGSG}\{\text{LYS(FITC)}\}\text{SGGSGCRG-CONH}_2$) was custom synthesized from Genscript. Conjugation was carried out in the exact same way as for ERY1.

1.2.7 ERY1 Conjugation with BMPH

ERY1 was dissolved at 30mg/ml with 3 M guanidine hydrochloride. The linker was dissolved to a 10mM (3mg/ml) solution in water free DMF. BMPH powder was stored under Argon atmosphere. 10 equivalents of the linker were added to the peptide, for 1 mg ERY1 add 75 μl of linker was added to the 30 μl of ERY1. Then 100 μl of PBS were added to keep a neutral pH. The reaction was carried out for at least 2 hours at room temperature while shaking and then dialysed against PBS. Alternatively the reaction can also be performed in DMF only by dissolving ERY1 in 25 μL of DMF.

ARSB was dialysed against the oxidation buffer (100mM Sodium Acetate, pH 5.5) overnight. Prepare 50 mM sodium meta periodate in the oxidation buffer. 25% of the original volume (volume of protein solution) of the 50mM sodium meta periodate buffer was added to the protein for an oxidation of the protein at 10 mM sodium meta periodate. The sodium meta periodate buffer has to be prepared fresh. Oxidation was carried out for exactly half an hour on ice protected from light. After half an hour dialysis against PBS was started. The oxidized protein is extensively dialyzed and protected from light. ERY1-BMPH was added in 10 molar excess to the protein and the reaction carried out for 2 hours with slight agitation at room temperature. The protein conjugate is then desalted twice with zeba desalting spin columns (ThermoFischer Scientific).

1.2.8 Conjugation of NHS-ester Dyes

For fluorescent OVA formulaitons, 5 equivalents Dy-649-NHS-ester (Dyomics) to OVA, or 5 equivalents of DY-750-NHS-ester (Dyomics) to OVA was added to the reaction and the reaction was stirred for another 1 h at room temperature. The reaction mixture was then filtered (0.22 M) and the conjugates were purified via size exclusion chromatography. The product was concentrated and used without further characterization.

1.2.9 Erythrocyte Binding by Flow Cytometry

To determine binding of the erythrocyte binding protein variants, a gradient from 1000 nM to 0.05 nM of protein was used to label 5×10^5 cells in PBSA 10 (PBS supplied with 10 mg/ml of BSA) in a total volume of 200 μ L for 1 h at 37 °C. Following a 4 min centrifugation at 200g, cells were resuspended in 200 μ L of PBSA-10 and a labeled antibody against the erythrocyte binding protein was added at a 1:100 dilution for 20 minutes on ice. After a final spin/wash cycle as above, cells were resuspended in PBSA-10 and analyzed on a flow cytometer. Cells are always kept on ice after initial binding of the protein.

1.3 Results

1.3.1 Immunogenicity of Ovalbumin, TER119-Ovalbumin and ERY1-Ovalbumin

To test the capability of the erythrocyte binding approach to introduce long term tolerance to foreign antigens an immunogenicity study with Ovalbumin was performed. Ovalbumin, the fusion protein TER119-Ovalbumin and the chemically conjugated ERY1-Ovalbumin were injected at 3 different doses i.v. once per week over a time of 12 weeks into C57BL/6 mice. 150, 30 and 6 pmol were chosen as different doses corresponding to 6.75, 1.35 and 0.27 μg Ovalbumin. Therefore the highest dose corresponds to 67.5 % of the dosing used in OTI deletion (fig.1.2) studies in the lab [69]. The experiment was analyzed by a two-way repeated measure ANOVA and the Bonferroni correction was used to calculate the p-values.

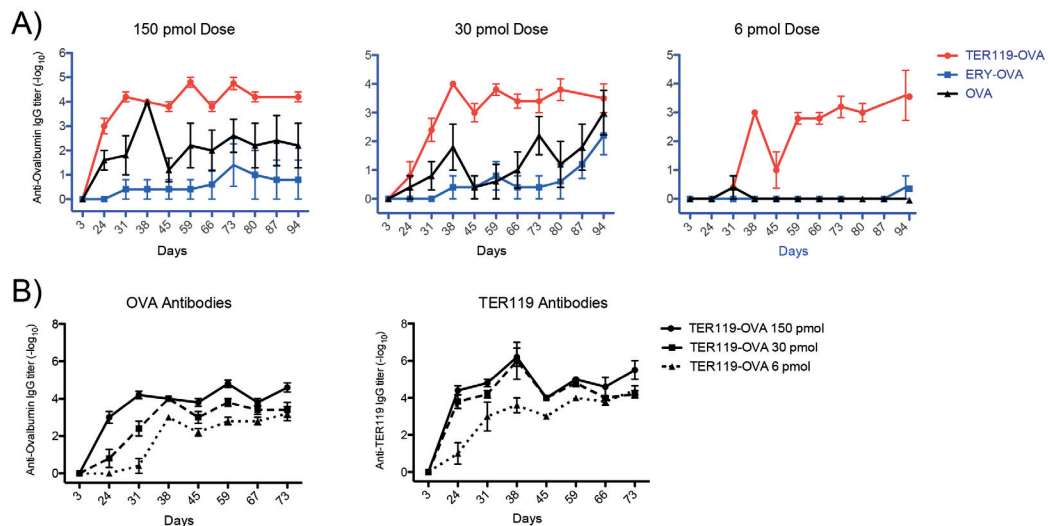


Figure 1.10 – A) Anti-Ovalbumin titers from repeated i.v. injections of Ovalbumin, TER119-Ovalbumin and ERY1-Ovalbumin at doses of 150, 30 and 6 pmol. No statistically significant differences between the treatment groups were found. B) Titers against Ovalbumin or TER119 in mice injected with TER119-Ovalbumin. Data represent mean \pm SD of n=5.

None of the treatments did improve the immunogenicity of Ovalbumin significantly at day 94. For the injections done at 6 pmol, we can see that only TER119-OVA leads to a significant antibody response. Comparing TER119-OVA against OVA at 6 pmol per injection shows that TER119-OVA is significantly more immunogenic ($p < 0.001$). The main reason no significance can be achieved between the groups is the relatively low immunogenicity of OVA, therefore making Ovalbumin a bad model to study the ability of tolerance induction of erythrocyte-binding technology. Further Ovalbumine does not have any clinical relevance.

1.3.2 Production and Characterization of Arylsulfatase B

Arylsulfatase B was produced transiently in CHO DG44 cells. Figure 1.11 A shows the western blot of the supernatant from the expression at day 7, 10 and 14. Highest levels of expression were achieved at day 14, however this was not reliably observed in repeats as cell viability could sharply decrease after day 9. Different media were tried out and JRH 302 Excel media supplemented with 4 mg/L of folic acid, 50 mg/L of L-serine and 80 mg/L of L-arginine was found to be the most efficient with a yield of 10 to 15 mg per liter of expression. This media is also used for expressing ARSB for medical use in recombinant continuous expression [98].

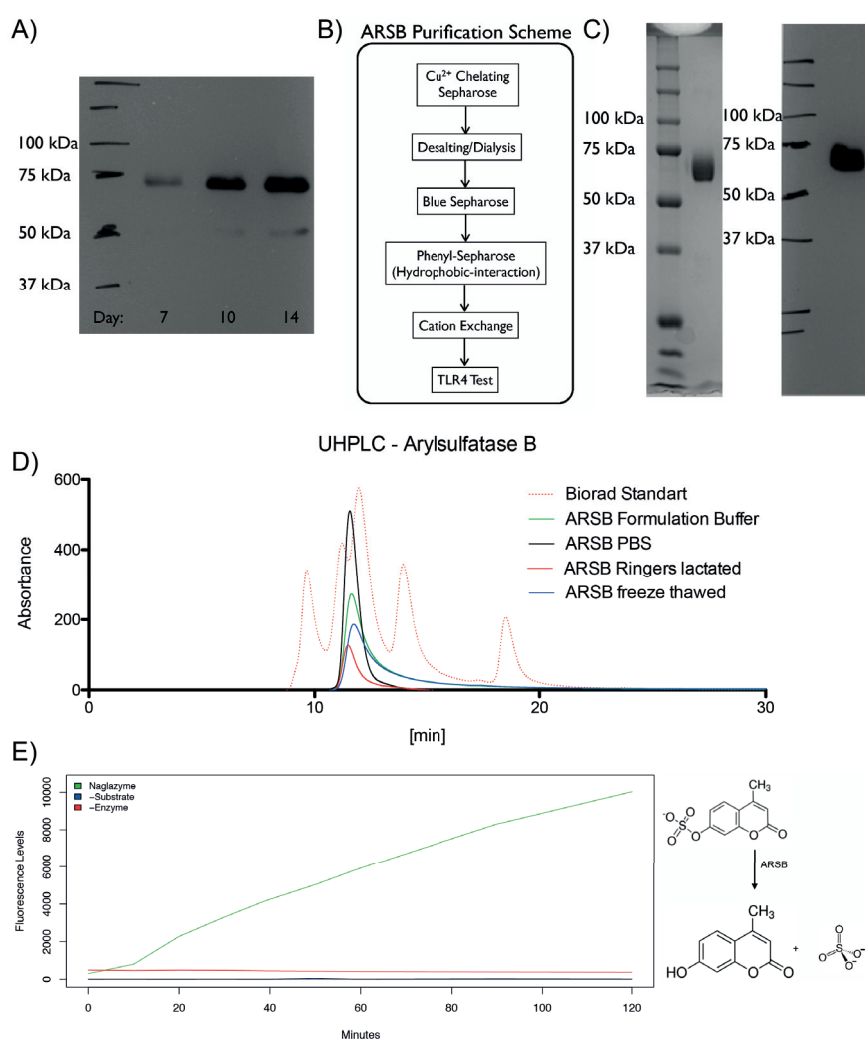


Figure 1.11 – A) Western blot analysis of ARSB expressed in CHO DG44 cells at day 7, 10 and 14. B) Purification scheme developed for purifying ARSB to a high purity (more than 99%). C) SDS-PAGE gel (left) and western blot of purified ARSB. D) HPLC profile of ARSB in different buffers and after freeze thawing. E) Fluorogenic activity assay for ARSB.

ARSB was expressed without a tag and was purified according to the scheme in figure 1.11 B. The scheme was adapted and changed for small scale and laboratory purpose from [98] where in a first step the supernatant is applied to a Cu^{2+} chelating sepharose column. The eluted protein was then dialyzed and further purified by affinity chromatography with blue sepharose followed by hydrophobic interaction and cation exchange chromatography. The protein obtained was more than 99% pure and tested for endotoxins with the HEK-blue mTLR4 test. The final protein is showed in figure 1.11 C on the left side in a coomassie blue stained SDS-PAGE gel and on the right in a western blot.

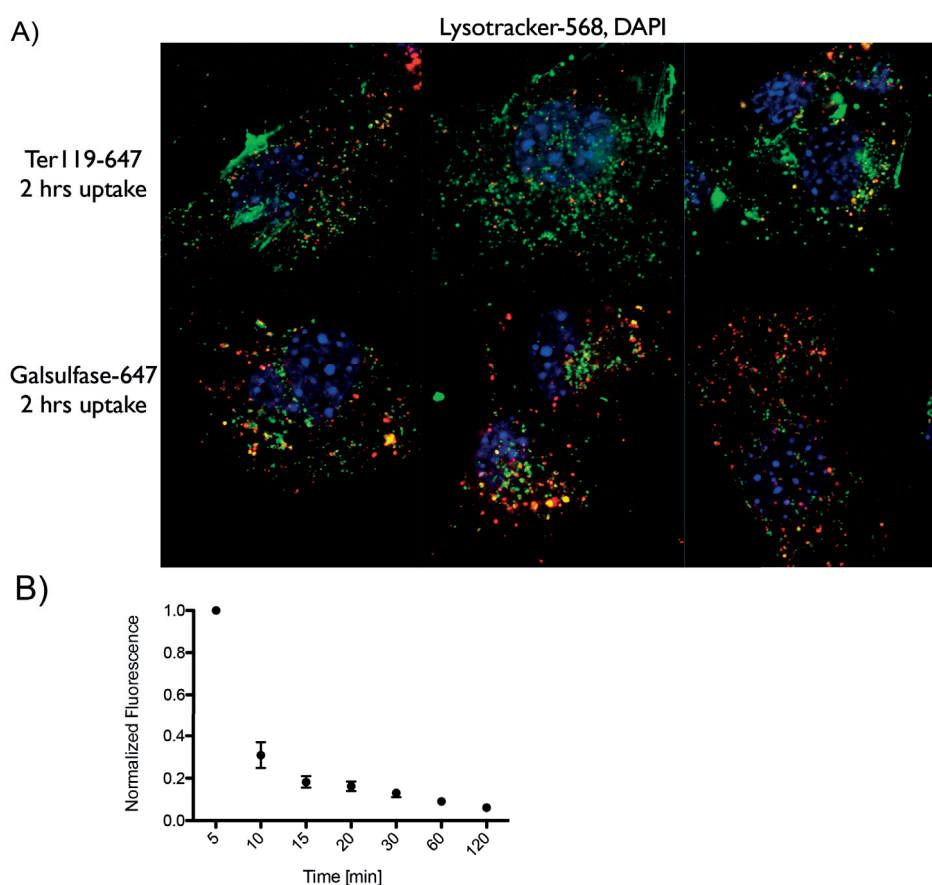


Figure 1.12 – A) Uptake of ARSB (Galsulfase) in NIH3T3 cells. Protein is shown in green, lysosome in red and the nucleus in blue. B) Normalized serum concentration of ARSB after injection of $15 \mu\text{g}$ i.v., data represent mean \pm SD of $n=5$.

The correct size of the protein was confirmed by UHPLC (fig. 1.11 D). The protein was tested in the formulation buffer used for injection (0.9% Sodium Chloride w/v), PBS, Ringers lactated buffer to simulate a physiological environment and in formulation buffer after freeze thawing. Neither a physiological buffer nor freeze thawing induces dimers or high molecular weight aggregates. The activity was tested in a fluorogenic activity assay with 4-methylumbelliferyl sulfate. The assay was conducted as published in [1] and activity was confirmed by measuring

Chapter 1. Tolerance Induction by Erythrocyte Binding

absorbance in twenty minutes intervals (fig 1.11 E). The amino acid sequence of the expressed and purified arylsulfatase b was determined by peptide mass fingerprinting (results not shown) and was confirmed to be the exact sequence of human arylsulfatase B.

Uptake of arylsulfatase B was measured *in vitro* in NIH 3T3 fibroblast cells. Arylsulfatase B and TER119 were labeled with Alex Fluor 647-NHS ester to compare uptake and localization to the lysosome. The tagged proteins were added to the media for two hours. The nucleus of the fibroblasts was then stained with DAPI and LysoTracker Red (Thermo Fischer Scientific) was used to stain the Lysosome. Figure1.12 A shows uptake and localization for three different images per protein. While both proteins are taken up, localization to the lysosome can be seen to a much higher degree for arylsulfatase B.

Clearance of arylsulfatase B was tested *in vivo* in three BALB/c and two C57/BL6 mice. Arylsulfatase B tagged with IRDye-750 was injected at 1 mg/kg i.v. and blood was drawn 5, 15, 20, 30, 60 and 120 minutes after the injection. The serum was then measured for fluorescence to determine the amount of ARSB. It can be seen that uptake of the protein is rapid and the serum half-life of the protein is about 5 to 10 minutes, which corresponds well with the serum half-life in humans [41]. Figure1.12 B shows the mean fluorescence in serum for 5 mice, the individual values for each mouse can be seen in appendix A.4.

1.3.3 Immunogenicity of Arylsulfatase B

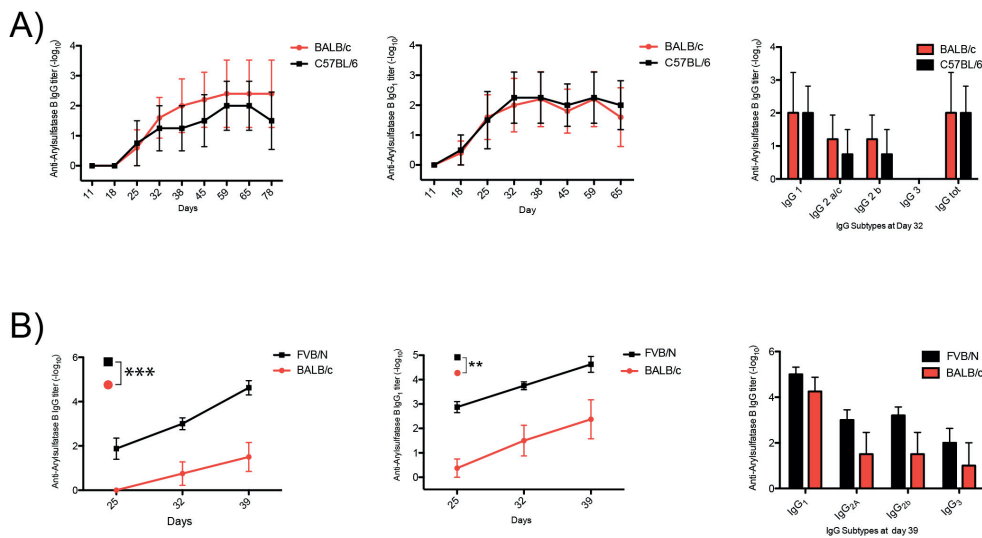


Figure 1.13 – A) Anti ARSB total IgG and IgG1 Titers in C57/BL6 and BALB/c mice and titers of different anti ARSB IgG subtypes at day 32. B) Anti ARSB total IgG and IgG1 Titers in FVB and BALB/c mice and titers of different anti ARSB IgG subtypes at day 32. ***P < 0.001, **P < 0.01. Data represent mean ± SE. Statistical analysis was done by two-way repeated measures ANOVA with post-hoc Bonferroni correction.

The immunogenicity of arylsulfatase B was first tested in C57/BL6 and BALB/c mice (fig. 1.13). The dose and frequency of the intra venous (i.v.) injection was calculated from the human therapy schedule [29] of 1mg/kg once per week. Both mice strains developed antibody titers against arylsulfatase B in 3 out of 5 mice. There was no significant difference between the two strains in total IgG titers. IgG subtypes were analyzed at day 32. IgG1 was found to be the dominant subtype, IgG2a and IgG2b were only detected in animals with very high total IgG1 levels. As IgG1 can be detected more efficiently than total IgG due to the sensitivity of the antibodies used, IgG1 titers were analyzed for the whole experiment. IgG1 titers measured were higher than total IgG for C57/BL6 mice but the same for BALB/c mice.

As only 60% of mice showed detectable levels of antibodies against arylsulfatase B and later experiments showed great variation especially in the C57/BL6 strain (Fig. 1.15) we decided to test the FVB/N strain. ARSB was intravenously injected at 1mg/kg once a week, with each group consisting of eight mice. Arylsulfatase B specific antibodies were measured by ELISA every week for total IgG and IgG1. Four out of eight mice developed antibodies against arylsulfatase B in the BALB/c strain while all eight animals of the FVB/N strain had measurable levels of anti-arylsulfatase B antibodies after 5 injections at day 39. The FVB/N strain showed significantly higher levels of antibody titers ($p < 0.001$) compared to the BALB/c strain measured by two-way ANOVA. No significant difference could be seen between total IgG and IgG1 titers. All IgG isotopes could be detected in both strains with no significant difference. In general there is a trend of higher IgG2a, IgG2b and IgG3 in FVB mice. The appearance of the subtypes is correlated with high IgG1 titers and therefore this effect is accredited to the higher overall immunogenicity of ARSB in FVB mice. The experiment was repeated in 5 FVB/N mice (Appendix A.5). All of them showed titres of four or higher after four injections.

1.3.4 Immunogenicity of ERY1-Arylsulfatase B and TER119-Arylsulfatase B

TER119-ARSB was expressed and purified with the same protocol as arylsulfatase B. The final protein had a higher than 99% purity (fig.1.14 A). ERY1 was conjugated to arylsulfatase B with SMCC. Binding was characterized by flow cytometry. While clear binding was observed, it was very weak and no reliable K_d could be established. From experience with the assay one can conclude that the binding is higher than $200\mu\text{M}$ (fig.1.14 B). This was attributed to the antibody who was not tested for flow and was even difficult for western blots. No better anti-arylsulfatase B antibody could be found though. To confirm efficient conjugation, time of flight mass spectrometry was conducted with arylsulfatase B and the ERY1-arylsulfatase B conjugate (fig.1.14 C). Arylsulfatase B was determined to have a size of 65.455 kDa and ERY1-arylsulfatase B of 76.615 kDa by time of flight mass spectrometry. This leads to a difference of 11.160 kDa, which corresponds quite exactly to the molecular weight of 5 ERY1 peptides and SMCC molecules (11.106 kDa). Therefore most ERY1 arylsulfatase B conjugates have 5 copies of ERY1, but as can be seen by the shoulders on the chromatogram we also expect conjugates with 3, 4, 6 and 7 copies of ERY1.

Chapter 1. Tolerance Induction by Erythrocyte Binding

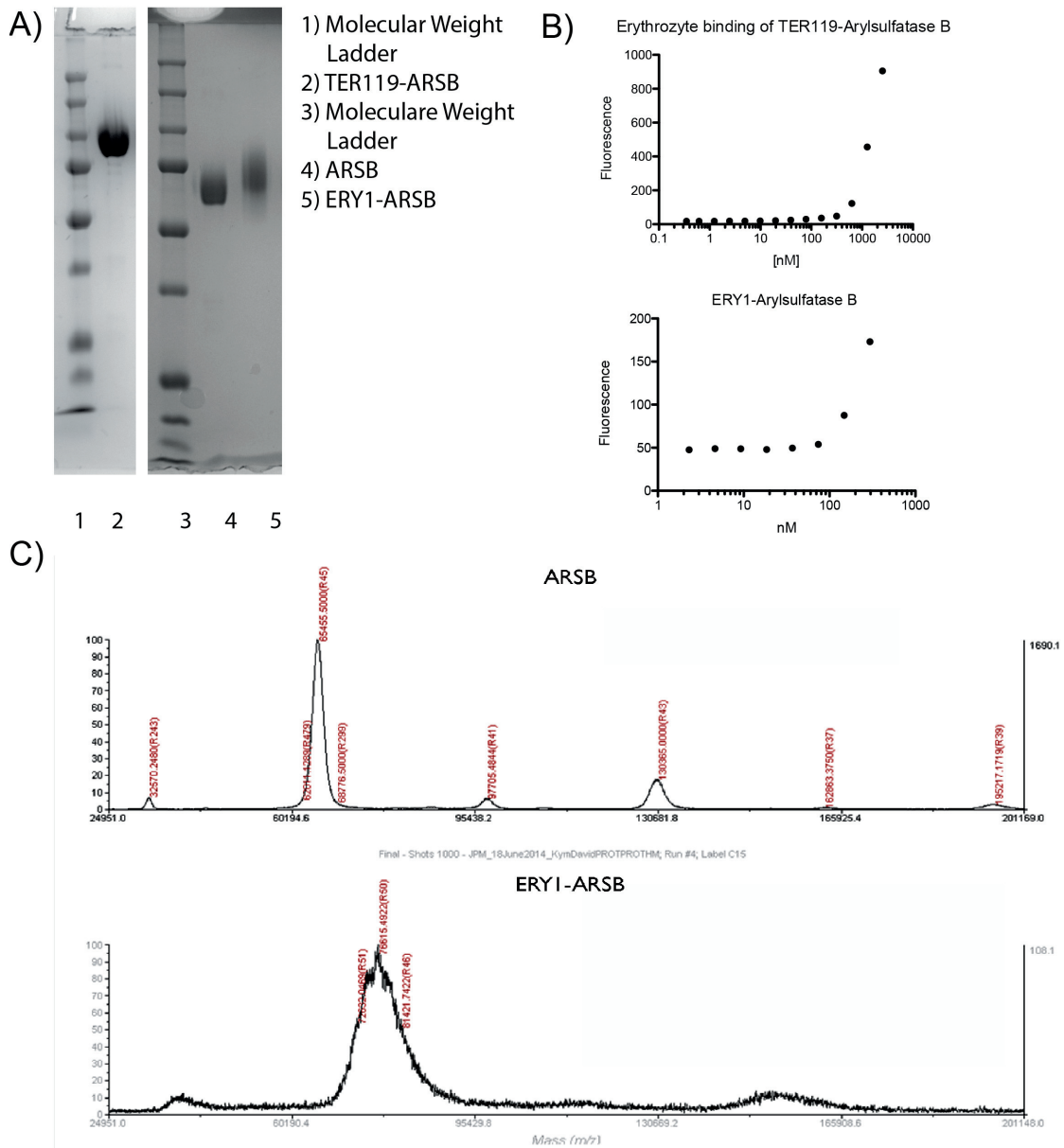


Figure 1.14 – A) Coomassie blue stained SDS-PAGE gels of TER119-ARSB, ARSB and ERY1-ARSB. B) Erythrocyte binding of TER119-ARSB and ERY1-ARSB measured by flow cytometry. C) MALDI-TOF chromatogram for ARSB and ERY1-ARSB.

The immunogenicity of ERY1-arylsulfatase B and TER119-arylsulfatase B was tested in C57/BL6 mice. Five mice per group were injected intravenously with either TER119-arylsulfatase B, ERY1-arylsulfatase B or arylsulfatase B at equimolar doses of 1 mg/kg arylsulfatase B once per week for nine weeks. One group of mice treated with TER119-arylsulfatase B was injected every second week to make sure the protein from the previous injection was completely cleared from circulation. Antibodies against arylsulfatase B in the blood serum were measured once a

week by ELISA.

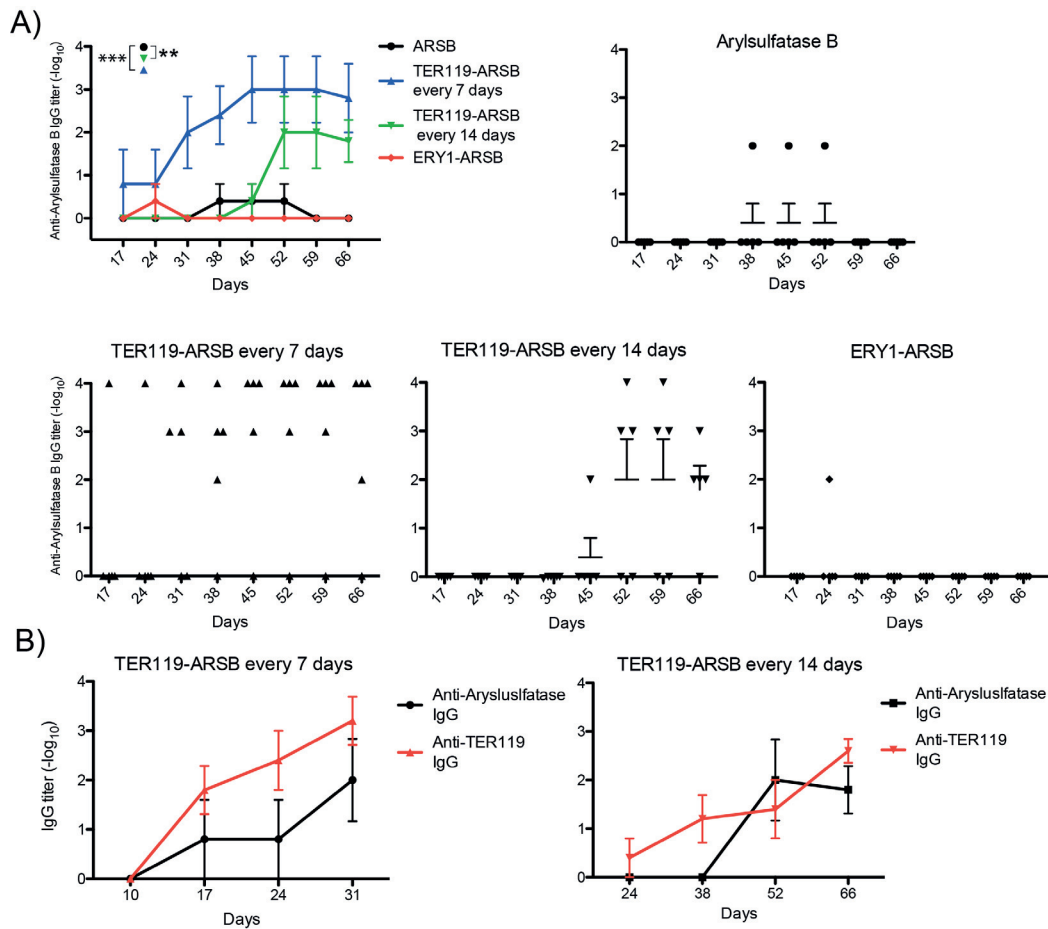


Figure 1.15 – A) Anti-arylsulfatase B titers shown as mean \pm SE as well as in every single mouse. ***P < 0.001, **P < 0.01. B) IgG titers against TER119 and ARSB in mice injected with TER119-ARSB every 7 days and every 14 days. Statistical analysis was done by two-way repeated measures ANOVA with post-hoc Bonferroni correction.

Comparing the TER119-arylsulfatase B group with weekly injections to the arylsulfatase B group, we can see that TER119-arylsulfatase B injected weekly has a significantly ($p < 0.001$) higher immunogenicity than arylsulfatase B. This also holds true for the TER119-arylsulfatase B group injected every second week, which has a significantly ($p < 0.01$) higher immunogenicity than arylsulfatase B. Surprisingly the immunogenicity of arylsulfatase B was very low in this experiment. No significant difference was observed between ERY1-arylsulfatase B and arylsulfatase B, as only one animal in the ERY1-arylsulfatase B group showed detectable antibodies against ARSB at day 24 and one animal of the arylsulfatase B group at day 38, 45 and 52.

In addition, antibody titers against TER-119 were measured (fig.1.15 B) in the two groups in which TER119-arylsulfatase B was injected. Titers against TER119 rose faster than titers

Chapter 1. Tolerance Induction by Erythrocyte Binding

against arylsulfatase B. In five out of 10 animals antibodies against the TER119 part of the fusion protein could be measured one week or more before antibodies against arylsulfatase B could be found. In no animal could antibodies against arylsulfatase B be detected before antibodies against TER119 were detected.

At a first look, it seems that injecting TER119-arylsulfatase B every 14 days makes it less immunogenic. However if we look at the immunogenicity by injections and not days we can see that the two are identical (Appendix A.6). Data was analyzed with a two-way repeated measures ANOVA and p-values were calculated with Bonferroni correction.

1.3.5 Tolerance Induction with ERY1-Arylsulfatase B

To test the capabilities of ERY1-arylsulfatase B to induce tolerance, FVB/N mice were injected twice with ERY1-arylsulfatase B one week apart with doses equimolar to 1mg/kg of arylsulfatase B and then switched to wild-type arylsulfatase B one week after the second ERY1-arylsulfatase B injection. They then received 1mg/kg of arylsulfatase B once every week. The control group received only the wild-type arylsulfatase B injections at 1mg/kg once a week (fig. 1.16 A). The FVB/N strain was used because it showed a stronger and more reproducible immune response against arylsulfatase B.

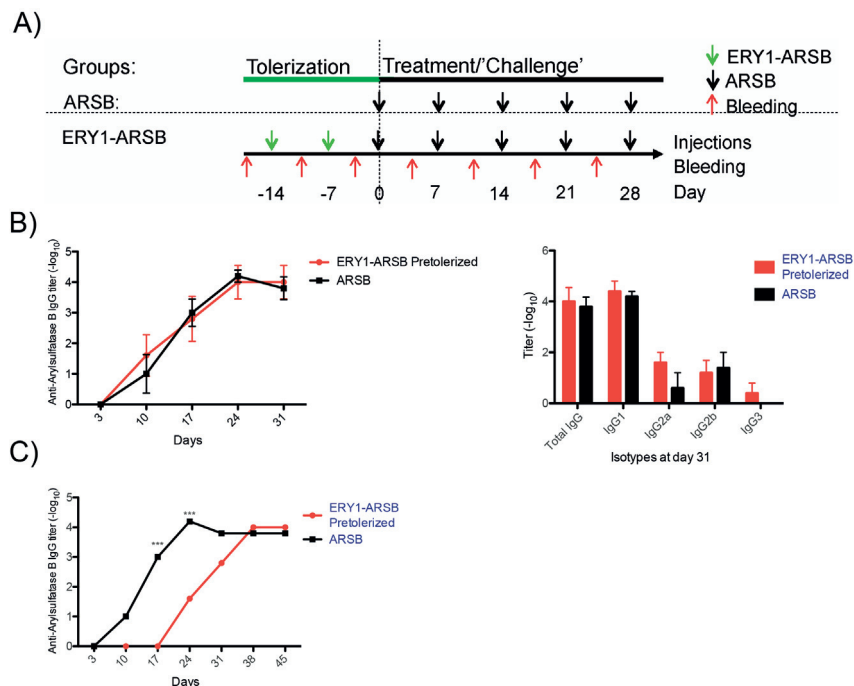


Figure 1.16 – A) Experimental protocol showing groups, dosing and bleeding. B) Anti-arylsulfatase B total IgG titers and anti-arylsulfatase B IgG subtypes. C) Anti-arylsulfatase B total IgG titers compare by total injections of 1mg/kg arylsulfatase B. *** $P < 0.001$. Data represent mean \pm SE. Statistical analysis was done by two-way repeated measures ANOVA with post-hoc Bonferroni correction.

Figure 1.16 B compares anti-arylsulfatase B titers of the two groups with day zero being where both animals receive their first wild-type ARSB injection. It can be seen that the titers of the two groups are very similar and there is no significant difference between ERY1-arylsulfatase B treated mice and the one receiving only arylsulfatase B. If we look at the IgG subtypes at day 31 we can see no significant difference between the groups either. As seen before in figure 1.13 all subtypes can be found with the most scarce being IgG3 and the dominant one being IgG1.

Figure 1.16 C shows the graph by comparing the two groups by total doses of arylsulfatase B injected, meaning that day 0 for the tolerized group is the first injection of ERY1-arylsulfatase B. This comparison makes sense in that it normalizes the time axes to the total amount of arylsulfatase B exposed. In this case there is a significant difference in anti-Arylsulfatase B titers at day 10 and 17 ($p < 0.001$) as a result of a delay in the induction of anti-arylsulfatase B antibodies in mice tolerized by ERY1-ARSB. Data was analyzed with a two-way repeated measures ANOVA and p-values were calculated with Bonferroni correction.

1.3.6 Tolerance Induction with deglycosylated ERY1-Arylsulfatase B

SMCC was switched to sulfo-SMCC for future experiments because it is less susceptible to hydrolysis and therefore made the chemical ERY1 conjugation more reproducible. Arylsulfatase B was deglycosylated to remove the rapid uptake dynamic from the native glycosylations. There are five known N-linked residues believed to be glycosylated in recombinant arylsulfatase B expressed in CHO. Those glycosylations are mannose rich and are recognized and taken up by the cation independent mannose-6-phosphate receptor [12, 23]. Deglycosylation was done with endoglycosidase F1, F2 and F3, to maintain the secondary and tertiary structure of the protein. The SDS-PAGE gel in figure 1.17 A shows the deglycosylated protein in lane 4. Compared to the wild type arylsulfatase B in lane 2 one can clearly see the loss of molecular weight from the deglycosylation. However, using glycostain revealed that the deglycosylation was not complete (result not shown). Lane five on the gel shows the ERY1 conjugates with deglycosylated arylsulfatase B after endotoxin removal by anion exchange chromatography.

Because the arylsulfatase B antibody did not work well for flow cytometry we designed an ERY1 variant that was labeled with one FITC molecule in the linker region of ERY1. To test the conjugation, reactions with ERY1(FITC) to arylsulfatase B, ERY1 to arylsulfatase B and ERY1-FITC to ovalbumin were performed side by side. The dissociation constant of the ERY1(FITC) constructs was measured by flow cytometry (fig. 1.17 B) and was found to be similar to previously measured K_d s [69]. Further the K_d of arylsulfatase B-ERY1(FITC) was in the same range as the one for the ERY1(FITC)-ovalbumin construct with 8.1 nM respectively 3.4 nM.

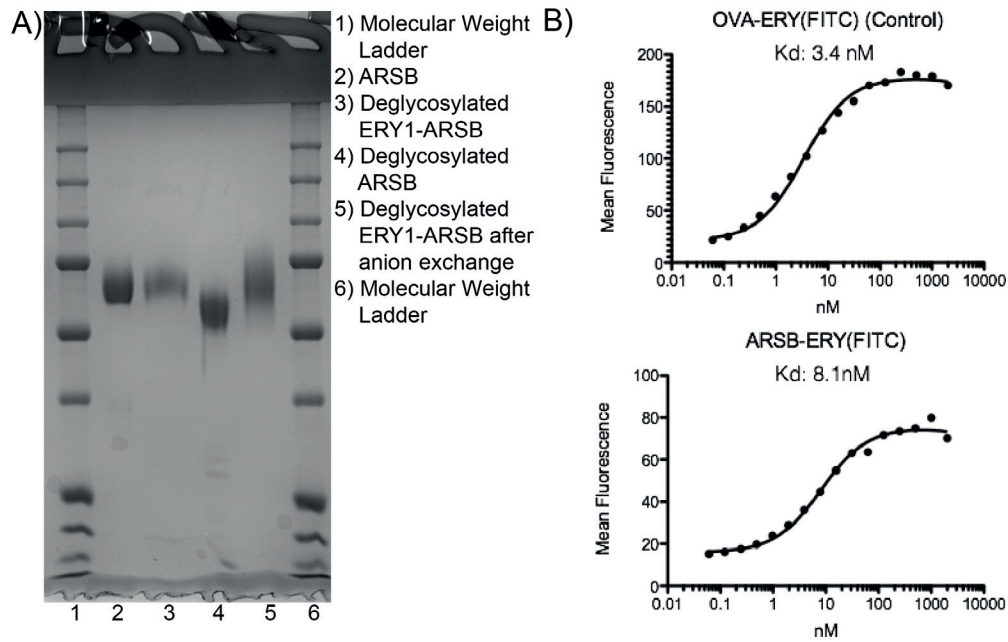


Figure 1.17 – A) Coomassie blue stained SDS-PAGE gel shows the weight loss upon deglycosylation with endoglycosidase F1, F2 and F3 and the ERY1-deglycosylated ARSB construct after endotoxin removal. B) Erythrocyte binding of ERY1(FITC)-ARSB and ERY1(FITC)-OVA measured by flow cytometry.

An animal experiment with four groups was performed in FVB mice with five mice per group. Two groups received 2 tolerizing injections of ERY1-arylsulfatase B or deglycosylated ERY1-arylsulfatase B at 1 mg/kg once a week followed by 1 mg/kg of arylsulfatase B once a week (fig.1.18 A). One group was injected with 1 mg/kg of ERY1-arylsulfatase once a week during the whole timespan of the experiment to measure the immunogenicity of the construct rather than its ability to induce tolerance. The "challenge" control group received 1 mg/kg arylsulfatase B once per week corresponding to the dosing used for the therapy in humans.

The anti-arylsulfatase B titers are shown in Figure 1.18 B. There was no significant difference between the groups by two way repeated measures ANOVA with post-hoc Bonferroni correction. There is a trend that mice injected with ERY1-arylsulfatase B weekly have a lower immunogenicity compared to mice injected weekly with arylsulfatase B, especially considering there are two mice that have not developed measurable titers against arylsulfatase B in mice injected with ERY1-arylsulfatase B weekly whereas in all other groups all mice have developed titers against arylsulfatase B at day 8 (Appendix A.7). Comparing the IgG subtypes IgG1, IgG2a, IgG2b and IgG3, we can see that the most dominant subtype in all groups is IgG1. There is no significant difference between the composition of subtypes and the appearance of the subtype IgG2a, IgG2b and IgG3 in mice seems to be directly correlated to the strength of the IgG1 titer (fig 1.18 C). For example, no mouse that has an IgG1 titer of 3 or lower has detectable levels of IgG3.

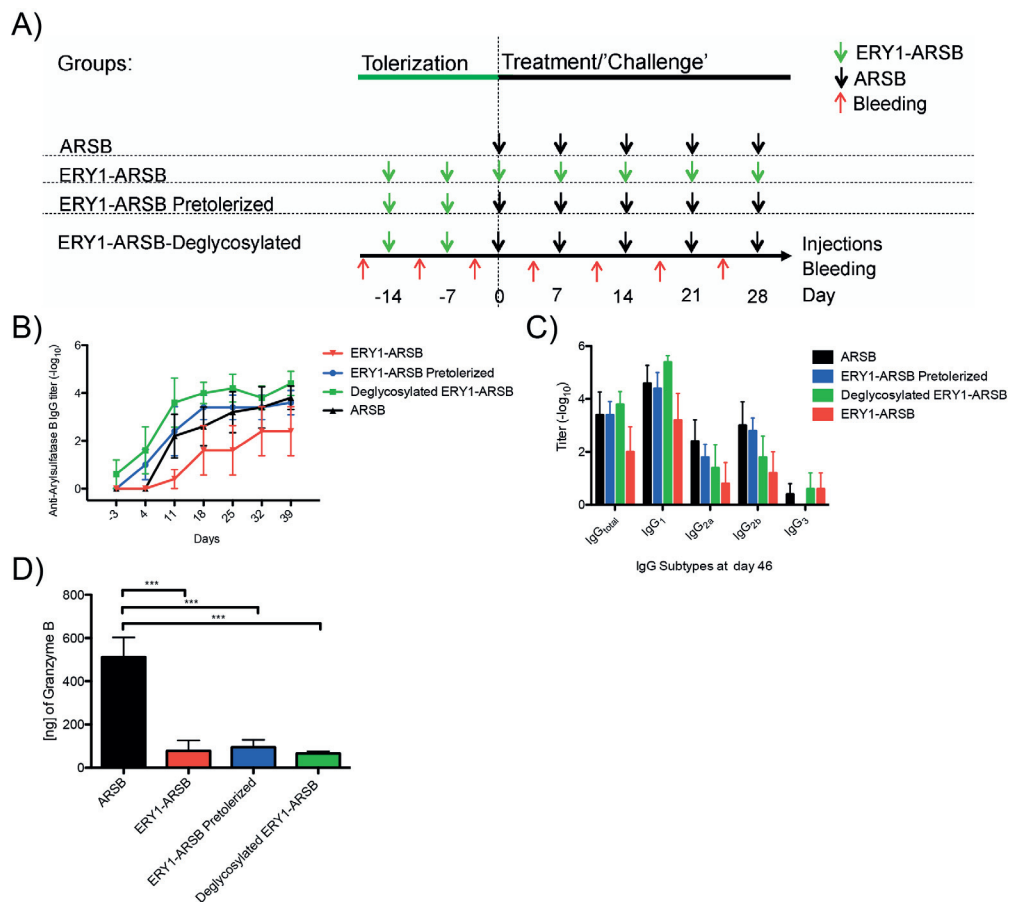


Figure 1.18 – A) Experimental Protocol showing different groups and injection and bleeding schedule. B) Anti-ARSB IgG titers measured by ELISA from blood serum. C) IgG subtype analysis measured by ELISA from blood serum. D) Granzyme B secreted by lymphocytes after 4 day restimulation with arylsulfatase B measured by ELISA. ***P<0.001. Data represent mean \pm SE. Statistical analysis was done by two-way repeated measures ANOVA with post-hoc Bonferroni correction for B and by one-way ANOVA with tukey's multiple comparison test for C and D.

Interestingly, upon four day restimulation of lymphocytes with arylsulfatase B, significant differences could be found in the amount of secreted granzyme B between all the groups receiving an ERY1-arylsulfatase B construct and the one receiving only arylsulfatase B by one-way ANOVA with tukey's multiple comparison test ($p < 0.001$). Granzyme B is released by activated CD8+ T-cells upon signaling from their T-cell receptor and induces apoptotic cell death by induction of the caspase cascade [43].

1.3.7 Tolerance Induction with ERY1-BMPH-Arylsulfatase B

To make sure ERY1 has maximal possible exposure, N- β -maleimidopropionic acid hydrazide (BMPH, ThermoFischer Scientific) was used as linker. BMPH has two reactive groups, a hy-

Chapter 1. Tolerance Induction by Erythrocyte Binding

drazide and a carbonyl, which allows conjugation of ERY1 on top of the glycosylations of arylsulfatase B. Further ERY1 (FITC) was used, which allows visualization of ERY1 (FITC) on SDS-PAGE gels by imaging with UV exposure. Arylsulfatase B and the conjugates are shown on an SDS-PAGE gel in figure 1.19 A as a coomassie blue stain on the left and the same gel imaged with UV exposure on the right. The K_D between red blood cells and ERY1-BMPH-arylsulfatase B was measured by flow cytometry and found to be 24.14 nM (fig. 1.19 C).

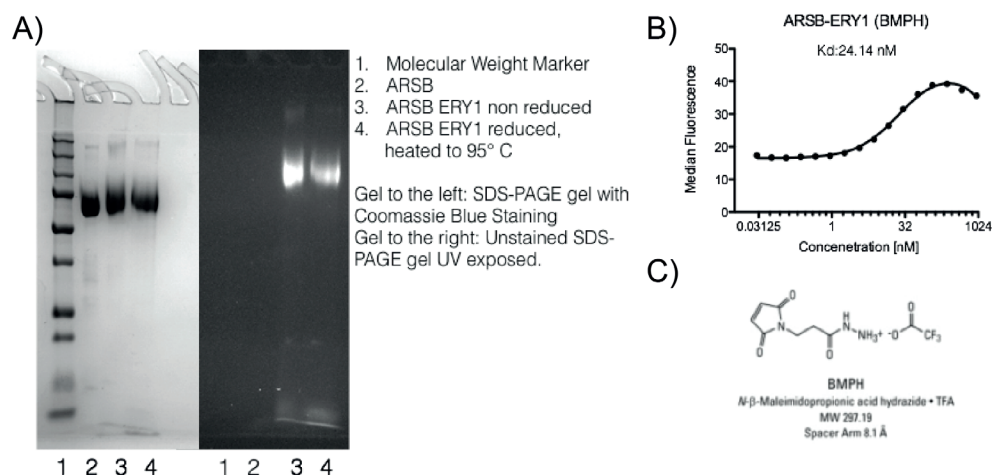


Figure 1.19 – A) SDS-PAGE gel showing ARSB and ERY1 (FITC)-ARSB (BMPH) by UV exposure (right side) and coomassie blue stain. B) Erythrocyte binding of ARSB-ERY1 (BMPH) by flow cytometry. C) Structure of BMPH (ThermoFischer Scientific).

The ability to induce tolerance of ERY1-BMPH-arylsulfatase B was tested in FVB mice with five mice per group. The mice got injected with ERY1-BMPH-arylsulfatase B once a week for two weeks with a dose equimolar to 1mg/kg of arylsulfatase B and were then switched to 1 mg/kg of arylsulfatase B once a week. This was compared to five mice injected with 1 mg/kg arylsulfatase B once per week starting when the other group gets the first arylsulfatase B injection.

If we look at tolerance, time point 0 on the x-axis is when the tolerized group switches to arylsulfatase B and the other group gets its first injection of arylsulfatase B (fig. 1.20 B). It can be seen that treatment with ERY1-BMPH-arylsulfatase B leads to a significant delay in the onset of titers with a significant difference in titers at day 18 ($p < 0.001$) by two-way repeated measures ANOVA with post-hoc Bonferoni correction. However this difference disappears at day 25 and long term tolerance is broken.

For comparison of the immunogenicity of the two injection methods used we should set day 0 for the first injection of ERY1-BMPH arylsulfatase B for the tolerized group and for the first injection of arylsulfatase B in the control group. This will normalize the time component to total amount of arylsulfatase B injected (fig. 1.20 C). Significant differences in titers were observed after 3 injections with $p < 0.05$ and after 4, 5 and 6 injections with $p < 0.001$, by two-way

repeated measures ANOVA with post-hoc Bonferroni correction.

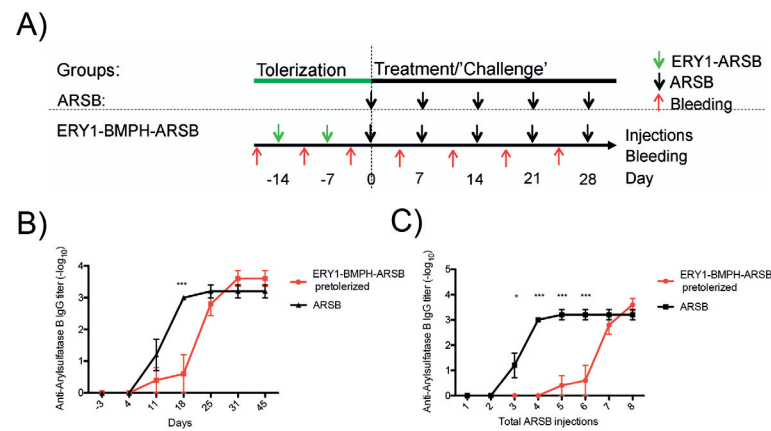


Figure 1.20 – A) Injection and bleeding schedule for the different groups (left side). B) Anti-arylsulfatase B IgG titers in mice tolerized with ERY1-ARSB (BMPH) and non-tolerized mice. Anti-arylsulfatase B IgG titers given the number of injections of ARSB at 1mg/kg. * $P < 0.05$, *** $P < 0.001$. Data represent mean \pm SE. Statistical analysis was done by two-way ANOVA with post-hoc Bonferroni correction.

1.4 Discussion

The immunogenicity experiment with different doses of Ovalbumin, ERY1-Ovalbumin and TER119-Ovalbumin showed that Ovalbumin does not raise a strong immunogenic response in C57BL/6 mice leading to very low levels of antibody titers. Ovalbumin is therefore not an ideal antigen to study the induction of tolerance. The experiment raised concerns about the immunogenicity of TER119, as high antibody titers against TER119 could be found after 3 injections for the 150 and 30 pmol dose and after 5 injections for the 6 pmol dose. However, TER119-Ovalbumin could not be purified to a high purity and therefore no conclusive judgment about the immunogenicity of TER119 could be made.

A protocol to produce and purify arylsulfatase B to an extremely high purity was developed. The protein was further shown to be active. The correct size of the protein was measured by UHPLC and freeze thawing was assessed to be a safe method to store the protein and was found to not introduce dimers, multimers or aggregation. Uptake and localization to the lysosome was confirmed *in vitro*. Rapid clearance of the protein from the plasma was found in mice and corresponds well with the data from human clinical trials [40]. The immunogenicity of arylsulfatase B was tested in C57/BL6, BALB/c and FVB mice. For C57/BL6 and BALB/c strains 50% of the mice developed measurable antibody titers against arylsulfatase B and no significant differences were found between these two strains. Most of the animals that did turn immunogenic developed high levels of antibody titers. In the FVB strain 100% of the mice developed measurable antibody titers against arylsulfatase B. Arylsulfatase B was significantly more immunogenic in the FVB strain compared to the C57/BL6 and BALB/c strains. No difference between the strains in IgG subtypes against arylsulfatase B was found in mice turned immunogenic. This high immunogenicity makes arylsulfatase B a well suited protein to study the induction of tolerance towards partly foreign proteins.

TER119-arylsulfatase B was found to have a significantly higher immunogenicity than arylsulfatase B in C57/BL6 mice. There was also a trend that higher antibody titers against the TER119 part of the fusion protein TER119-arylsulfatase B, rather than the arylsulfatase B part. Furthermore in 50% of the mice, anti-TER119 IgG titers could be measured one week before arylsulfatase B titers could be measured. It was therefore concluded that TER119 has an inherent immunogenicity and is not suitable for tolerance induction by erythrocyte binding.

Measuring the binding of ERY1-arylsulfatase B to erythrocytes proved to be difficult as there is no existing anti-arylsulfatase B antibody suited for flow cytometry. The mass of arylsulfatase B and ERY1-arylsulfatase B was measured by MALDI-TOF and revealed a mean of five ERY1 peptides per arylsulfatase B protein.

While ERY1-arylsulfatase B fails to induce tolerance (fig. 1.16 B) upon challenge with arylsulfatase B, if we compare the total injections of arylsulfatase B at 1mg/kg we find a significant delay in the onset of titers (fig. 1.16 C). One hypothesis is that the strong uptake of arylsulfatase B through the mannose-6-phosphate receptor interferes with efficient tolerance induction. To measure the direct dissociation constant we used an ERY1 variant that is tagged with FITC

in the linker. Binding to erythrocytes with a high affinity of 8.1 nM could be measured for ERY1(FITC)-arylsulfatase B. But this variant also showed no capacity to induce long term tolerance against arylsulfatase B. Furthermore a deglycosylated variant of arylsulfatase B-ERY1 was used for tolerance induction but was not performing significantly different from the glycosylated variant (fig 1.18 B). The deglycosylation was shown to be incomplete even though a large shift in mass could be observed on SDS-PAGE gels. There is a trend that injecting only ERY1-arylsulfatase B has a lower immunogenicity compared to arylsulfatase B, especially because two animals treated with ERY1-arylsulfatase B did not develop measurable anti-arylsulfatase B IgG titers over the span of the experiment - a result never observed with arylsulfatase B injections in the FVB strain, in which always 100% of the animals had measurable IgG titers against arylsulfatase B. Interestingly, upon 4 day restimulation of lymphocytes with arylsulfatase B all the groups receiving erythrocyte binding variants of arylsulfatase B showed significantly lower levels of Granzyme B. Granzyme B is related to the cytotoxic activity of CD8+ T-cells [43].

BMPH was used as a linker to ensure maximal exposure of ERY1 and the possibility that by conjugating to the glycosylations of arylsulfatase B, uptake by the mannose-6-phosphate receptor can be reduced. While a significantly slower rise of anti-arylsulfatase IgG titers could be observed, this effect was only true for one week, after which tolerance to arylsulfatase B was fully broken (fig. 1.20 B). The delay of the onset in the production of anti-arylsulfatase B antibodies is even more clear when the data is plotted by looking at the number of injections of 1mg/kg of arylsulfatase B (fig. 1.20 C).

While it is not clear why the tolerance to arylsulfatase B is broken and the induction of tolerance to arylsulfatase B only leads to a significant delay in the production of anti-arylsulfatase B IgG there is a hypothesis: Heavily glycosylated proteins can be targeted to dendritic cells, macrophages and B-cells [121]. While we are able to delete the CD8+ and CD4+ T-cells, arylsulfatase B is able to activate B-cells in a T-cell independent fashion [25]. Especially T-cell independent immune responses against polysaccharides have been shown to elicit memory B-cells [92]. This would also mean that regulatory T-cells capable of suppressing those B-cells [48] were not induced. This hypothesis is further supported by the fact that erythrocyte binding technology worked for asparaginase which is expressed in *Escherichia coli* and therefore has no glycosylations. Further it is possible that expression of arylsulfatase B in CHO cells leads to non human glycosylation patterns and the erythrocyte technology only induces long term tolerance towards foreign peptides but not glycosylations.

To try to address these questions inactive arylsulfatase B was expressed in *Escherichia coli* to have a variant of the protein that has no glycosylation. This would allow us to directly compare the tolerance induction process of a heavily glycosylated protein against a non glycosylated variant of it. While the expression of the protein works fine no soluble form of the protein could be expressed.

2 Searching new Binders to Erythrocytes by Phage Display

2.1 Introduction

2.1.1 Motivation to Search for new Erythrocyte Binders

Chapter one showed that the single-chain variable fragment of the rat antibody TER119, which recognizes a glycoprotein A associated molecule, is immunogenic (fig. 1.15). However its ability to efficiently delete CD8+ and CD4+ T-cells with only two injections has been shown and the deletion of CD8+ T-cells would be highly beneficial in a diseases like diabetes. Therefore, the aim was to find a less immunogenic antibody or antibody fragment against mouse glycoprotein A (GYPA) and for translation of the approach to the clinic antibodies against human and monkey glycoprotein A. The decision fell on domain antibodies, as they are relatively small molecules of about 14 kDa and can easily be fused to other proteins. The library used has further the advantage that all domain antibodies it contains should not aggregate and be monomeric [53].

2.1.2 Phage Display Technology, the Human Domain Antibody Library

Phage display was first described in 1985 [109] for selection of peptides and 5 years later it was shown that filamentous phages can display antibodies correctly [83]. Phage display is based on genetic engineering of the coat proteins of filamentous phage, like M13, that uses *E. coli* as a host. Phage assemble by the polymerization of the coat protein pVIII (geneVIII) that is then capped of by the terminal coat protein pIII (geneIII). Genetic fusion of the desired protein for display can be made to both coat proteins. Fusion to pVIII leads to high level display as there are more than a thousand copies of pVIII and fusion to pIII leads to low level display with only 5 present copies. Phage display has the big advantage over hybridoma technology that it allows to screen against self-antigens by completely bypassing the use of animals.

The library used in the search of new binders towards human, mouse and monkey glycoprotein A is the human domain antibody library [17]. The library uses human domain antibodies,

Chapter 2. Searching new Binders to Erythrocytes by Phage Display

which consist only of a single variable heavy chain (VH) domain from an antibody. Such single domain antibodies have been observed in camels [101] and sharks [104]. The antibody repertoire in this library is based on the human VH3-23 germline segment, which is known to bind to protein A [50]. Synthetic diversity was introduced into all three complementarity determining regions (CDR1-3) by PCR mutagenesis. The library uses the phagemid, a pIII-domain antibody fusion expressing plasmid in combination with a helper phage. The rest of the proteins needed for phage assembly and most copies of the pIII protein are derived from the helper phage, only a small proportion stem from the phagemid. This leads to mostly monovalent display, with in average less than one pIII-domain antibody fusion per phage [93]. The advantage is, that monovalent display leads to the selection of higher affinity binders compared to multivalent display [78].

2.2 Materials and Methods

2.2.1 Glycophorin A Isolation

Blood from BALB/c and C57BL/6 mice was washed twice with twice the volume of PBS in 50 ml falcon tubes (spun at 2000 g for 20 min.). The resulting cell pellet was lysed in a buffer of 10 mM phosphate buffer and 1 mM MgCl₂ at pH 7.6 (add 20 times of the original volume of blood). Lysis was carried out for 10 minutes at room temperature. The cells were then spun at 12'000 g for 15 minutes at room temperature. The supernatant was discarded and the pellet dissolved in the same amount of lysis buffer, spinning and re suspending was done for at least three times or until the obtained pellet was white and not red anymore. The obtained white pellet is then resuspended in a 0.15 M NaCl buffer (1.3 times the initial blood volume) and 1.5 times the volume of 75% w/v of phenol in water is added (for example, 20 ml of 0.15 M NaCl and 30 ml of 75% w/v of phenol). Glycophorin A is then extracted for 30 minutes at 65° C. The solutions is then left at room temperature for 30 minutes and then frozen at - 20° C. The extraction was thawed up and the organic phase was dialysed extensively against milli-Q water (water was changed at least 5 times). The extracted glycophorin A was then lyophilized and resuspended in PBS.

2.2.2 Biotin Conjugation and Binding to Magnetic Beads

Biotin-NHS was added in a 5 molar excess to glycophorin A. The reaction was carried out for one hour in PBS, the remaining biotin was then removed by dialysis. Conjugation of biotin was measured by ELISA - flat bottom 96 well plates were coated with 5 µg of glycophorin A-biotin. The same amount of Ovalbumin was used as negative control. A normal ELISA protocol was followed by using and anti streptavidin-HRP conjugated antibody. The magnetic beads (Thermo Fisher Scientific, Dynabeads, M-280 Streptavidin) were washed 3 times with PBS. 20 µg of glycophorin A-biotin was added to 1mg of beads in 200 µl. Reaction was carried out for one hour at room temperature with gentle agitation. The beads were washed 3 times with PBS.

2.2.3 Phage Display

The phage was amplified as described in [72]. For each round of selection 4×10^{12} phages were used. The selection was carried out in PBS supplied with 50 mg/ml of BSA (binding buffer).

For selection on beads, 4×10^6 beads were used for a round of selection. The first round of screening had a negative selection against unmodified beads. The beads and the phage was incubated for 1 hour at 37° C in a total volume of 4 ml in binding buffer. After 1 hour the beads were removed by centrifugation. Glycophorin A beads were added to the phage and incubated at 37° C for one hour, the beads were then removed with the help of a magnet. The beads were washed twice with 4 ml of binding buffer and then left for 10 min at 37° C for dissociation at

Chapter 2. Searching new Binders to Erythrocytes by Phage Display

room temperature. Round two used two 10 minutes dissociation steps and round 3 used one 15 min and two 10 minutes dissociation steps. The beads were washed another 3 times and trypsin cleavage was carried out as described in [72].

For selection with erythrocytes, 4×10^6 erythrocytes were incubated in 4 ml of binding buffer with the phage for 1 hour at 37° C. Unbound phage was removed by centrifugation in Percoll. This step also ensured that no other cells from blood than erythrocytes were present. The erythrocytes were then washed twice by centrifugation and left for a 5 min dissociation step at room temperature. Round 2 had two 10 min dissociation steps and Round three a 10, 15 and 20 minute dissociation step. Subsequent rounds used the same dissociation steps as round 2. The Erythrocytes were then washed 3 more times and trypsin cleavage was carried out as described in [72].

Phage ELISA was carried out as described in [72], expression of the domain antibodies and purification was carried out as described in [103].

2.2.4 Erythrocyte Binding by Flow Cytometry

To determine phage binding, approximately 10^{10} phage particles were used to label 5×10^5 cells in PBS with 5 mg/ml of BSA in a total volume of 200 μ L for 1 h at 37 °C. Following a 4 min centrifugation at 200g, cells were resuspended in 200 μ L of PBS with 5 mg/ml of BSA and anti-phage-PE was added at a 1:20 dilution for 1 h at room temperature. After a final spin/wash cycle as above, cells were resuspended in PBS with 5 mg/ml of BSA and analyzed on a flow cytometer.

The same protocol was used to determine protein binding, but it was carried out in a known concentration of protein (2000 nM) and anti-myc-FITC was used to label the domain antibody binding to the erythrocyte.

2.3 Results

2.3.1 Screening against Mouse and Human Glycophorin A

Murine glycophorin A (GYPA) was chemically extracted from blood of BALB/c and C57BL/6 mice, conjugated with Biotin-hydrazide and bound to magnetic streptavidin beads as described in materials and methods. The Glycophorin A extract used is shown in figure 2.1 A as glycostained SDS-PAGE gel. Human glycophorin A was bought from (Sigma Aldrich, CAS: 76416-15-4) and human glycophorin A beads were created as described in materials and methods.

3 rounds of panning against human and mouse glycophorin A beads were conducted as described with more stringent washes every round. Phage titers were determined after every round of selection and are shown in figure 2.1 B. Titers after the first round were in the expected range for the library and rose in subsequent rounds for both screens against human and mouse glycophorin A. Rounds 2 and 3 were sent for sequencing. The amino acid sequence of the complementarity determining regions for domain antibodies that appeared multiple times in the sequencing are shown in table 2.1 with the percentage that the sequence made up from the total obtained sequences.

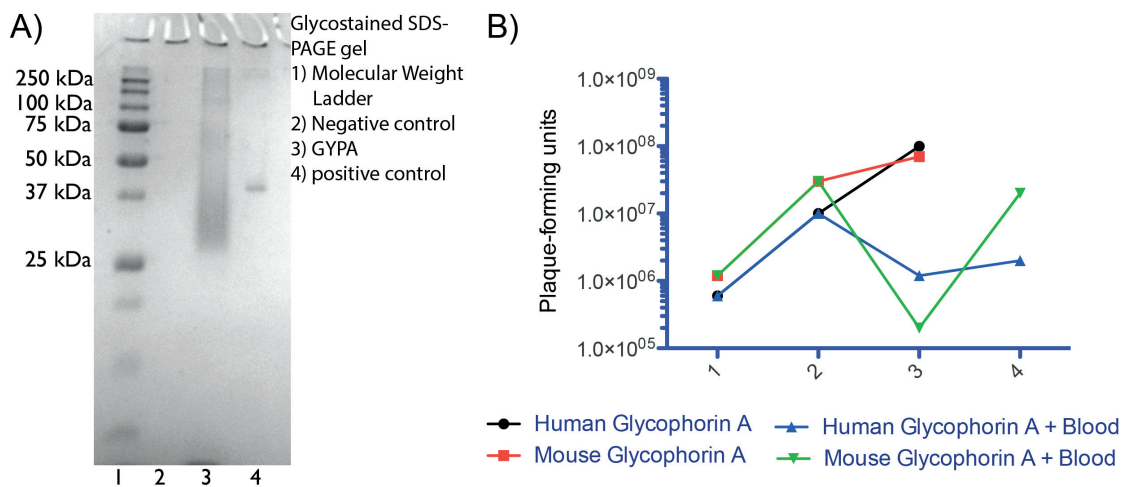


Figure 2.1 – A) Chemically isolated mouse GYPA on a glycostained SDS-PAGE gel. B) Phage titers for 3 rounds of screening against mouse and human glycophorin A and 2 rounds of panning against human and mouse glycophorin A followed by two rounds against human and mouse erythrocytes.

After 2 rounds of panning against human glycophorin A one sequence (hA3) made up 28% of all the sequences after two rounds and 60% after 3 rounds. The same sequence can also be seen in the display against mouse glycophorin A, where after 2 rounds it takes up 44% of the sequences and 30% of the sequences after 3 rounds of panning. Another sequence (mE2) made up another 30% of the sequences after 3 rounds of panning against mouse sequences. Both

Chapter 2. Searching new Binders to Erythrocytes by Phage Display

these sequences were tested for their ability to bind glycophorin A by phage-ELISA against human and mouse glycophorin A. hA3 was found to bind mouse and human glycophorin A and sequence mE2 bound to Mouse glycophorin A by phage-ELISA. However neither of the specific phage clones for these sequences (mE2,hA3) bound to human or mouse erythrocytes measured by flow cytometry.

Round	Species	Identifier	Percentage	CDR-H1	CDR-H2	CDR-H3
2	Human	hA3	28	DMFNDDDDMG	TISTSSGSTYYADSV	GELSVLGQSAQAYINF
3	Human	hA3	60	DMFNDDDDMG	TISTSSGSTYYADSV	GELSVLGQSAQAYINF
2	Mouse	hA3	44	DMFNDDDDMG	TISTSSGSTYYADSV	GELSVLGQSAQAYINF
3	Mouse	hA3	30	DMFNDDDDMG	TISTSSGSTYYADSV	GELSVLGQSAQAYINF
3	Mouse	mE2	30	VSITAESMS	TITMRDGGSTYYADSV	ARAMYPLRSSQLES

Table 2.1 – Complementarity determining regions of the domain Antibodies found more than once in a given round of screening against human or mouse glycophorin A

2.3.2 Screening against Mouse and Human Erythrocytes after Glycophorin A Screen

After two rounds of screening against human or mouse glycophorin A the obtained phage libraries were panned against human respectively mouse erythrocytes for two rounds. The phage titers dropped sharply after the first round of screening against the erythrocytes compared to the former second round of screening against glycophorin A (fig. 2.1). The drop for the screening against mouse glycophorin A was larger. The subsequent round saw phage titers rising for the screens against human as well as against mouse erythrocytes, though the one against mouse rose higher.

Round	Species	Identifier	Percentage	CDR-H1	CDR-H2	CDR-H3
1	Human	hA3	5	DMFNDDDDMG	TISTSSGSTYYADSV	GELSVLGQSAQAYINF
1	Human	hG6	23	DMLTPENMG	SIPAPSGSTYYADSV	GWGYSWGRLLYSHPLWY
1	Human	hE12	8	FMVIYQYMG	SAIHGASGSTYYADSV	AFYIGEWSGHNTFGY
2	Human	hC3	5	FMITDEYMT	GIVDDDGSTYYADSV	SEVWCDCCKDVSY
2	Human	hG6	25	DMLTPENMG	SIPAPSGSTYYADSV	GWGYSWGRLLYSHPLWY
2	Human	hA11	5	DRVTDYDMG	SILIPNGSTYYADSV	SGQWACGGWDGLYSPIDF
1	Mouse	hA3	9	DMFNDDDDMG	TISTSSGSTYYADSV	GELSVLGQSAQAYINF
1	Mouse	mC10	25	DMLTPENMG	SIPAPSGSTYYADSV	GWGYSWGRLLYSHPLWY
2	Mouse	mC10	31	DMLTPENMG	SIPAPSGSTYYADSV	GWGYSWGRLLYSHPLWY

Table 2.2 – Complementarity determining regions of the domain Antibodies found more than once in a given round of screening against human or mouse erythrocytes after two rounds of screening against human or mouse glycophorin A

Both rounds were sequenced, and the complementarity determining regions are shown in table 2.2 for sequences appearing more than once per round. The dominant sequence from screening against glycophorin A, hA3, was found in the first round of selection against human or mouse erythrocytes but disappeared in the second round. The sequence hG6 makes up 23% respectively 25% in the first and second round of screening against human erythrocytes. In the first and second round of screening against mouse glycophorin A the sequence mC12 made up 25% respectively 31%. All the clones shown in table 2.2 were expressed on a phage

level and tested for binding against human or mouse erythrocytes by flow cytometry, but no binding could be observed.

2.3.3 Screening against Mouse, Monkey and Human Erythrocytes

The library was screened for 2 rounds against monkey erythrocytes, 3 rounds against mouse erythrocytes and 4 rounds against human erythrocytes. The endpoints of the screens were based on the rise of the phage titers after panning and sequence conversion. The screen against monkey erythrocytes was stopped after two rounds because of the high sequence conversion (complete sequencing is shown in appendix A.13). On the other hand the human phage display was continued for four rounds because phage titers did not rise after 2nd 3rd or 4th round. It was stopped after four rounds due to the high sequence conversion.

The complete sequencing for the last two rounds can be found in appendix A.8 and A.9 for the display against human erythrocytes, in appendix A.10 and A.11 for the display against mouse erythrocytes and in appendix A.12 and A.13 for the display against monkey erythrocytes. The complementarity determining regions are shown in table 2.3 for sequences appearing more than once in the last two rounds with the percentage the sequence makes up from the total obtained sequences per round. Sequences were tested for binding towards blood on the phage level and then expressed as proteins as described in [103] and tested for binding against erythrocytes.

Round	Species	Identifier	Percentage	CDR-H1	CDR-H2	CDR-H3
3	Human	mH10	32	VKFNAQDMG	AIHGTNGSTYYADSV	RRRRRTANFRY
3	Human	hE10	6	YMFSTQNMG	SIRMDNGSTYYADSV	HVKWLSRSHSHQVKY
4	Human	mH10	36	VKFNAQDMG	AIHGTNGSTYYADSV	RRRRRTANFRY
4	Human	mH8	10	DRVSYKFMA	SIRGNDGSTYYADSV	KGKRHYELPY
4	Human	hH4	12	DRVSYKFMA	TIKTKSGSTYYADSV	RGRESQTPVNYW
4	Human	hG1	5	DMISHEYMA	TIYTDDGSTYYADSV	QGQDDEPTVTS
2	Monkey	moG3	12	FRFSDNFMA	TIEAAGGSTYYADSV	SQPGSQKRLRY
2	Monkey	moC6	10	DNITYDYMA	TIQADDGSTYYADSV	LAQFRPSKLS
2	Monkey	moC09	8	DNITDKYMG	TISDDSGSTYYADSV	GRQGPTYKLTS
2	Monkey	moE03	3.5	DSFSNEYMT	TISDQDGSTYYADSV	RWRVATKQITF
2	Mouse	mH8	5	DRVSYKFMA	SIRGNDGSTYYADSV	KGKRHYELPY
2	Mouse	mF10	3.5	DRFNSKNMA	SINNQDGSTYYADSV	RHRMSSAIKY
2	Mouse	mH10	5	VKFNAQDMG	AIHGTNGSTYYADSV	RRRRRTANFRY
3	Mouse	mH8	25	DRVSYKFMA	SIRGNDGSTYYADSV	KGKRHYELPY
3	Mouse	mA3	3.5	DTFIHQDMG	GIREHDGSTYYADSV	SVGAPPYHMYS
3	Mouse	mB3	3.5	FRLIAQFMG	TINIKGGSTYYADSV	GIPSYQSEFQS
3	Mouse	mA10	3.5	VRIIDDVMA	TIHMPNGSTYYADSV	PLQTGTGRMYDFPTALGF

Table 2.3 – Complementarity determining regions of the domain Antibodies found more than once in a given round of screening against human, mouse or monkey erythrocytes

Sequence mH10 was found in 32 % and 36 % of the 3rd respectively 4th round panning against human erythrocytes and with 5 % in the second round against mouse erythrocytes. The sequence was tested for binding against mouse and human erythrocyte. While weak binding against human erythrocytes could be observed, the human domain antibody could

Chapter 2. Searching new Binders to Erythrocytes by Phage Display

not be expressed in the *e. coli* expression system. The sequence hE10 accounted for 6 % of the sequences in the 3rd round against human erythrocytes but no binding to erythrocytes could be detected on a phage level by flow cytometry and the corresponding human domain antibody could not be expressed. Sequence mH8 was found in the 2nd and 3rd round of display against mouse erythrocytes with 5 % and 25 %, it was further found in the 4th round against human erythrocytes (10 %). The sequence showed strong binding on a phage level towards blood and the human domain antibody was expressed. On the protein level the antibody was shown to bind human and mouse CD45+ blood cells by flow cytometry. hH4 made up 12% of total sequences in the 4th round of panning against human erythrocytes. The sequence showed weak binding to human erythrocytes on a phage level, but no binding could be observed on the protein level. Sequence hG1 was found in the fourth round of screening against human erythrocytes (5 %). It showed strong binding on the phage level, but expressed as protein no binding towards erythrocytes or any other blood cells could be found.

The sequences mF10 and mA10 were found in the second respectively third round panning against mouse erythrocytes (both 3.5 %) and showed weak binding towards mouse blood on a phage level. The corresponding human domain antibodies were expressed and found to bind CD 45+ mouse blood cells. mA3 was found in the 3rd round of screening against mouse erythrocytes (3.5 %) and showed no interaction with mouse blood cells on a phage level. The corresponding human domain antibody could not be expressed. Sequence mB3 was found in the third round of screening against mouse erythrocytes (3.5 %) and showed binding towards mouse erythrocytes on a phage level but not on a protein level.

All the monkey sequences showing up more than once were found to bind monkey erythrocytes by flow cytometry (Appendix A.14). Sequence monE3 and monC9 were expressed in *e. coli* and binding to red blood cells was measured by flow cytometry. For monC9 a K_d of 167 nM was measured and for monE3 a K_d of ca. 400 nM was measured.

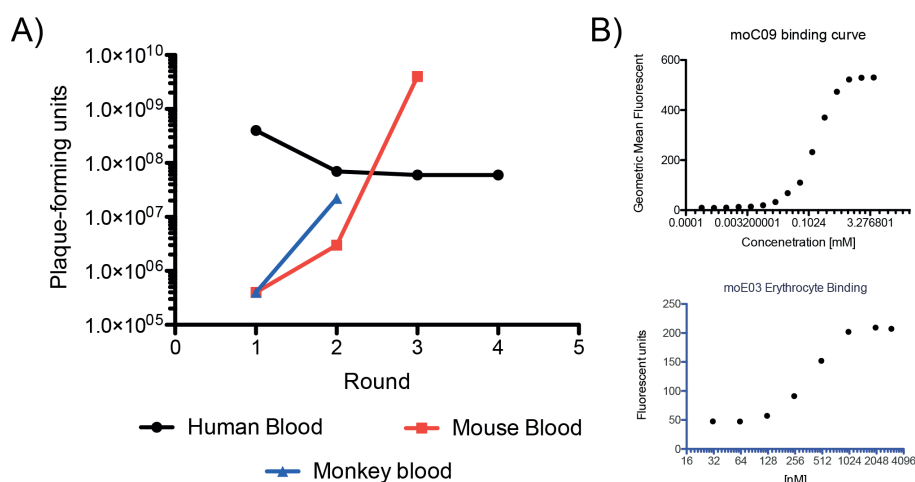


Figure 2.2 – A) Phage titers for panning of 2 rounds against monkey erythrocytes, 3 rounds against mouse erythrocytes and 4 rounds against human erythrocyte. B.) Binding of the human domain antibodies monC9 and monE3 against monkey erythrocytes by flow cytometry.

2.4 Discussion

Even though glycoporphin A has a large extracellular part (amino acids 1-108 of 168) [3, 45, 64], by screening against human and mouse glycoporphin A on magnetic beads only binders against the transmembrane (amino acids 109-131 of 168) or the cytoplasmic region (amino acids 132-168 of 168) were found. This was shown by the capability of the clones obtained through sequencing to bind human and mouse glycoporphin A by phage ELISA but not on erythrocytes measured by flow cytometry.

To amplify sequences that bind against the extracellular part of glycoporphin A, the library was screened against human and mouse erythrocytes after two rounds of screening against human respectively mouse glycoporphin A. The clones identified from this screening were tested for binding against human or mouse blood on a phage level and no binding was observed.

The library was then screened against mouse, human and monkey erythrocytes. While on the phage level a domain antibody clone for all the species was found to bind blood, some of those were shown to bind CD45+ positive blood cells, while others lost its binding capacity, when expressed as a protein. Remarkably, the four domain antibodies found against monkey erythrocytes all bound on a phage level and binding curves for two was measured on a protein level. The affinity was relatively high with a K_d of 167 nM and ca. 400 nM.

It's not clear why clones against monkey erythrocytes could be found after just 2 rounds, while no functional domain antibodies against mouse or human erythrocytes could be found after 3, respectively 4 rounds of panning, as all the screens followed the exact same protocol. Further non of the clones against monkey erythrocyte showed binding to CD45+ cells in blood, even though the same approach was used to isolate erythrocytes from blood in all screens. It could be that negative fluorescent sorting by flow cytometry of erythrocytes from blood would lead to better results compared to the isolation with Percoll used in this protocol. Purer erythrocytes may lead to successful phage display, because a considerable part of the domain antibody repertoire present after the 2nd and 3rd round of panning against mouse erythrocytes and the 4th round against human erythrocytes was shown to bind to CD45+ cells in blood.

3 Tolerance Induction by Antigens Bearing Synthetic Glycosylations

3.1 Introduction

3.1.1 Liver Targeting for Tolerance Induction by Synthetic Antigen Glycosylation

The liver represents an interesting organ to target for introducing tolerance towards foreign or partly foreign proteins as it has been shown extensively to induce and maintain tolerance towards auto- and food-derived antigens [20, 75, 113]. Its tolerogenic effect is attributed to the hepatic antigen presenting cells such as dendritic cells (DC's), liver sinusoidal endothelial cells (LSECs), Kupffer cells (KCs), and hepatocytes [27, 47, 75]. The liver microenvironment contains anti-inflammatory cytokines which are secreted by the hepatic antigen presenting cells [65, 66]. These cells further express the inhibitory molecule PD-L1 [46, 94, 123]. This leads to a tolerogenic milieu that induces anergy, deletion or the induction of regulatory T-cells in CD4+ and CD8+ T-cells by antigen presentation by hepatic antigen presenting cells on the major histocompatibility complex I and II [15, 114].

Synthetic polymers were developed by Dr. David Scott Wilson and synthesized by reversible addition-fragmentation chain-transfer (RAFT) polymerization. The polymers are composed of random co-polymers of monomers bearing either β -linked *N*-Acetylgalactosamine (pGal) or β -linked *N*-Acetylglucosamine (pGlu) or α -linked *N*-Acetylmannosamine (pMan) residues and a biologically inert co-monomer (fig. 3.1 A). The polymers are attached via a reduction sensitive self-immolating linker, that after uptake into the cell undergoes disulfide reduction and releases the antigen from the polymer into its native form. The rationale behind the polymer lies in targeting C-type lectin receptors expressed by hepatic antigen presenting cells [11, 21]. These receptors can play a role in clearing apoptotic cell debris and maintaining tolerance to self [16]. Apoptosis increases desialylation of *N*-Acetylgalactosamine (pGal) [49] and the release of intracellular proteins bearing *N*-Acetylglucosamine (pGlu) [24], which are then taken up by hepatic antigen presenting cells via C-type lectins [4, 16].

3.1.2 Antigen Specific Tolerance Induction in CD4+ and CD8+ T-cells by Synthetic Glycosylated Ovalbumin

Wilson et al. (unpublished data) showed that ovalbumin conjugated to pGlu and pGal leads to a significant greater hepatic load when injected intra venous (i.v.). C57BL/6 mice were injected i.v. with fluorescent labeled pGlu-ovalbumin and pGal-ovalbumin. After 3 hours the hepatic antigen presenting cells were analyzed by flow cytometry. Increased uptake of pGal-ovalbumin was observed in hepatocytes and liver sinusoidal endothelial cells (LSECs) and pGlu-ovalbumin showed increased uptake in dendritic cells, kuppfer cells, hepatocytes and liver sinusoidal endothelial cells (fig. 3.1 B, C). Although the same percentage of LSECs is targeted by all constructs, the amount of antigen, identified by the mean fluorescence of the LSECs, is significantly higher for pGal- and pGlu-ovalbumin compared to ovalbumin and pGlu-ovalbumin leads to significant higher uptake in LSECs than pGal-ovalbumin.

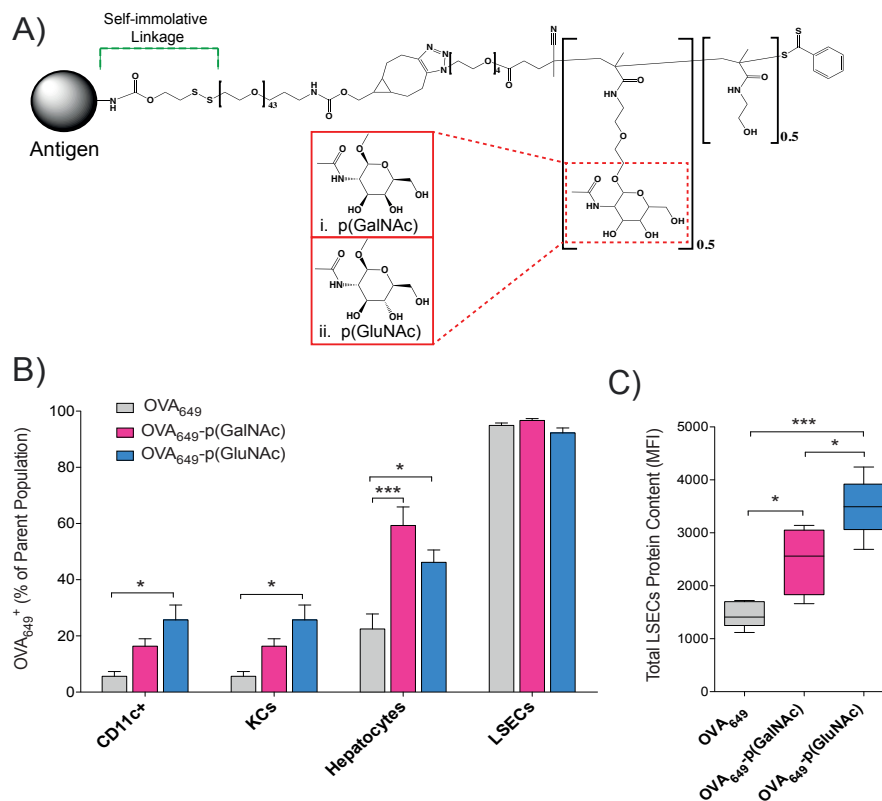


Figure 3.1 – A) Structure of pGlu- and pGal-ovalbumin. B) Uptake of pGal- and pGlu-Ovalbumin compared to Ovalbumin as percentage of parent in hepatocytes, DCs, KCs and LSECs. C) Uptake of pGal- and pGlu-Ovalbumin compared to Ovalbumin in LSECs by mean fluorescence. Unpublished, data provided by Dr. David Scott Wilson.

Using the OTI and OTII transfer model Dr. Wilson showed that treatment with ovalbumin-glycopolymer leads to the induction of antigen specific T-cell tolerance in CD8+ and CD4+ T-cells. Following transfer with OTI and OTII cells they were treated with either saline, 10 μ g

of ovalbumin, 10 μg of pGlu-ovalbumin or 10 μg of pGal-ovalbumin (fig. 3.2 A) at day 1 and day 7. 9 days later the mice were challenged via an intra dermal (i.d.) injection of OVA and lipopolysaccharide (LPS), 5 days later the mice were sacrificed. Fewer OTI and OTII cells were found in the draining lymph nodes of mice treated with pGlu- or pGal-ovalbumin compared to mice receiving ovalbumin (fig. 3.2 B). Further a lower percentage of OTI and OTII cells treated with pGlu- or pGal-ovalbumin produced IFN γ upon restimulation (fig 3.2 C, D), demonstrating tolerance towards ovalbumin. Finally, mice treated with pGlu- or pGal-ovalbumin showed significantly higher percentage of OTII regulatory cells in the draining lymph nodes (fig. 3.2 E) and the spleen (fig. 3.2 F) compared to mice receiving OVA or saline.

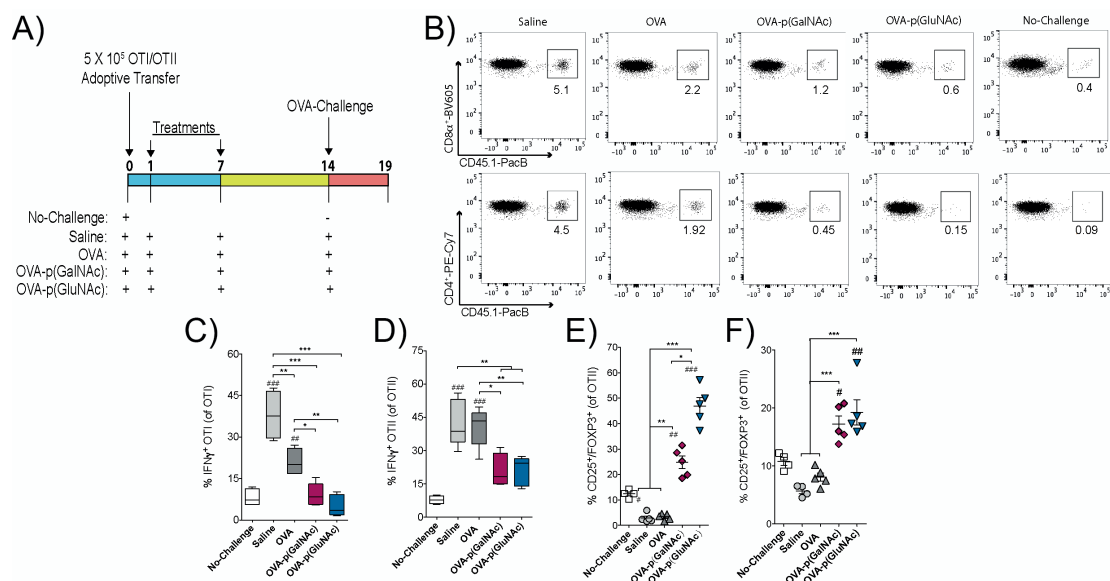


Figure 3.2 – A) Treatment schedule for all the groups. B) OTI and OTII cell expansion or deletion after challenge in the draining lymph nodes by flow cytometry. C) Percentage of OTI cells from the draining lymph nodes producing IFN γ upon restimulation. D) Percentage of OTI cells from the draining lymph nodes producing IFN γ upon restimulation. E) Percentage of regulatory T-cells of OTII cell in the draining lymph node. E) Percentage of regulatory T-cells of OTII cell in the draining lymph node. Unpublished, data provided by Dr. David Scott Wilson.

Dr. Wilson then showed that antigens modified with synthetic glycosylations induce endogenous functional regulatory T-cells which are necessary in maintaining tolerance. Mice were treated with three injections of either saline, 5 μg of ovalbumin or 5 μg of pGlu-ovalbumin at days 1,4 and 7. Half of the mice treated with pGlu-ovalbumin received a single intraperitoneal injection of 400 μg anti-CD25 antibody to reduce the regulatory T-cell compartment. On day 29 all mice received an adoptive transfer of OTI and OTII cells. All mice were challenged the following day with ovalbumin LPS i.d. (fig. 3.3 A). Five days after challenge the ovalbumin specific immune response in the draining lymph nodes was assessed via flow cytometry.

Chapter 3. Tolerance Induction by Antigens Bearing Synthetic Glycosylations

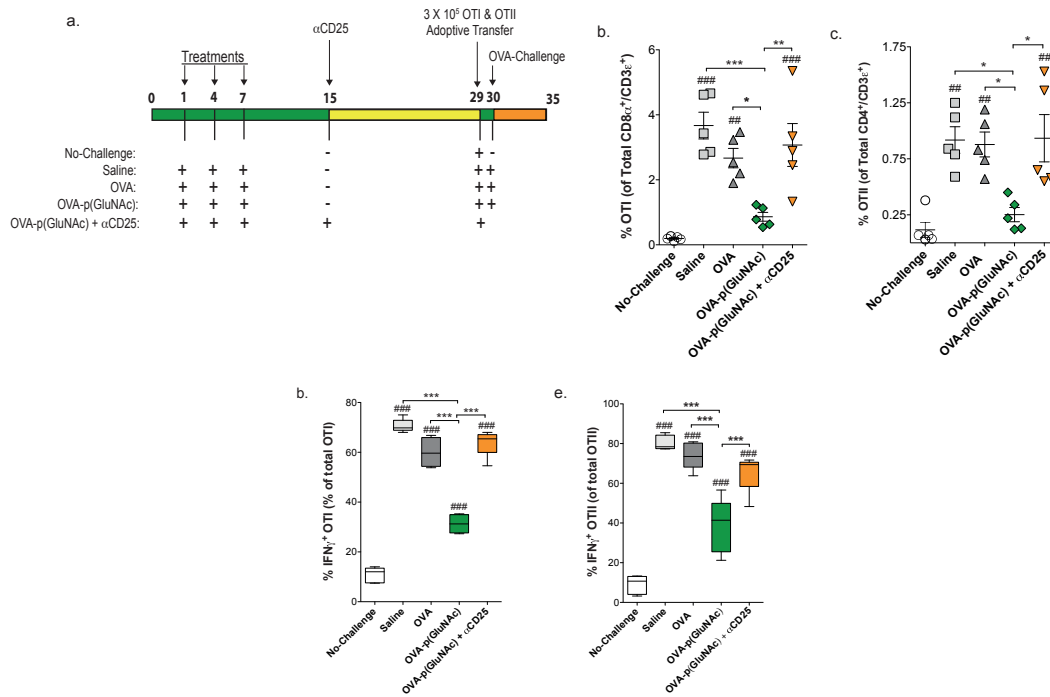


Figure 3.3 – A) Treatment schedule for all the groups. B) Percentage of OTI cells from total CD8+ T-cells B) Percentage of OTII cells from total CD8+ T-cells C) Percentage of IFN γ producing OTI cell. E) Percentage of IFN γ producing OTII cell. Unpublished, data provided by Dr. David Scott Wilson.

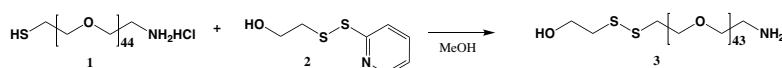
Mice treated with pGlu-ovalbumin significantly reduced the OTI and OTII cells in the draining lymph nodes compared to mice treated with ovalbumin or pGlu-ovalbumin and then anti-CD25 antibody (fig. 3.3 B, C), while mice treated with pGlu-ovalbumin and then anti-CD25 antibody had the same amount of OTI and OTII cells in the draining lymph nodes as saline or ovalbumin treated mice. Lymphocytes from the draining lymph node were restimulated with the immunodominant CD8 peptide. A lower percentage of OTI and OTII cells expressed IFN γ when treated with pGlu-ovalbumin than the ones treated with ovalbumin or pGlu-ovalbumin and then anti CD25 antibody. These results show that antigen modification with synthetic glyco polymers induce tolerance by CD4+ and CD8+ T-cell deletion and further induce regulatory T-cells which critically involved in maintaining tolerance.

3.2 Materials and Methods

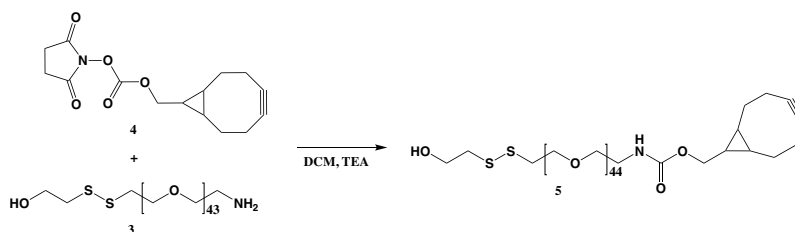
3.2.1 Chemical Synthesis

The following chemical synthesis protocol has been developed and was kindly provided by Dr. David Scott Wilson

All reactions were performed under an atmosphere of nitrogen, unless otherwise stated. Unless otherwise stated, chemicals were purchased from Sigma-Aldrich

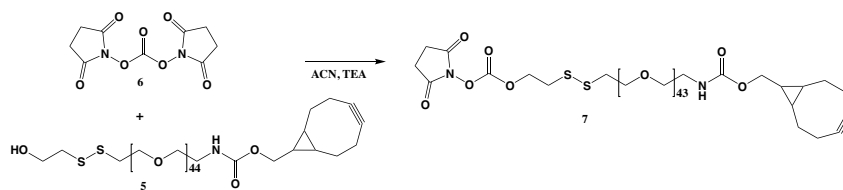


Ethanol disulfaneyl polyethylene glycol amine (3). A solution of thiol polyethylene glycol amine HCl 1 (JenKem Technology USA) (1.0 g, 0.5 mmol) in dichloromethane (DCM) (5ml) was added dropwise to a stirred solution of 2-(2-pyridinyldithio)ethanol 2 (467.5 mg, 2.5mmol) in methanol (MeOH) (3ml). The solution was stirred at room temperature for 10 h then approximately half the solvent was removed via rotary evaporation. The remaining crude product was then decanted into ice cold hexanes (40 ml) and placed at -20°C for 4 h. The precipitate and solvent mixture was centrifuged at 2000g for 3 min. The solvent was then decanted and excess solvent was removed from the pelleted precipitate under reduced pressure. The crude product was then used in the next step without further purification (65% crude yield).

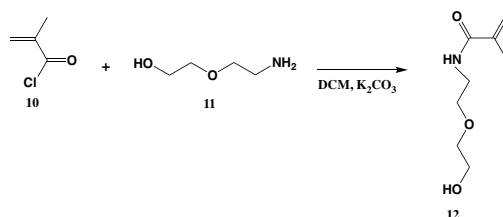


Ethanol disulfaneyl polyethylene glycol (1R,8S,9s)-Bicyclo[6.1.0]non-4-yn-9-ylmethyl carbamate (5). A solution of (1R,8S,9s)-Bicyclo[6.1.0]non-4-yn-9-ylmethyl N-succinimidyl carbonate 4 (90 mg, 0.30 mmol) in DCM (0.5 ml) was added dropwise to an ice-cooled stirred solution of ethanol disulfaneyl polyethylene glycol amine 3 (0.5 g, 0.24 mmol) and trimethylamine (48 mg, .48 mmol) in DCM (5 ml). After the addition of 4, the reaction was allowed to come to room temperature and stirred for another 6h. The reaction mixture was then poured into ice-cold hexanes (40 ml) and placed at -20°C for 4 h. The precipitate and solvent mixture was centrifuged at 2000g for 3 min. The solvent was then decanted and excess solvent was removed from the pelleted precipitate under reduced pressure. The crude product was then used in the next step without further purification (75% crude yield).

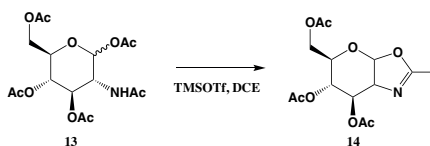
Chapter 3. Tolerance Induction by Antigens Bearing Synthetic Glycosylations



N-succinimidyl carboamate Ethanol disulfaneyl polyethylene glycol (1R,8S,9s) - Bicyclo [6.1.0] non-4-yn-9-ylmethyl carbamate (Self-immolative Linker) (7). A solution of Ethanol disulfaneyl polyethylene glycol (1R,8S,9s)-Bicyclo[6.1.0]non-4-yn-9-ylmethyl carbamate 5 (300 mg, 0.13 mmol) in anhydrous acetonitrile (ACN) (1.5 ml) was added drop wise to a stirred solution of *N,N'*-Disuccinimidyl carbonate 6 (0.5 g, 0.24 mmol) and trimethylamine (48 mg, .48 mmol) in anhydrous ACN (5 ml). The reaction mixture was stirred overnight and was then poured into ice-cold hexanes (40 ml) and placed at -20°C for 4 h. The precipitate and solvent mixture was centrifuged at 2000g for 3 min. The solvent was then decanted and excess solvent was removed from the pelleted precipitate under reduced pressure. The crude product was purified via silica gel flash chromatography DCM:MeOH (85:15) (yield: 43%, 129mg)



N-[2-(2-Hydroxyethoxy)ethyl]methacrylamide (12). To 200 ml of an ice-cold solution of 2-(2-aminoethoxy ethanol) 11 (24 ml, 240 mmol) and potassium carbonate (15g) in DCM was slowly added a solution of methacryloyl chloride 10 (24 ml, 250 mmol) in DCM (50ml). The reaction was allowed to come to room temperature and stirred for another 4 h. After 4h the reaction mixture was filtered through celite and the solvent was removed via rotary evaporation. The crude product was loaded onto silica gel and purified via flash chromatography, Ethyl Acetate (EtOAc):Hexanes (90:10), to give 12 as a colorless oil. (Yield: 72%) ¹H NMR: (400 MHz, CDCl₃-d₆): δ (ppm), 6.53 (s, 1H); 5.66 (m, 1H); 5.29 (m, 1H); 3.71 (s, 2H); 3.56 (m, 4H); 3.48 (m, 2H); 1.91 (m, 3H). ¹³C NMR: (75 MHz, CDCl₃-d₆): δ(ppm), 169.34; 141.72; 120.37; 72.43; 69.82; 61.63; 39.81; 18.86. MS *m/z*: [M + H]⁺ 174.11.



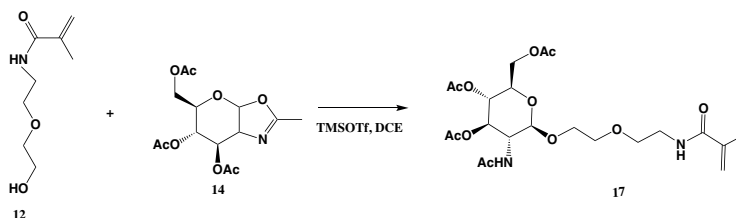
2-Methyl-(3,4,6-tri-O-acetyl-1,2-dideoxy-α-D-glucopyrano)[1,2-d]-1,3-oxazoline (14). D-glucosamine penta-acetate 13 (10g, 25.6mmol) was dissolved in dichloroethane (DCE) (150

3.2. Materials and Methods

mL). Then trimethylsilyl trifluoromethanesulfonate (TMSOTf) (5.5 ml, 30 mmol) was added, and the mixture was stirred at 50°C for 1h. The mixture was then removed from the heat and stirred for 16h. Triethylamine(2ml) was added to the mixture at room temperature. The mixture was then stirred for 10 min then the solvent was removed via rotary evaporation. The crude material was loaded onto silica gel and purified via flash chromatography, EtOAc (100) to give 14 as a pink oil (Yield: 61%). ¹H NMR: (400 MHz, CDCl₃-d₆): δ (ppm), 5.86 (d, J=7.4 Hz, 1H, H-4); 5.22 (t, J=2.1 Hz, 1H, H-5); 4.87 (d, J=9.3 Hz, 1H, H-4); 4.12-4.05 (m, 3H, H-2, H-6, H-6'); 3.54-3.57 (m, 1H, H-3); 2.06 (s, 3H); 2.03 (s, 6H); 2.01 (s, 3H). ¹³C NMR: (125 MHz, CDCl₃-d₆): δ (ppm), 170.41; 169.55; 169.18; 166.34; 99.27; 70.04; 68.17; 67.43, 64.98, 63.12, 20.55, 20.34, 20.42, 13.91. MS *m/z*: [M + H]⁺ 330.12.



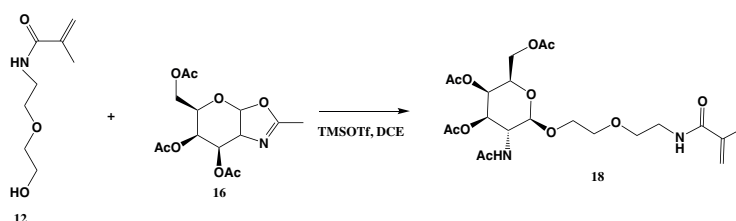
2-Methyl-(3,4,6-tri-O-acetyl-1,2-dideoxy- α -D-galactopyrano)[1,2-*d*]-1,3-oxazoline (16). D-galactosamine penta-acetate 15 (2.0g, 5.15 mmol) was dissolved in dichloroethane (DCE) (20 mL). Then trimethylsilyl trifluoromethanesulfonate (TMSOTf) (1 ml, 5.53 mmol) was added, and the mixture was stirred at 50°C for 9h. The mixture was then removed from the heat and stirred for 7h. Triethylamine(2ml) was added to the mixture at room temperature. The mixture was then washed with a saturated solution of NaHCO₃ and then dried with sodium sulfate. The organic phase was then filtered and the solvent was removed via rotary evaporation and the residue was loaded onto silica gel. The product was purified via column chromatography on silica gel with EtOAc (100) to yield 16 as a yellow viscous solid. (Yield: 64%) ¹H NMR: (400 MHz, CDCl₃-d₆): δ (ppm), 5.97 (d, J=6.9 Hz, 1H, H-4); 5.45 (t, J=3.0 Hz, 1H, H-5); 4.92 (dd, J=7.6 Hz, 3.4 Hz, 1H, H-4); 4.26 (td, J=6.7 Hz, 2.8 Hz, 1H); 4.25-4.13 (m, 1H, H-3); 3.99 (s, 1H); 2.13 (s, 3H); 2.07 (s, 6H); 2.05 (s, 3H). ¹³C NMR: (125 MHz, DMSO-d₆): δ (ppm), 170.0; 169.55; 168.11; 165.21; 100.9; 70.66; 68.2; 65.02, 63.00, 61.8, 20.5, 20.44, 20.42, 13.91. MS *m/z*: [M + H]⁺ 330.12.



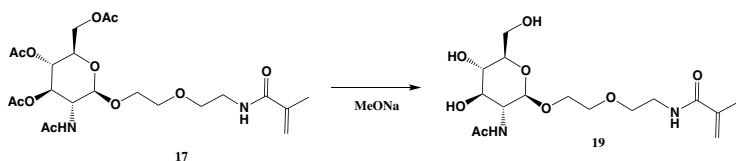
2-(2-Hydroxyethoxy)ethyl methacrylamide-2-acetamido-3,4,6-tri-O-acetyl-2-deoxy- α -D-galucopyranoside (17). A flask was charged with compound 14 (2.0g, 6.0mmol), 12 (1.1g, 6.6mmol), 4 A molecular sieves (2.5g), and DCE (20 ml). The solution was stirred for 30 min. TMSOTf (464 μ L, 2.6 mmol) was added and the mixture was stirred at room temperature for 19

Chapter 3. Tolerance Induction by Antigens Bearing Synthetic Glycosylations

h, then TMSOTf (464L, 2.6 mmol) was added again and the reaction was allowed to stir for an additional 8 h. Triethylamine was then added to the reaction and the reaction was stirred for another 1 h. The solvents were removed via rotary evaporation and the crude product was loaded onto silica gel and purified via column chromatography, hexane: EtOAc (80:20), to yield 17 as a viscous solid (Yield: 51%).¹H NMR: (500 MHz, CD₃OD): δ (ppm), 5.7 (s, 1H), 5.45 (s, 1H), 4.97 (dd, J = 10.5, 10.5 Hz, 1H), 4.65 (d, J = 8.5 Hz, 1H), 4.32 (d, J = 8.5 Hz, 1H), 4.27 (dd, J = 5.0, 10.5 Hz, 1H), 4.17-3.69 (m, 6H), 2.01 (s, 3H), 1.99 (s, 3H), 1.97 (s, 3H), 1.89 (s X 2, 6H). MS *m/z*: [M + H]⁺ 503.31.



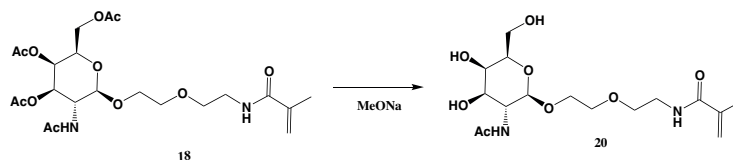
2-(2-Hydroxyethoxy)ethyl methacrylamide-2-acetamido-3,4,6-tri-O-acetyl-2-deoxy- α -D-galactopyranoside (18). A flask was charged with compound 16 (2.0g, 6.0mmol), 2-(2-Aminoethoxyethanol) methacrylamide 12 (1.1g, 6.6mmol), 4 Å molecular sieves (2.5g), and DCE (20 ml). The solution was stirred for 30 min. TMSOTf (464 μ L, 2.6 mmol) was added and the mixture was stirred at room temperature for 19 h, then TMSOTf (464L, 2.6 mmol) was added again and the reaction was allowed to stir for an additional 8 h. Triethylamine was then added to the reaction and the reaction was stirred for another 10 min. The solvents were removed via rotary evaporation and the crude product was loaded onto silica gel and purified via column chromatography, hexanes: EtOAc (80:20), to yield 18 as a viscous solid (Yield: 43%).¹H NMR: (500 MHz, CD₃OD): δ (ppm), 5.72 (s, 1H), 5.35 (s, 1H), 4.67 (m, 1H), 4.65 (m, 1H), 4.32 (d, J = 8.5 Hz, 1H), 4.27 (dd, J = 5.0, 10.5 Hz, 1H), 4.17-3.69 (m, 6H), 2.01 (s, 3H), 1.99 (s, 3H), 1.97 (s, 3H), 1.89 (s X 2, 6H). MS *m/z*: [M + H]⁺ 503.22.



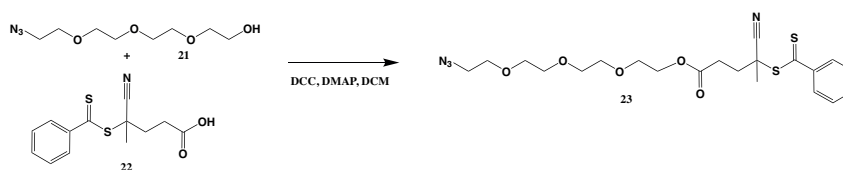
2-(2-ethoxy)ethyl methacrylamide 2-acetamido-2-deoxy- β -D-glucopyranoside (19). Compound 17 (2.0g, 3.98mmol) was dissolved in 10 ml of MeOH and stirred at room temperature. Sodium methoxide (4 mmol) was added to the reaction and the reaction was stirred at room temperature. After 6 h, the solution was neutralized with Amberlite IR120 and then filtered. The solvent was removed via rotary evaporation and loaded on to silica gel. The products was purified via column chromatography using DCM:MeOH (83:17) to give 19 as a clear solid.¹H NMR: (400 MHz, D₂O): δ (ppm), 5.7 (s, 1H), 5.45 (s, 1H), 4.44 (d, J = 8.5Hz, 1H), 3.83-3.66 (m, 5H), 3.60-3.36 (m, 6H), 2.01 (s, 3H), 1.91 (s, 3H). ¹³C NMR: (125 MHz, D₂O): δ (ppm), 176.2;

3.2. Materials and Methods

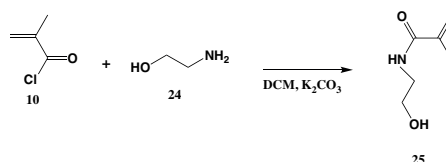
169.34; 141.72; 120.37; 103.0; 76.5; 72.43; 72.5; 69.82; 69.3; 61.63; 62.4; 53.9; 39.81; 18.86; 11.0. MS m/z : $[M + H]^+$ 377.18.



2-(2-ethoxy)ethyl methacrylamide 2-acetamido-2-deoxy- β -D-galactopyranoside (20). Compound 18 (2.0g, 3.98mmol) was dissolved in 10 ml of MeOH and stirred at room temperature. Sodium methoxide (4 mmol) was added to the reaction and the reaction was stirred at room temperature. After 6 h, the solution was neutralized with Amberlite IR120 and then filtered. The solvent was removed via rotary evaporation and loaded on to silica gel. The products was purified via column chromatography using DCM:MeOH (83:17) to give 20 as a clear solid. (Yield: 78%) ^1H NMR: (400 MHz, D_2O): δ (ppm), 5.69 (s, 1H), 5.44 (s, 1H), 4.46 (d, $J = 8.5$ Hz, 1H), 3.92 (d, $J = 3.2$ Hz, 1H), 3.90-3.63 (m, 10H), 3.45 ($J = 10.1$ Hz, $J = 6.5$ Hz), 2.01 (s, 3H), 1.91 (s, 3H). ^{13}C NMR: (125 MHz, D_2O): δ (ppm), 176.2; 169.34; 141.72; 120.37; 103.0; 76.5; 73.6; 72.43; 72.5; 69.82; 69.3; 61.63; 62.4; 53.9; 39.81; 23.5; 18.86; 11.0. MS m/z : $[M + H]^+$ 377.19.



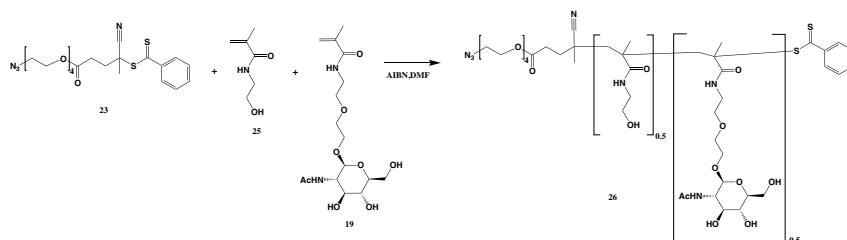
N3TEG-RAFT (23) Azido-tetraethylene glycol 21 (219g, 1.0mmol), DMAP (12 mg, 0.1mmol) and RAFT agent 22 (279.0mg, 1.0mmol) were added to 10 ml of DCM and stirred on ice for 30 min. A solution of DCC (206 mg, 1.0mmol) in DCM was added dropwise to the reaction mixture. The reaction mixture was allowed to come to room temperature and stirred for another 3 hours. The reaction was filtered and the solvent was removed via rotary evaporation. The product was loaded onto silica gel and separated via column chromatography using EtOAc to yield 23 as a pink liquid. (Yield: 23%) ^1H NMR: (400 MHz, CDCl_3-d_6): δ (ppm), 7.76(m, 2H), 7.43 (m,1H), 7.28 (m, 2H), 4.11 (m, 2H), 3.57 (m, 2H), 3.51 (m, 12H), 3.23(m, 2H), 2.75-2.45 (m, 4H), 1.79 (s, 3H). ^{13}C NMR: (125 MHz, CDCl_3-d_6): δ (ppm), 221.2; 171.34; 144.72; 135.37; 129.0; 126.5; 119.6; 68.43; 65.5; 44.82; 31.3; 29.64; 24.5; 12.4. MS m/z : $[M + H]^+$ 481.17.



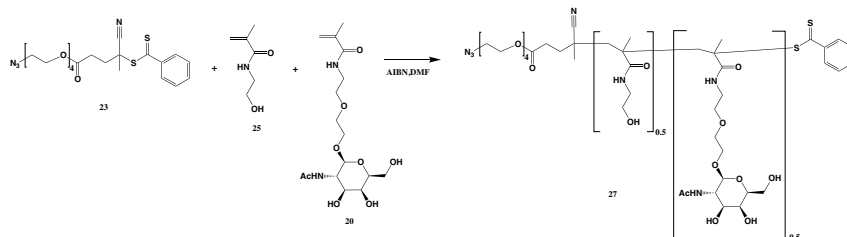
N-(2-Hydroxyethyl) methacrylamide (25). To 200 ml of an ice-cold solution of ethanolamine

Chapter 3. Tolerance Induction by Antigens Bearing Synthetic Glycosylations

24 (12 ml) and potassium carbonate (15g) in DCM was slowly added a solution of methacryloyl chloride 10 (9 ml) in DCM (50ml). The reaction was allowed to come to room temperature and stirred for another 4 h. After 4h the reaction mixture was filtered through celite and the solvent was removed via rotary evaporation. The crude product was loaded onto silica gel and purified via flash chromatography, Ethyl Acetate (EtOAc):Hexanes (90:10), to give 25 as a colorless oil. (Yield: 75%) $^1\text{H NMR}$: (400 MHz, CDCl_3-d_6): δ (ppm) 6.87 (m, 1H), 5.7 (m, 1H), 5.3 (m, 1H), 4.29 (s, 1H), 3.66 (t, $J = 5.1$ Hz, 2H), 3.4 (dt, $J = 5.3, 5.1$ Hz, H2), 1.96 (s, H3). $^{13}\text{C NMR}$: (125 MHz, CDCl_3-d_6): δ (ppm), 166.5, 139.2, 120.1, 61.2, 42.3, 18.4. MS m/z : $[\text{M} + \text{H}] + 130.08$.



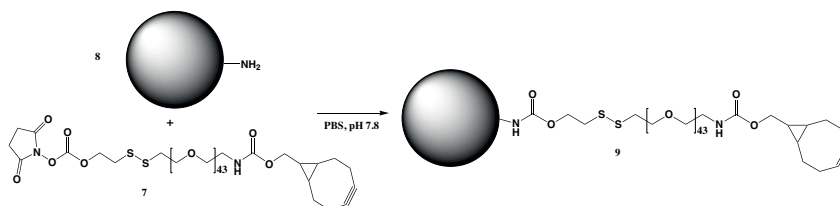
p(GluNAc) (26). Compound 25 (129mg, 1.0mmol), compound 19 (377mg, 1.0mmol), compound 23 (9.62mg, 0.02mmol), and AIBN (0.656mg, 0.004mmol) were added to dimethylformamide (DMF) (2.0 ml) were added to a schlenk flask and subjected to 4 freeze-thaw degassing cycles. The reaction mixture was then headed to 65°C for 12 h. After 12h 0.328 mg of AIBN were added to the reaction, and the mixture was allowed to stir at 65°C for another 8 h. The reaction mixture was then cooled to room temperature and then precipitated in acetone. The polymer product rapidly crashed out of the mixture and the solvent was decanted. Residual solvent was then removed from the product under vacuum.



p(GalNAc) (26). Compound 25 (129mg, 1.0mmol), compound 20 (377mg, 1.0mmol), compound 23 (9.62mg, 0.02mmol), and AIBN (0.656mg, 0.004mmol) were added to dimethylformamide (DMF) (2.0 ml) were added to a schlenk flask and subjected to 4 freeze-thaw degassing cycles. The reaction mixture was then headed to 65°C for 12 h. After 12h 0.328 mg of AIBN were added to the reaction, and the mixture was allowed to stir at 65°C for another 8 h. The reaction mixture was then cooled to room temperature and then precipitated in acetone. The polymer product rapidly crashed out of the mixture and the solvent was decanted. Residual solvent was then removed from the product under vacuum.

3.2.2 Protein Conjugation to Synthetic Polymeric *N* - Acetylglucosamine, *N* - Acetylgalactosesamine and *N* - Acetylmannosesamine

Asparaginase-immolative linker conjugate (9). Asparaginase (5 mg, 222.2 nmol) and self-immolative linker (10 molar equivalents of asparaginase) 7 were added to an endotoxin free tube. PBS pH 7.6 (200 L) was added to the tube and the tube was stirred at 6 h at room temperature. Unconjugated linker was then removed with zeba spin columns.



pGal-, pGlu- or pMan-asparaginase. Asparaginase self-immolative linker (5.0mg) was added to a solution of excess pGlu pGal or pMan polymer in PBS pH 7.4. The reaction was stirred at room temperature for 2 h. The conjugate was then cleaned up by Size-exclusion chromatography. Size-exclusion chromatography (SEC) was done on a GE Healthcare life sciences ÄKTA pure 25 L system, using PBS as the mobile phase and a GE HiLoad 16/600 Superdex 200 prep grade column.

3.3 Results

3.3.1 Synthetic Polymeric *N*-Acetylglucosamine for Tolerance Induction towards Asparaginase

To study the ability of synthetic polymeric *N*-Acetylglucosamine (pGlu) to introduce tolerance towards therapeutic proteins, the immunogenicity of asparaginase was assessed in mice tolerized with pGlu-asparaginase and naive mice (fig. 3.4 A). pGlu-asparaginase was produced by chemical conjugation, as described in material and methods, and then purified by size exclusion. While pGlu-asparaginase appears as a single symmetric peak on the size exclusion chromatogram (Appendix A.15), it is a large smear on a coomassie blue stained SDS-Page gel (fig. 3.4 B). This behavior can be attributed to asparaginase being a tetramer in solution and a monomer on the gel due to the chaotropic property of SDS. While the pGlu conjugation seems to be fairly homogeneous on the tetramer level, it seems that when broken down to monomers the extend of pGlu conjugation varies greatly. This is especially true as we can see a small band for monomeric unconjugated asparaginase below the smear. As intended the glycosylation in pGlu-asparaginase disappear upon reducing conditions and we can detect two single bands with one of them having the exact same weight as asparaginase (fig. 3.4 B). To quantify the amount of glucose residues introduced by the conjugation, an SDS-PAGE gel was glycostained. The gel shows that a higher molecular weight on the SDS-PAGE gel leads a higher degree of glycosylation. This does not mean that the glycosylations are not homogeneously distributed per molecule as the SDS-PAGE gel looks at the monomer level and pGlu-asparaginase is a tetramer in solution.

Five BALB/c mice per group were injected with 2.5 or 15 μg of pGlu-asparaginase i.v. once a week for 3 weeks and were then switched to 15 μg of Asparaginase i.v. once a week for 8 weeks. One group received 15 μg of asparaginase once a week i.v. for 8 weeks. To test if pGlu-asparaginase can induce tolerance in the presence of asparaginase a mix of 2.5 μg pGlu-asparaginase and 12.5 μg asparaginase was injected once a week for 8 weeks i.v.. The detailed experimental schedule is shown in figure 3.4 A.

A significant difference in anti-asparaginase IgG was observed between mice pretolerized with pGlu-asparaginase and naive mice after 8 weeks of asparaginase treatments ($p < 0.001$). There was no significant difference between the mice tolerized with 15 or 2.5 μg of pGlu-asparaginase but there was a trend that the lower dose works better. Administration of the tolerogenic pGlu-asparaginase and the immunogenic asparaginase leads to no significant difference between those groups, but there is a trend that the co-administration leads to higher anti-asparaginase IgG titers. The progression of the anti-asparaginase titers is shown in figure 3.4 C. Statistical analysis was done by two-way repeated measures ANOVA with post-hoc Bonferroni correction.

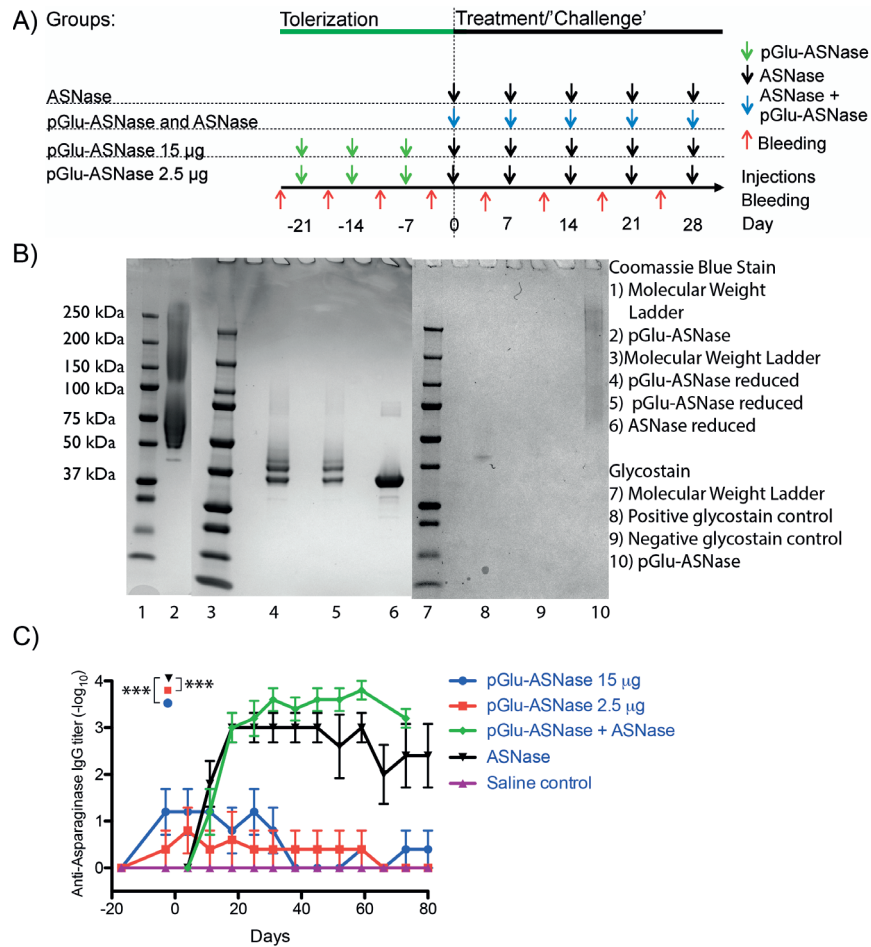


Figure 3.4 – A) Injection and bleeding schedule B) Coomassie blue stained SDS-PAGE gel displaying pGlu-asparaginase, reduced pGlu-asparaginase and asparaginase. C) Anti-asparaginase titers from blood serum. *** $P < 0.001$ by two-way repeated measures ANOVA with post-hoc Bonferroni correction. Data represent mean \pm SE.

While 3 animals in the group receiving 15 µg of pGlu-asparaginase had measurable levels of anti asparaginase IgG, only one mouse in the group tolerized with 2.5 µg had measurable IgG titers more than once. The anti asparaginase IgG titers for each single animal per group are displayed in figure 3.5 A. Comparing the IgG subtypes between the groups at day 38 all IgG subtypes can be found in the groups receiving asparaginase and the one receiving the mix of asparaginase and pGlu-asparaginase while only IgG1 is present in the groups pretolerized with pGlu-asparaginase (fig. 3.5 B). There is a significant difference in all the subtypes between the group preteolerized with 2.5 µg of pGlu-asparaginase and the groups receiving only asparaginase (IgG1 $P < 0.05$, IgG2a $P < 0.05$, IgG2b $P < 0.01$, IgG3 $P < 0.001$), with the biggest difference in IgG type 3 anti-asparaginase titers. To verify that these differences are not just a result of the difference in total IgG anti-asparaginase titers at day 38, anti-asparaginase IgG subtypes at day 4 and 11 were measured (fig. 3.5 C). At day 4 we can only

Chapter 3. Tolerance Induction by Antigens Bearing Synthetic Glycosylations

measure IgG3 anti-asparaginase titers in two mice, at day 11 all titers from all subtypes can already be observed, with 5 mice showing anti-asparaginase IgG3 and IgG1 titers. While the IgG response in pGlu-asparaginase is dominated by IgG1, asparaginase seems to first induce the IgG3 subtype. These differences in subtypes hint at a different mechanism in the immune response to pGlu-asparaginase and asparaginase. Statistical analysis was done by one-way ANOVA with post-hoc Tukey's multiple comparison test.

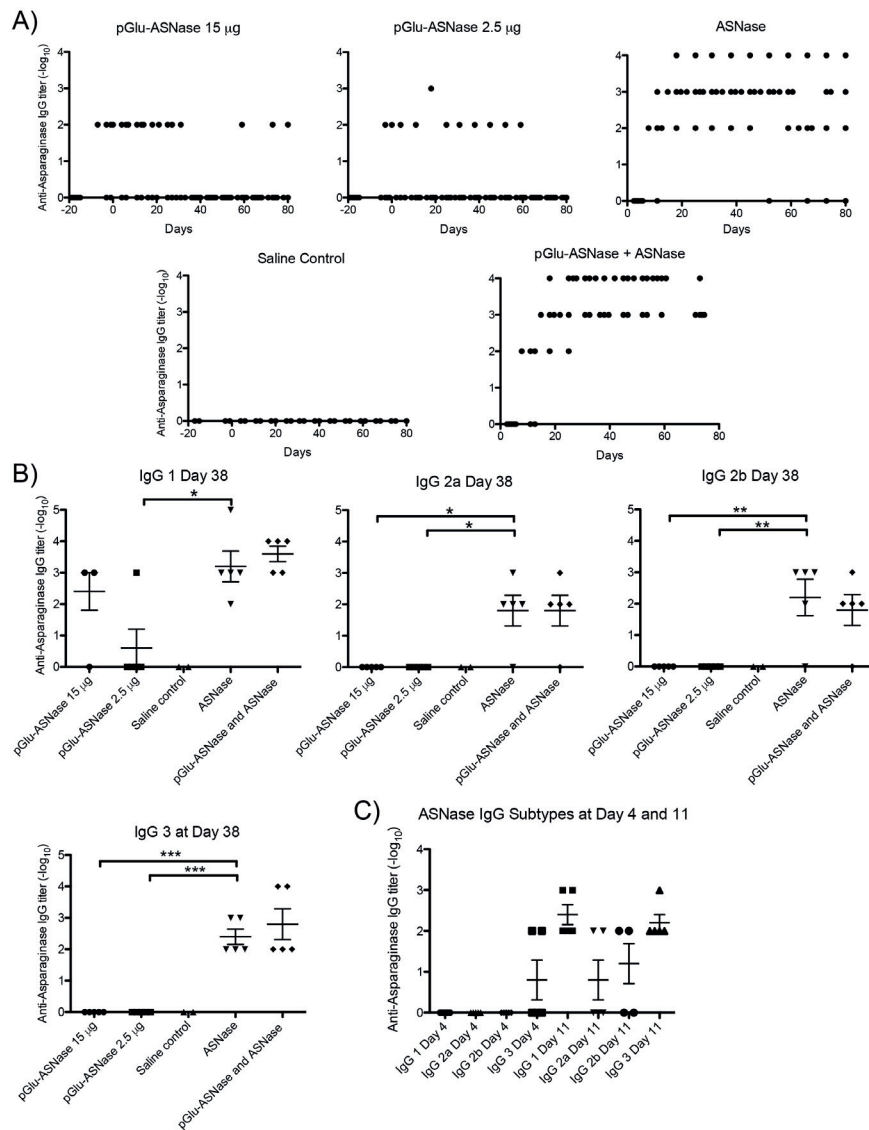


Figure 3.5 – A) Anti-asparaginase titers showed for each single animal for all experimental groups. B) Compares different treatment groups in regard to the anti-asparaginase IgG subtypes at day 38. * $P < 0.05$, ** $P < 0.01$, *** $P < 0.001$, C) Anti-asparaginase IgG subtypes for the group treated with asparaginase at day 4 and 11. Statistical analysis was done by one-way ANOVA with post-hoc Tukey's multiple comparison test. Data represent mean \pm SE.

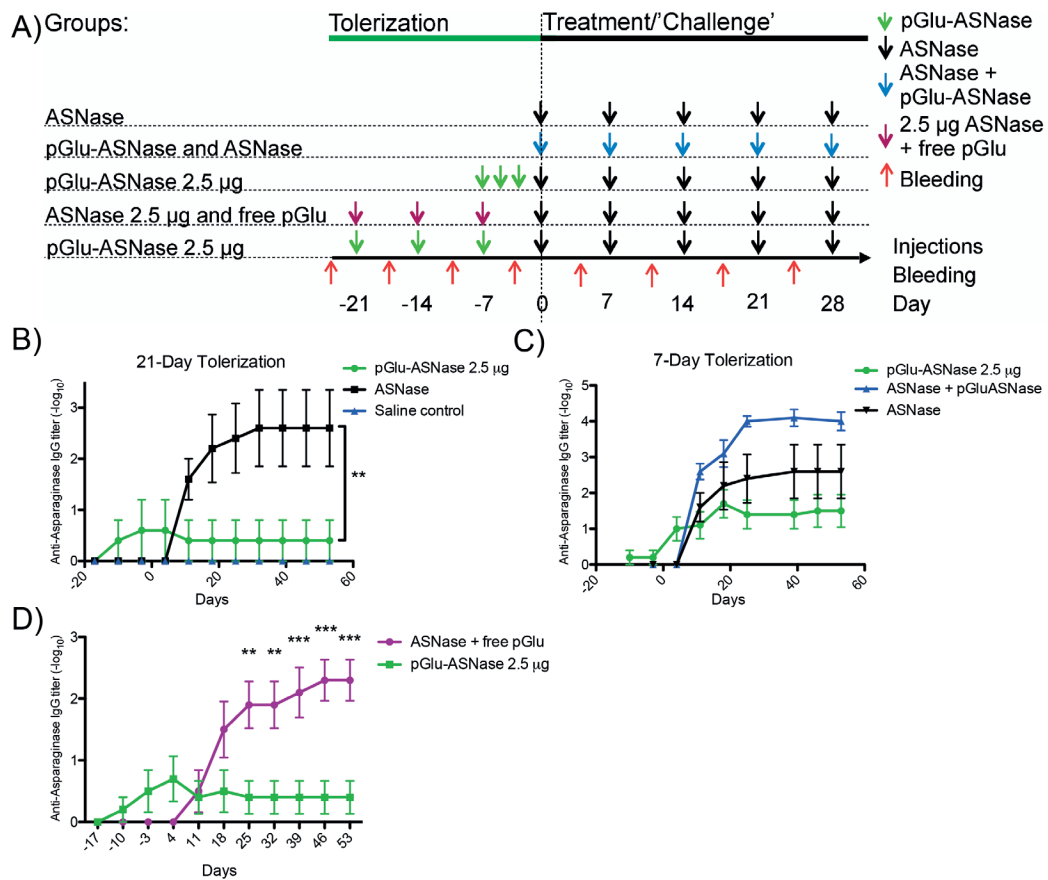


Figure 3.6 – A) Injection and bleeding schedule B) Anti-asparaginase IgG titers for animals in which tolerance was induced over 21 days. C) Anti-asparaginase IgG titers for animals in which tolerance was induced over 7 days. D) Anti-asparaginase IgG titers comparing the tolerance induction of pGlu-asparaginase to free pGlu and asparaginase. ** $P < 0.01$, *** $P < 0.001$ Statistical analysis for B was done by one-way ANNOVA with post-hoc Tukey's multiple comparison test and for C and D by two-way repeated measures ANOVA with post-hoc Bonferroni correction. Data represent mean \pm SE.

The experiment was repeated with a new batch of pGlu-asparaginase, which is displayed in appendix A.16. Groups of 5 BALB/c mice were injected with 2.5 µg of pGlu-asparaginase i.v. for once a week for 3 weeks and were then switched to 15 µg of Asparaginase i.v. once a week for 8 weeks. A group in which the mice received pGlu-asparaginase and asparaginase as a mix, was included again but the ratio was changed to 7.5 µg pGlu-asparaginase and 7.5 µg asparaginase once a week for 8 weeks i.v.. The immunogenicity of asparaginase was measured in a group of mice receiving 15 µg of asparaginase once a week for 8 weeks. A faster injection schedule for tolerization with pGlu-asparaginase was tested. Mice were injected with 2.5 µg three times 2 days apart, 3 days after the last injection the mice were switched to 15 µg of asparaginase per week for 8 weeks. To show that conjugation of pGlu to the antigen is needed to induce tolerance a group of 10 mice received 2.5 µg of asparaginase and 1 µg of free pGlu for 3 weeks once a week i.v. and was then switched to 15 µg of asparaginase i.v. once a week

Chapter 3. Tolerance Induction by Antigens Bearing Synthetic Glycosylations

for 8 weeks. The group was compared to the groups tolerized with 2.5 μg asparaginase once a week for 3 weeks in this experiment and the experiment described in figure 3.5. The detailed experimental schedule is displayed in figure 3.6 A.

Mice tolerized with 2.5 μg of pGlu-asparaginase once a week for three weeks had significant lower anti-asparaginase IgG titers compared to the mice only receiving asparaginase after 8 weeks of treatment with asparaginase ($P < 0.01$ by one-way ANNOVA with post-hoc Tukey's multiple comparison test). The faster injection schedule for the tolerizing doses with 2.5 μg of pGlu-asparaginase every 2 days showed no significant effect on anti asparaginase IgG titers compared to the mice receiving asparaginase only (fig. 3.6 B). Mice receiving a mix of pGlu-asparaginase and asparaginase showed no beneficial effect on anti-asparaginase IgG titers compared to the mice receiving asparaginase only. Comparing mice receiving 2.5 μg pGlu-asparaginase for 3 weeks once a week to mice receiving 2.5 μg of asparaginase and 1 μg of free pGlu showed significant lower anti asparaginase IgG titers after 8 weeks of treatment with asparaginase ($P < 0.01$ at day 25 and 32 and $P < 0.001$ at day 39, 46 and 53). Statistical analysis was done by two-way repeated measures ANOVA with post-hoc Bonferroni correction.

3.3.2 Synthetic Polymeric *N* - Acetylgalactoseamine and *N* - Acetylmannoseamine for Tolerance Induction towards Asparaginase

Asparaginase was conjugated to synthetic polymeric *N*-Acetylgalactoseamine (pGal) and *N*-Acetylmannoseamine (pMan) and purified by size exclusion. The conjugates are shown on a coomassie blue stained SDS-PAGE gel in appendix A.17. The gel also shows the release of pMan and pGal from asparaginase by the self-immolative linker in a reductive environment.

To test the ability of these constructs to induce tolerance, 2.5 μg of pGal-asparaginase or pMan-asparaginase were injected i.v. into 5 BALB/c mice once a week for three weeks and then switched to 15 μg asparaginase for 5 weeks. A group of 5 mice was injected with 15 μg of asparaginase i.v. for 5 weeks. The detailed experimental schedule is displayed in figure 3.7 A.

Mice pretolerized with pGal-asparaginase showed by a factor 12 reduced anti-asparaginase IgG titers at the end of the experiment compared to mice receiving only asparaginase, however the effect was not significant. Mice tolerized with pMan-asparaginase lowered anti-asparaginase titers 400 fold compared to mice receiving asparaginase, with only one mouse having measurable anti asparaginase IgG titers ($P < 0.001$ two-way repeated measures ANNOVA with post-hoc Bonferroni correction). Anti-asparaginase IgG titers are displayed in figure 3.7 B.

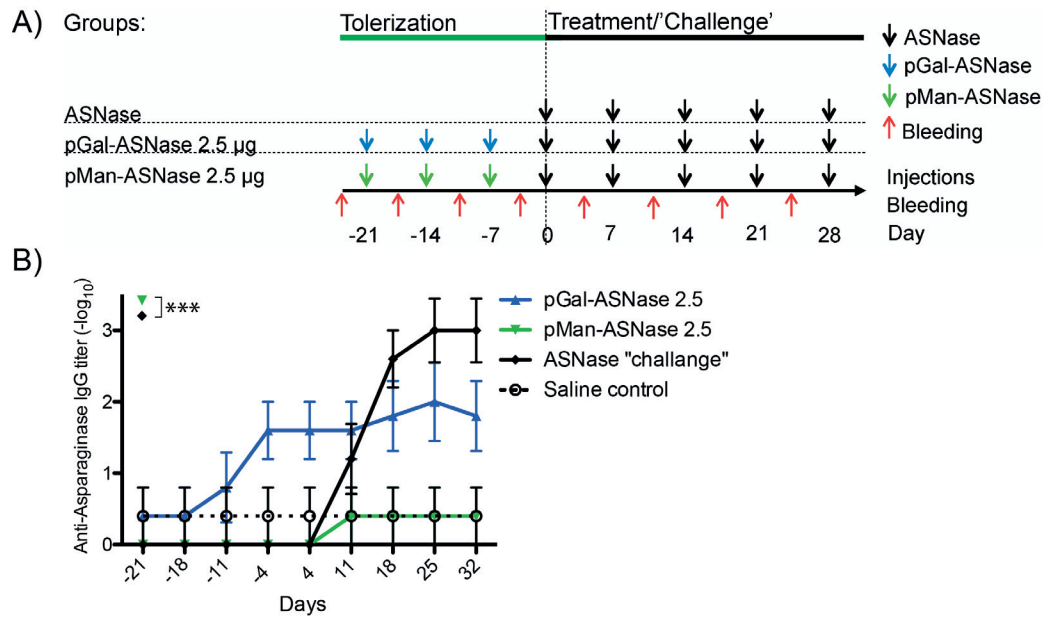


Figure 3.7 – A) Injection and bleeding schedule B) Anti-asparaginase titers for mice tolerized with pMan- or pGal-asparaginase compared to mice receiving no pretolerization after 5 weeks of treatment with asparaginase. *** $P < 0.001$, two-way repeated measures ANNOVA with post-hoc Bonferroni correction. Data represent mean \pm SE.

3.4 Discussion

Pretolerization with pGlu-asparaginase leads to a significant reduction in anti-asparaginase titers during an 8 week asparaginase treatment period when compared to non-tolerized animals. This result was obtained twice with two independently produced pGlu-ASNase batches. If we pool both experiments, pretolerization with pGlu-asparaginase reduces anti-asparaginase titers in average 125 fold after 8 weeks of treatment. It was found that pGlu-asparaginase can not efficiently induce tolerance when applied simultaneously with asparaginase, showing that the signal that induces an immune response towards asparaginase is stronger than the tolerance inducing one from pGlu-asparaginase. The injection schedule was sped-up, to test if we can shorten the pretolerization phase. Animals that were pretolerized with 3 doses of pGlu-asparaginase every two days had similar titers compared to animals not receiving any pretolerization after 8 weeks of treatment with asparaginase. One theory was that we overload the liver with antigen because it can not be cleared fast enough. This has been confirmed as people in the Hubbell lab have shown the presence of antigen, injected as pGlu conjugate, for 4 days in the liver. This might not be the only reason as it is not clear how fast the tolerance inducing process actually can be.

If we look at anti-asparaginase IgG titers in single mice, in both experiments where pGlu-asparaginase was used to pretolerize, we find that only one mouse out of 5 has measurable titers and that they were at the lowest measurable level of 2. Further it was found that if an antibody response against asparaginase can be measured in mice pretreated with pGlu-ASNase, it is of the IgG1 subtype. In comparison, mice that only receive the asparaginase doses show all subtypes, and IgG3 is the subtype that can be detected at the earliest time points. This result suggests that the induction of antibody production follows a different process involving different cells leading to the induction of a different subtype pattern.

Pretolerization with pGlu-asparaginase was then compared to pretolerization with free pGlu and asparaginase. Both groups followed the same dosing regimen and were treated with 8 injections of asparaginase over 8 weeks after tolerization. A significant difference in anti-asparaginase titers was found between the two groups after the third week of asparaginase treatment with the pGlu-asparaginase treated mice having much lower titers. Further, there is no difference in anti-asparaginase IgG titers between mice that did not receive pretolerization and mice pretolerized with free pGlu and asparaginase. This result demonstrates that the targeting of the protein, achieved by the conjugation of pGlu, is responsible for tolerance induction.

The experiment was then repeated with pGal-asparaginase and pMan-asparaginase. Pretolerization with 3 injections of pGal-asparaginase reduced the titers by a factor of 12 but was not significant after 5 weeks of treatment with asparaginase when compared to mice not receiving tolerizing injections. Pretolerizing injections with pMan-asparaginase were highly efficient and reduced anti-asparaginase IgG titers 400 fold after 5 weeks of treatment with asparaginase compared to mice that were not tolerized.

These results show that pMan-asparaginase and pGlu-asparaginase induce long term tolerance towards asparaginase. To further gain evidence that this platform has great potential in inducing tolerance towards protein drugs, work on producing tolerance inducing variants of Humira and Myalept has begun.

Humira is a human monoclonal antibody used to treat rheumatoid arthritis and has recently been shown to lose efficacy in patients with high anti-humira antibody titers. One potential problem when inducing tolerance to antibodies is recycling of antibodies by the Fc receptor [102]. When pGlu-antibody is taken up by a cell, pGlu is released by reduction of the self-immolative linker and the free antibody is brought back into circulation by the Fc receptor instead of degraded and presented to the immune system. This fear was confirmed when an experiment with 3 pretolerizing doses of pGlu-Humira showed no tolerizing effect (data not shown). In fact 3 doses of pGlu-Humira induced the exact same titers as 3 doses of Humira. However another approach can be used to induce tolerance towards Humira in humans, as it has been shown that the antibodies against Humira generated in patients are all directed against the variable region [116]. It is therefore sufficient to tolerize with a Fab to induce tolerance towards Humira, with a Fab having the advantage that it is not affected by Fc recycling. The Humira-F(ab')₂ has recently been produced by pepsin digestion of Humira. After the digestion the Humira-F(ab')₂ was cleaned up by protein A purification followed by size exclusion. However the Humira-F(ab')₂ was not endotoxin free as a result of the pepsin digest. Endotoxin removal for the F(ab')₂ can easily be achieved by cation exchange.

Myalept is a human leptin analog produced in *Escherichia coli*. It was approved by the FDA in 2014 for the treatment of leptin deficiencies. 84% of the patients which receive Myalept develop Antibodies against it [30]. Myalept was successfully cloned and expressed in a small scale. Scale up of the protein expression is planned with the goal to create a tolerance inducing version of pMan-Myalept. Myalept is an excellent drug for the study of tolerance induction because i) it is produced in *Escherichia coli* and has therefore no native glycosylations that might interfere with the targeting of the synthetic sugar polymer. ii) loss of efficacy in patients with high anti-drug antibody titers has already been shown.

To gain a better understanding of how pGlu-asparaginase induces tolerance, a version of asparaginase that has no catalytic activity has been generated by a single point mutation [42]. Integrity of the structure was shown by analytical size exclusion. This mutant allows us to use asparaginase in restimulation assays, as the wild type can not be used in cell culture due to its catalytic activity. This has already been used to show by ELISPOT that tolerance induction with pGlu-asparaginase leads to less memory B-cells compared to mice that were not pretolerized after exposure to asparaginase over 8 weeks (data not shown). This asparaginase mutant will allow us to further study the molecular and cellular mechanisms at play in tolerance induction with pGlu-asparaginase.

A Appendix

Antibody name	Company	Type	Target	Indication(s)	Reported immunogenicity
Muromanab (OKT3)	Ortho Biotech	Murine	CD3	Allograft rejection	25% (24)
Abciximab (Reopro)	Centocor (Johnson & Johnson)	Chimeric Fab	GP1Ib/IIIa	PTCA adjunct	6%–44% (36)
Rituximab (Rituxan)	Genentech (Roche)/Biogen Idec	Chimeric	CD20	Non-Hodgkin lymphoma	11% (2578)
Daclizumab (Zenapax)	Hoffman LaRoche	Humanized	IL2R	Transplant rejection	14–34%
Trastuzumab (Herceptin)	Genentech (Roche)	Humanized	Her2/neu	Breast cancer	<1%
Palivizumab (Synagis)	MedImmune (Astra Zeneca)	Humanized	RSV F	RSV prophylaxis	0.7%–2% (1002–639)
Basiliximab (Simulect)	Novartis	Chimeric	IL2R	Transplant rejection	1–2% (138–339)
Infliximab (Remicade)	Centocor (Johnson & Johnson)	Chimeric	TNF α	RA/Crohn	10–15%
Arcitumomab (CEA-scan)	Immunomedics	Murine	CEA	Colorectal cancer	<1% (3/400)
Canakinumab (Ilaris)	Novartis	Human	IL-1 β	Cryopyrin-associated periodic syndrome	0% (64)
Fanolesomab (Neutrospec)	Palatin Tech.	Murine	CD15	Imaging for appendicitis	0–16.6% (30–54)
Imciromab (Myoscint)	Centocor (Johnson & Johnson)	Murine	Myosin	Cardiac imaging for MI	<1% (914)
Capromab (Prostascint)	Cytogen	Murine	PSMA	Prostate cancer diagnostic	8%–19% (27–239)
Nofetumomab (Verluma)	Boehringer Ingelheim	Murine	40 kDa glycoprotein	Detection of SCLC	6% (53)
Gemtuzumab (Mylotarg)	Wyeth Pharma (Pfizer)	Humanized	CD33	Acute myeloid leukemia	0% (277)
Alemtuzumab (Campath)	Ilex Pharma (Genzyme)	Humanized	CD52	B cell chronic lymphocytic leukemia	1.9–8.3% (133–211)
Ibritumomab (Zevalin)	Idec Pharma (Biogen Idec)	Murine	CD20	Non-Hodgkin lymphoma	1.3% (446)
Adalimumab (Humira)	Abbott	Human	TNF α	RA/Crohn/PsA/JIA/Ankylosing spondylitis/plaque psoriasis	2.6%–26%
Omalizumab (Xolair)	Genentech (Roche)	Humanized	IgE	Asthma	<0.1% (1723)
Efalizumab (Raptiva)	Genentech (Roche)	Humanized	CD11a	Psoriasis	6.3% (1063)
Tositumomab (Bexxar)	GSK	Murine	CD20	Non-Hodgkins lymphoma	11% (230)
Cetuximab (Erbix)	Imclone (Eli Lilly)	Chimeric	EGFR	Colorectal cancer	5% (1001)
Bevacizumab (Avastin)	Genentech (Roche)	Humanized	VEGF	Colorectal, breast, renal and NSCL cancer	0% (~500)
Panitumumab (Vectibix)	Amgen	Human	EGFR	Colorectal cancer	4.6% (613)
Ranibizumab (Lucentis)	Genentech (Roche)	Humanized	VEGF	Macular degeneration	1–6%
Eculizumab (Soliris)	Alexion Pharma	Humanized	C5	Paroxysmal nocturnal hemoglobinuria	2% (196)
Natalizumab (Tysabri)	Biogen Idec	Humanized	α -4 integrin	MS & Crohn	9% (627)
Golimumab (Simponi)	Centocor (Johnson & Johnson)	Human	TNF α	RA/PsA/Ankylosing spondylitis	4% (1425)
Cetolizumab pegol (Cimzia)	UCB	Humanized	TNF α	RA/Crohn	8% (1509)
Ofatumumab (Arzerra)	GSK	Human	CD20	CLL	0% (79)
Ustekinumab (Stelara)	Centocor (Johnson & Johnson)	Human	IL-12/IL-23	Plaque psoriasis	3–5% (743–1198)
Tocilizumab (Actemra)	Genentech (Roche)	Humanized	IL-6R	Rheumatoid arthritis	2% (2876)
Denosumab (Prolia)	Amgen	Human	RANKL	Osteoporosis	<1% (8113)

Figure A.1 – FDA approved antibody therapeutics showing the level of reported immunogenicity observed in patients from prescribing information available at FDA.com. Figure adapted from [6].

Biologic name	Company	Type	Target	Indication(s)	Reported immunogenicity
Prolastin	Talecris biotherapeutics	PD	α 1-proteinase inhibitor	α 1-antitrypsin deficiency	None reported
Aralast	Baxter Healthcare	PD	α 1-proteinase inhibitor	α 1-antitrypsin deficiency	None reported
Zemaira	Aventis Behring (CSL Behring)	PD	α 1-proteinase inhibitor	α 1-antitrypsin deficiency	None reported
Kogenate FS	Bayer (Bayer Schering Pharma)	rHu	Factor VIII	Hemophilia A	15%
ReFacto	Genetics Institute (Wyeth)	rHu	Factor VIII	Hemophilia A	30%
Zyntha	Wyeth (Pfizer)	rHu	Factor VIII	Hemophilia A	2.2% (89)
NovoSeven	NovoNordisk	rHu	Factor FVII	Hemophilia	<1%
Benefix	Wyeth (Pfizer)	rHu	Factor IX	Hemophilia B	3%
ATryn	GTC Biotherapeutics	rHu	Anti-thrombin	Thromboembolism	None reported
BabyBIG	California Department of Health Services	PD	Botulism Immune Globulin Intravenous Human	Infant botulism	
Berinerit	CSL Behring	rHu	C1 Esterase Inhibitor	Angioedema	
Cinryze	Lev Pharmaceuticals	rHu	C1 Esterase Inhibitor	Angioedema	
Rhophylac	CSL Behring	PD	Rho(D) Immune Globulin	ITP	0% (447)
Evithrom	OMRIX Biopharmaceuticals	rHu	Thrombin, Topical	Coagulation	3.3%
Recothrom	ZymoGenetics	rHu	Thrombin, Topical	Coagulation	1.2–1.5%
Wilate	Octapharma	PD	von Willebrand Factor	Coagulation	1.5–3%
Cerezyme	Genzyme	rHu	β -glucocerebrosidase	Gacher Disease	15%
Exenatide or Byetta	Amylin Pharmaceuticals/Eli Lilly	R	Glucagon Like Peptide-1	Type II diabetes	6%
IntronA	Schering Corp (Bayer Schering Pharma)	rHu	IFN α	Leukemia, Kaposi sarcoma, hepatitis B/C	<3–13%
Betaseron	Bayer Schering Pharma	rHu	IFN β	Multiple sclerosis	16.5–25.2%
NovoLog	NovoNordisk	rHu	Insulin analog	Type II diabetes	Transient antibodies
Leukine	Genzyme	rHu	GM-CSF	Preventing infection in cancer	2.3%
NEUPOGEN (Filgrastim)	Amgen	rHu	G-CSF	Preventing infection in cancer	3%
Retavase	PDL Biopharma	rHu	TPA	Myocardial infarction, pulmonary embolism	0% (2400)
Humatrope	Eli Lilly	rHu	Growth hormone	Dwarfism	1.6%
Adagen	Enzon Pharmaceuticals	Bovine	ADA Adenosine deaminase	Inherited immunodeficiency	Not reported (SCID)
Pulmozyme	Genentech (Roche)	rHu	DNase I	Cystic fibrosis	2–4%
Procrit	Amgen	rHu	EPO	Anemia in chronic renal disease	
Proleukin	Novartis	rHu	IL-2	Oncology	<1%

Figure A.2 – FDA approved other biologics showing the level of reported immunogenicity observed in patients from prescribing information available from FDA.com. Figure adapted from [6].

Disease	Product	Enzyme	Product status	Patients with IgG antibody (%)	Reference
Gaucher's	Ceredase	Alglucerase	Licensed	12.8	18
	Cerezyme	Imiglucerase	Licensed	13.8	Product label
Fabry's	Fabrazyme	Agalsidase beta	Licensed	90	20
Hurler's (MPS I)	Aldurazyme	α -L-iduronidase	Licensed	91	55
Pompe's	Myozyme	Acid- α -glucosidase	Licensed	89	Product label
Hunter's (MPS II)	Elaprase	Iduronate-2-sulfatase	Licensed	51	Product label
Maroteaux-Lamy (MPS VI)	Naglazyme arylsulfatase B	N-acetylgalactosamine-4-sulfatase	Phase 3 completed	97	87

MPS, mucopolysaccharidosis.

Figure A.3 – Immune responses to replacement lysosomal enzymes. Figure adapted from [120].

Appendix A. Appendix

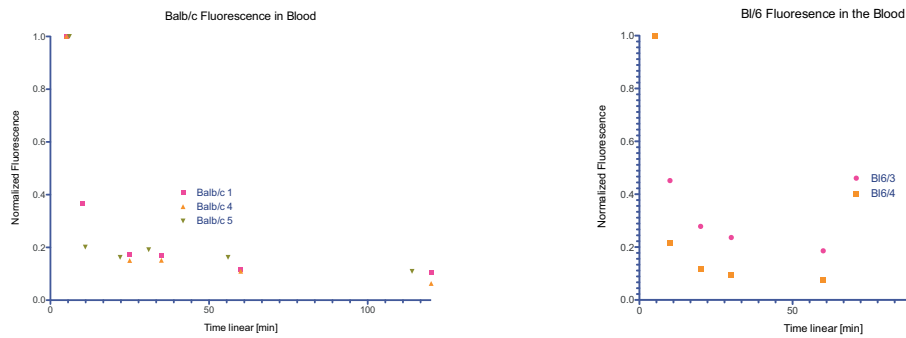


Figure A.4 – Uptake of arylsulfatase B from serum after i.v. injection in every mouse.

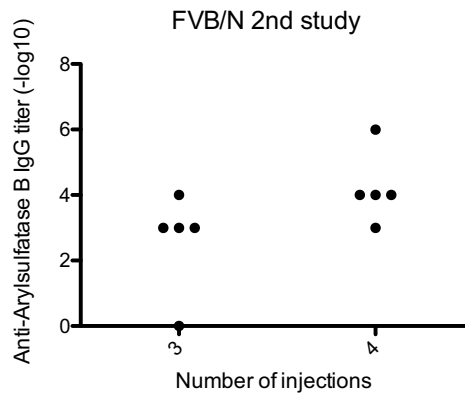


Figure A.5 – Anti-arylsulfatase B titers after 3 and 4 injections of arylsulfatase B in FVB/N mice.

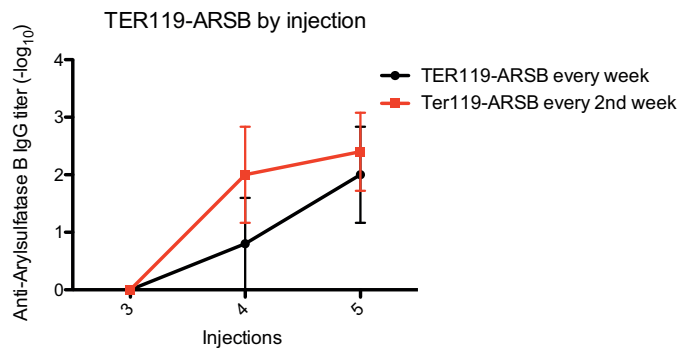


Figure A.6 – Anti-Arylsulfatase B titers in mice injected weekly or every 2nd week with TER119-arylsulfatase B by injections received.

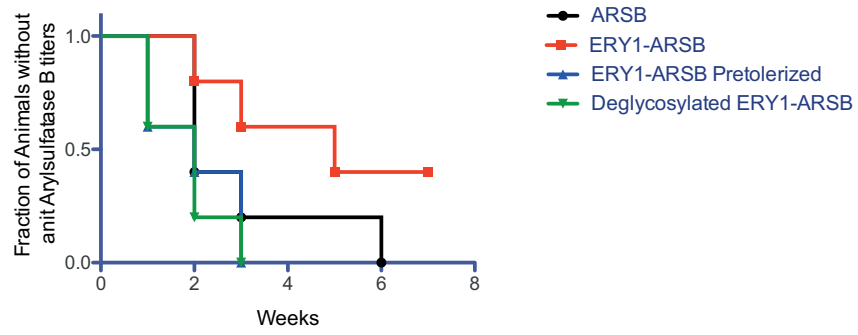
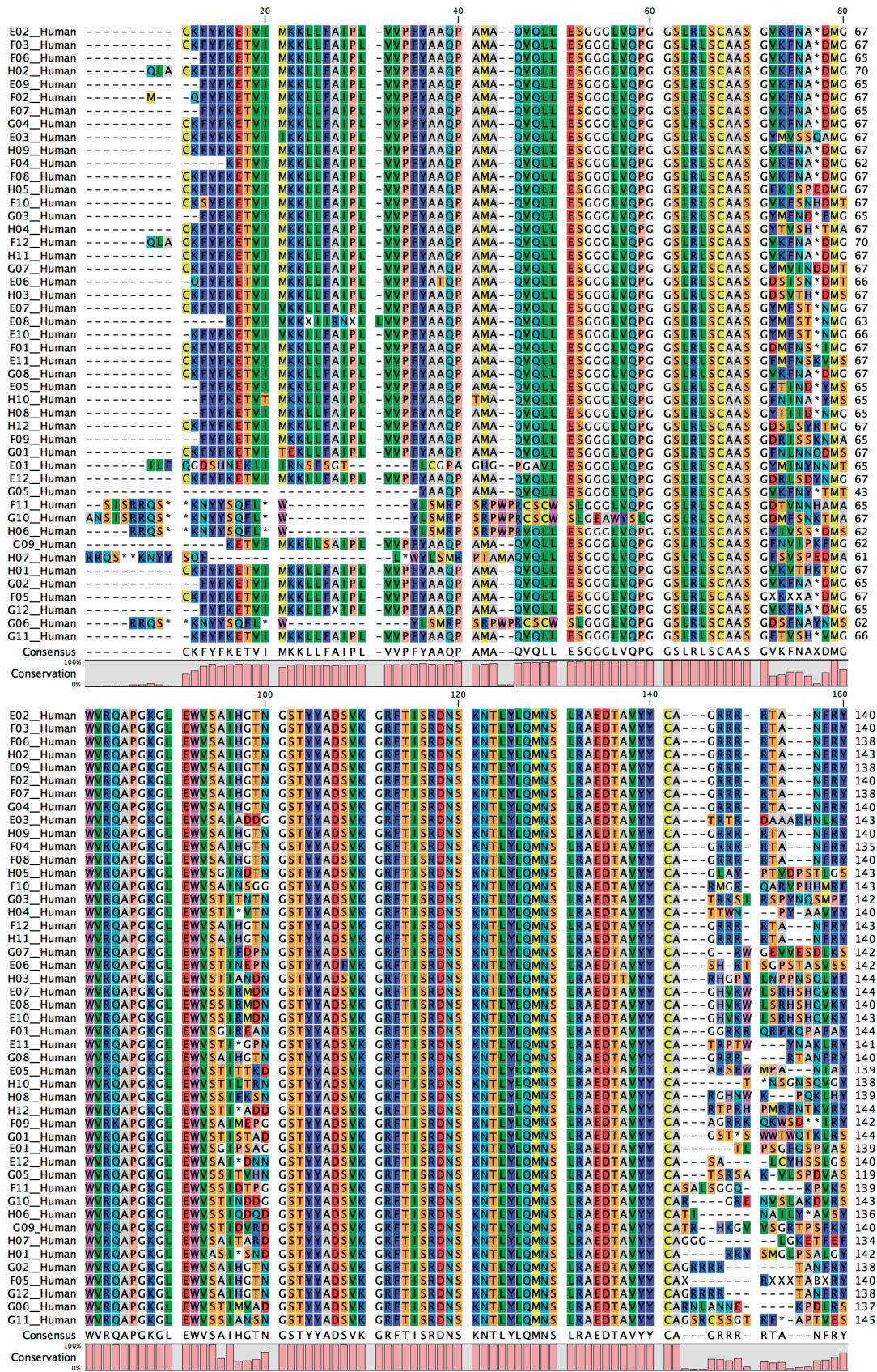


Figure A.7 – Percentage of mice not showing detectable levels against ARSB, ERY1-ARSB, deglycosylated ERY1-ARSB pretolerized and ERY1-ARSB pretolerize

Appendix A. Appendix



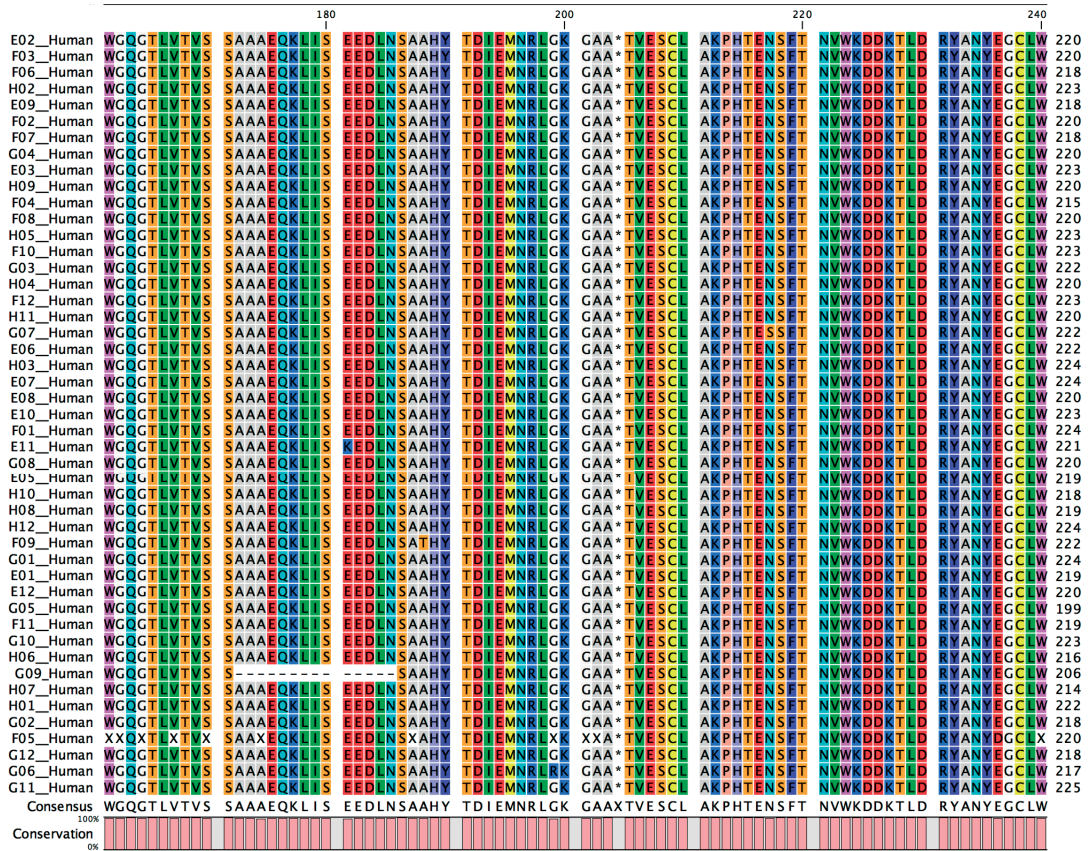


Figure A.8 – Complete Sequencing results from third Round of Phage Display against Human Erythrocytes

Appendix A. Appendix

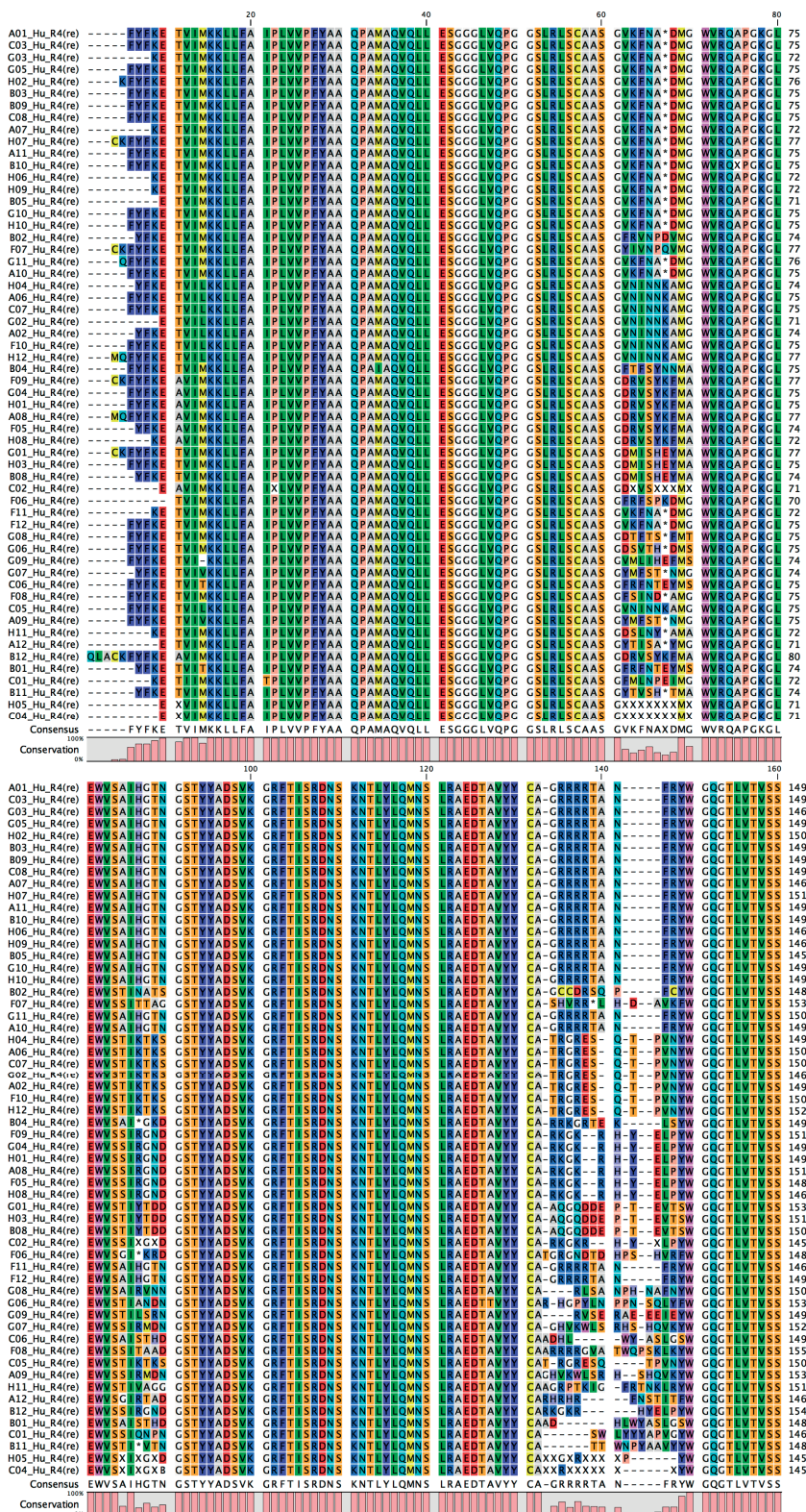
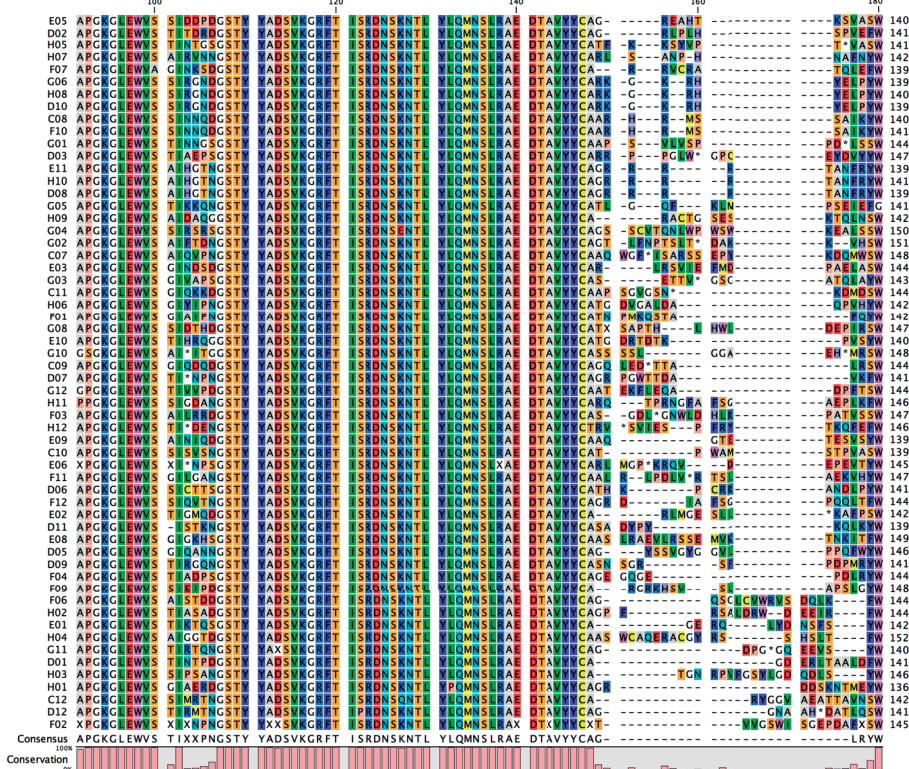
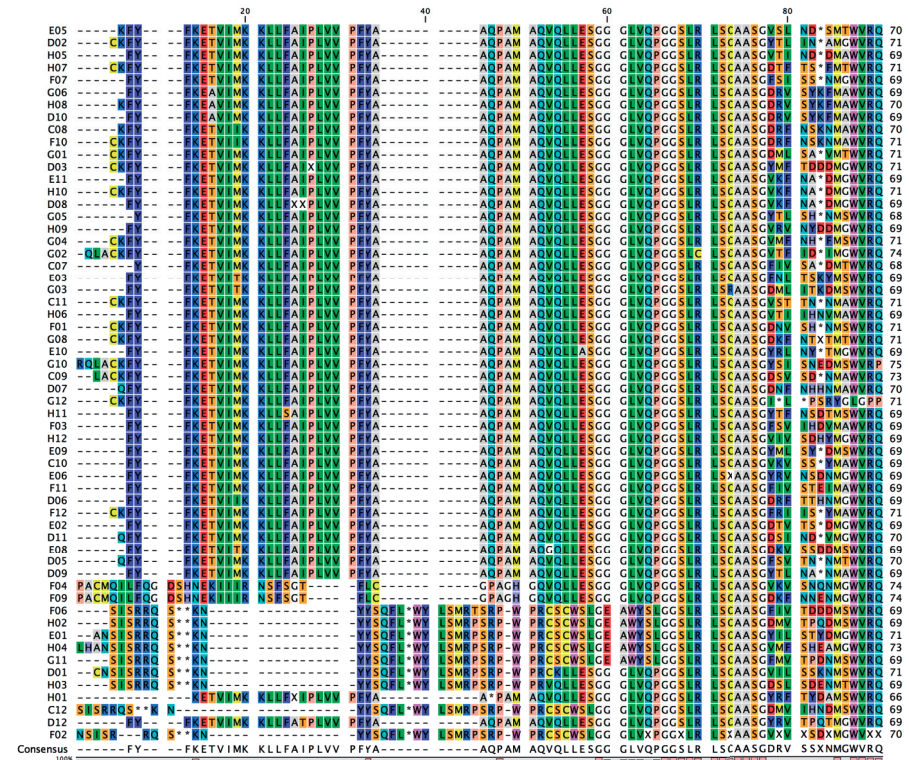


Figure A.9 – Complete Sequencing results from fourth Round of Phage Display against Human Erythrocytes



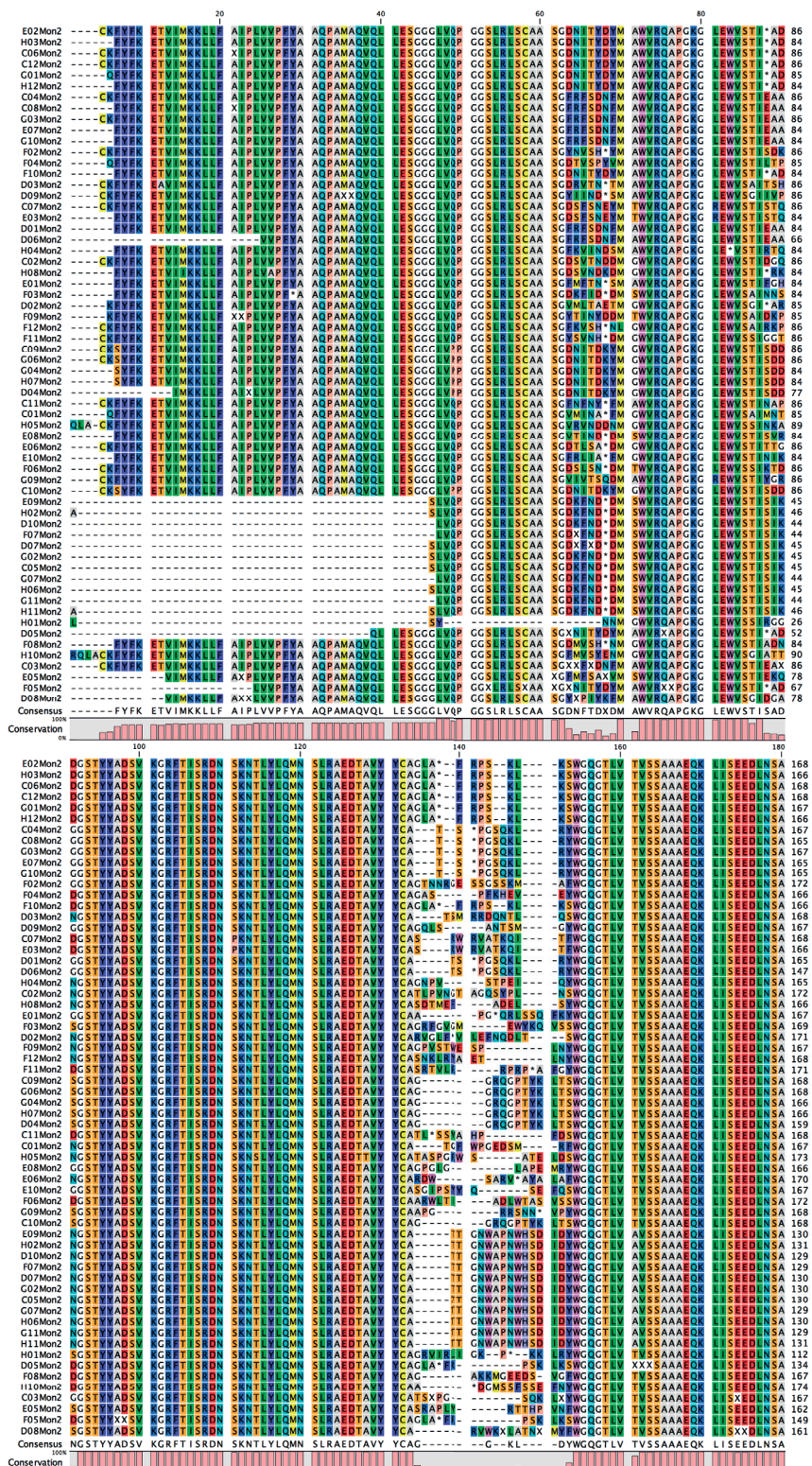


Figure A.13 – Complete Sequencing results from second Round of Phage Display against Monkey Erythrocytes

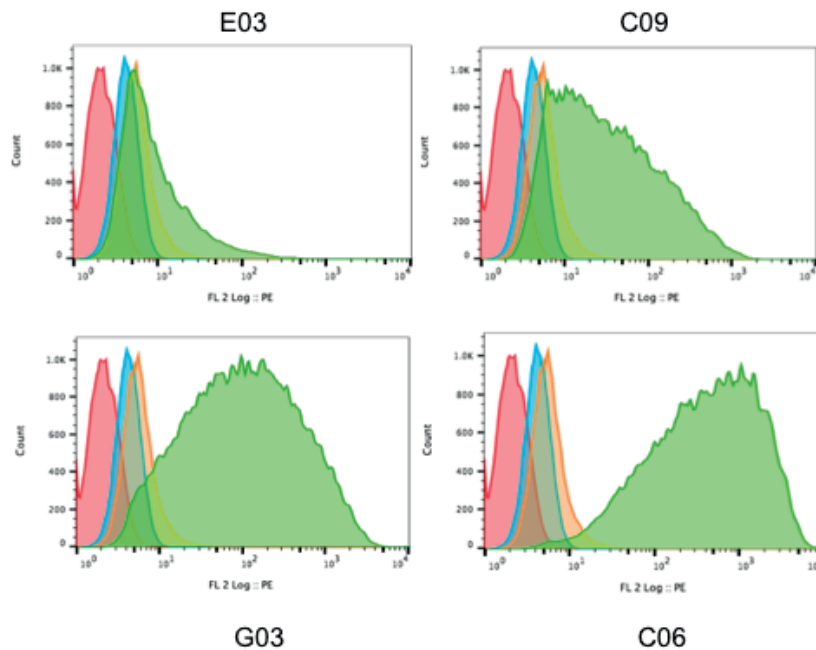


Figure A.14 – Binding of moC9, moE3, moG03 and moC06 human domain antibodies identified by phage display against monkey blood towards monkey blood on a phage level. Red area shows absorbance of blood only, blue is blood stained with anti-M13 pIII antibody, orange is blood with the control phage from the library and stained with anti-M13 pIII antibody, green is blood with the phage for the given sequence stained with anti-M13 pIII antibody

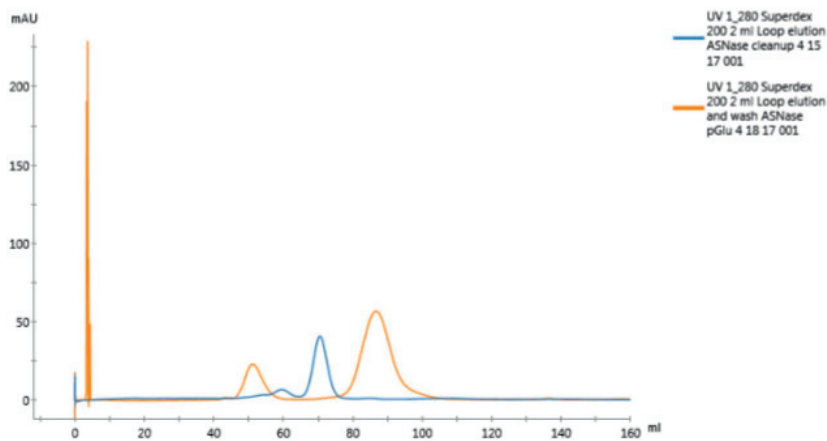


Figure A.15 – Size exclusion Chromatogram of Asparaginase and pGlu-Asparaginase with the blue line being the absorbance at 280 nm, the peak of the asparaginase as tetramer is at 70 minutes. The blue line represents the absorbance at 280 nm during the pGlu-asparaginase run, with the peak at 50 minutes being pGlu-asparaginase and the free pGlu polymer at 90 minutes.

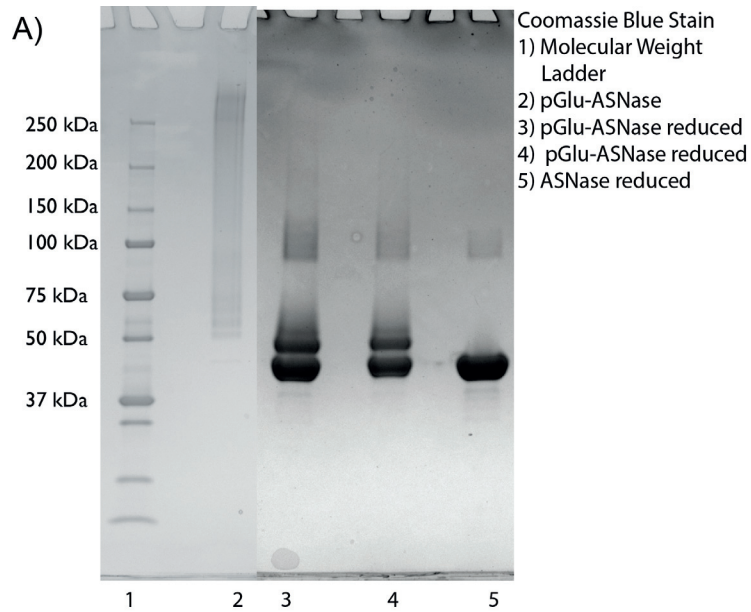


Figure A.16 – Coomassie blue stained SDS-PAGE gel showing reduced and unreduced pGlu-asparaginase and reduced asparaginase

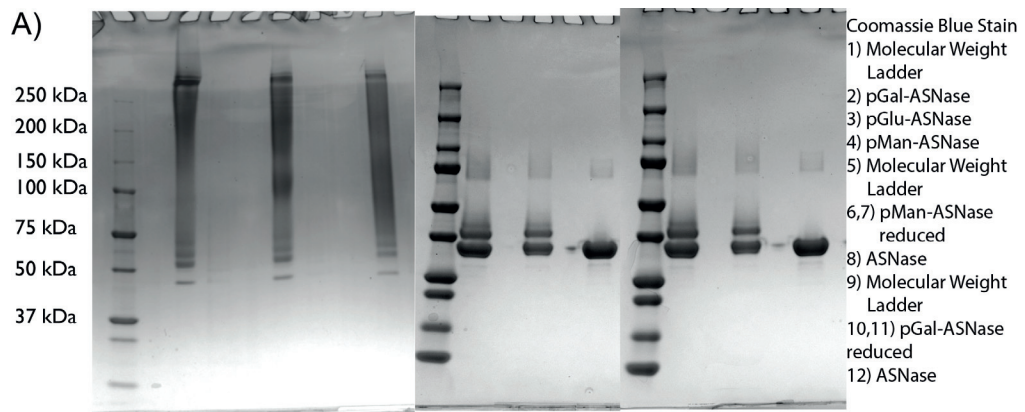


Figure A.17 – Coomassie blue stained SDS-PAGE gel showing unreduced and reduced pGal-asparaginase and pGlu asparaginase

Bibliography

- [1] Differential assay of arylsulfatase A and B activities: a sensitive method for cultured human cells. *Anal Biochem*, 117(2):382–389, November 1981.
- [2] D S Anson, J A Taylor, J Bielicki, G S Harper, C Peters, G J Gibson, and J J Hopwood. Correction of human mucopolysaccharidosis type-VI fibroblasts with recombinant N-acetylgalactosamine-4-sulphatase. *Biochem J*, 284 (Pt 3):789–794, June 1992.
- [3] Nagisa Arimitsu, Nobuyoshi Akimitsu, Norihiro Kotani, Seiichi Takasaki, Tatsuo Kina, Hiroshi Hamamoto, Koushirou Kamura, and Kazuhisa Sekimizu. Glycophorin A requirement for expression of O-linked antigens on the erythrocyte membrane. *Genes to Cells*, 8(9):769–777, September 2003.
- [4] G Ashwell and J Harford. Carbohydrate-specific receptors of the liver. *Annual review of biochemistry*, 1982.
- [5] Katja Aviszus, Megan K L Macleod, Greg A Kirchenbaum, Thiago O Detanico, Ryan A Heiser, James B St Clair, Wenzhong Guo, and Lawrence J Wsocki. Antigen-specific suppression of humoral immunity by anergic Ars/A1 B cells. *J Immunol*, 189(9):4275–4283, November 2012.
- [6] Matthew P Baker, Helen M Reynolds, Brooke Lumicisi, and Christine J Bryson. Immunogenicity of protein therapeutics: The key causes, consequences and challenges. *Self/nonself*, 1(4):314–322, October 2010.
- [7] Geertje M Bartelds, Charlotte L M Krieckaert, Michael T Nurmohamed, Pauline A van Schouwenburg, Willem F Lems, Jos W R Twisk, Ben A C Dijkmans, Lucien Aarden, and Gerrit Jan Wolbink. Development of Antidrug Antibodies Against Adalimumab and Association With Disease Activity and Treatment Failure During Long-term Follow-up. *Jama*, 305(14):1460–1468, April 2011.
- [8] Facundo D Batista and Naomi E Harwood. The who, how and where of antigen presentation to B cells. *Nat Rev Immunol*, 9(1):15–27, January 2009.
- [9] Tahira Batool, Essam A Makky, Muna Jalal, and Mashitah M Yusoff. A Comprehensive Review on L-Asparaginase and Its Applications. *Applied biochemistry and biotechnology*, 178(5):900–923, March 2016.

Bibliography

- [10] C P Berg, I H Engels, A Rothbart, K Lauber, A Renz, S F Schlosser, K Schulze-Osthoff, and S Wesselborg. Human mature red blood cells express caspase-3 and caspase-8, but are devoid of mitochondrial regulators of apoptosis. *Cell Death Differ*, 8(12):1197–1206, December 2001.
- [11] Rostyslav Bilyy and Rostyslav Stoika. Search for novel cell surface markers of apoptotic cells. *Autoimmunity*, 40(4):249–253, July 2009.
- [12] C S Bond, P R Clements, S J Ashby, C A Collyer, S J Harrop, J J Hopwood, and J M Guss. Structure of a human lysosomal sulfatase. *Structure (London, England : 1993)*, 5(2):277–289, February 1997.
- [13] H Braley-Mullen, J G Tompson, G C Sharp, and M Kyriakos. Suppression of experimental autoimmune thyroiditis in guinea pigs by pretreatment with thyroglobulin-coupled spleen cells. *Cell Immunol*, 51(2):408–413, May 1980.
- [14] Bronwen R Burton, Graham J Britton, Hai Fang, Johan Verhagen, Ben Smithers, Catherine A Sabatos-Peyton, Laura J Carney, Julian Gough, Stephan Strobel, and David C Wraith. Sequential transcriptional changes dictate safe and effective antigen-specific immunotherapy. *Nature Communications*, 5:ncomms5741, September 2014.
- [15] Antonella Carambia, Barbara Freund, Dorothee Schwinge, Markus Heine, Alena Laschtowitz, Samuel Huber, David C Wraith, Thomas Korn, Christoph Schramm, Ansgar W Lohse, Joerg Heeren, and Johannes Herkel. TGF- β -dependent induction of CD4CD25Foxp3 Tregs by liver sinusoidal endothelial cells. *Journal of Hepatology*, 61(3):594–599, September 2014.
- [16] A Chionna, E Panzarini, and P Pagliara. Hepatic clearance of apoptotic lymphocytes: simply removal of waste cells? *European journal of . . .*, 2003.
- [17] Daniel Christ, Kristoffer Famm, and Greg Winter. Repertoires of aggregation-resistant human antibody domains. *Protein Engineering Design and Selection*, 20(8):413–416, August 2007.
- [18] A C Crawley, D A Brooks, V J Muller, B A Petersen, E L Isaac, J Bielicki, B M King, C D Boulter, A J Moore, N L Fazzalari, D S Anson, S Byers, and J J Hopwood. Enzyme replacement therapy in a feline model of Maroteaux-Lamy syndrome. *J Clin Invest*, 97(8):1864–1873, April 1996.
- [19] A C Crawley, K H Niedzielski, E L Isaac, R C Davey, S Byers, and J J Hopwood. Enzyme replacement therapy from birth in a feline model of mucopolysaccharidosis type VI. *J Clin Invest*, 99(4):651–662, February 1997.
- [20] I N Crispe. Hepatic T cells and liver tolerance. *Nature reviews Immunology*, 2003.
- [21] Luciana Dini, Francesco Autuori, Alessandro Lentini, Serafina Oliverio, and Mauro Piacentini. The clearance of apoptotic cells in the liver is mediated by the asialoglycoprotein receptor. *FEBS letters*, 296(2):174–178, January 1992.

- [22] H S Dua, D S Gregerson, and L A Donoso. Inhibition of experimental autoimmune uveitis by retinal photoreceptor antigens coupled to spleen cells. *Cell Immunol*, 139(2):292–305, February 1992.
- [23] M Dürrschmid, C Jursik, N Borth, R Grabherr, and O Doblhoff-Dier. Investigations on Mannose-6-Phosphate Receptor Mediated Protein Uptake. In *Investigations on Mannose-6-Phosphate Receptor Mediated Protein Uptake*, pages 43–49. Springer-Verlag, Berlin/Heidelberg, 2005.
- [24] E Duvall, A H Wyllie, and R G Morris. Macrophage recognition of cells undergoing programmed cell death (apoptosis). *Immunology*, 56(2):351–358, October 1985.
- [25] S Fagarasan. T-Independent Immune Response: New Aspects of B Cell Biology. *Science*, 290(5489):89–92, October 2000.
- [26] FDA. Asparaginase package insert. 16(2):73–76, July 2013.
- [27] Zhigang Tian Fenglei Li. The liver works as a school to educate regulatory immune cells. *Cellular and Molecular Immunology*, 10(4):292–302, July 2013.
- [28] Brian T Fife, Indira Guleria, Melanie Gubbels Bupp, Todd N Eagar, Qizhi Tang, Helene Bour-Jordan, Hideo Yagita, Miyuki Azuma, Mohamed H Sayegh, and Jeffrey A Bluestone. Insulin-induced remission in new-onset NOD mice is maintained by the PD-1-PD-L1 pathway. *J Exp Med*, 203(12):2737–2747, November 2006.
- [29] Food and Drug Administration. Naglazyme (galsulfase) prescription information, Biomarin Pharmaceutical Inc. pages 1–10, March 2013.
- [30] Food and Drug Administration. FULL PRESCRIBING INFORMATION MYALEPT. pages 1–55, February 2014.
- [31] Elena Garrido, Bru Cormand, John J Hopwood, Amparo Chabás, Daniel Grinberg, and Lluïsa Vilageliu. Maroteaux–Lamy syndrome: Functional characterization of pathogenic mutations and polymorphisms in the arylsulfatase B gene. *Molecular Genetics and Metabolism*, 94(3):305–312, July 2008.
- [32] Daniel R Getts, Aaron J Martin, Derrick P McCarthy, Rachael L Terry, Zoe N Hunter, Woon Teck Yap, Meghann Teague Getts, Michael Pleiss, Xunrong Luo, Nicholas JC King, Lonnie D Shea, and Stephen D Miller. Microparticles bearing encephalitogenic peptides induce T-cell tolerance and ameliorate experimental autoimmune encephalomyelitis. *Nature Biotechnology*, 30(12):1217–1224, December 2012.
- [33] Daniel R Getts, Derrick P McCarthy, and Stephen D Miller. Exploiting apoptosis for therapeutic tolerance induction. *J Immunol*, 191(11):5341–5346, December 2013.
- [34] Daniel G Gibson, Hamilton O Smith, 3rd Clyde A Hutchison, J Craig Venter, and Chuck Merryman. Chemical synthesis of the mouse mitochondrial genome. *Nat Methods*, 7(11):901–903, November 2010.

Bibliography

- [35] S K Gregorian, L Clark, E Heber-Katz, E P Amento, and A Rostami. Induction of peripheral tolerance with peptide-specific energy in experimental autoimmune neuritis. *Cell Immunol*, 150(2):298–310, September 1993.
- [36] Alizée J Grimm, Stephan Kontos, Giacomo Diaceri, Xavier Quaglia-Thermes, and Jeffrey A Hubbell. Memory of tolerance and induction of regulatory T cells by erythrocyte-targeted antigens. *Nature Publishing Group*, 5(1):15907, October 2015.
- [37] P Harmatz, W G Kramer, J J Hopwood, J Simon, E Butensky, and S J Swiedler. Pharmacokinetic profile of recombinant human N-acetylgalactosamine 4-sulphatase enzyme replacement therapy in patients with mucopolysaccharidosis VI (Maroteaux-Lamy syndrome): a phase I/II study. *Acta Paediatr Suppl*, 94(447):61–8; discussion 57, March 2005.
- [38] Paul Harmatz, Roberto Giugliani, Ida Schwartz, Nathalie Guffon, Elisa Leão Teles, M Clara Sá Miranda, J Edmond Wraith, Michael Beck, Laila Arash, Maurizio Scarpa, Zi-Fan Yu, Janet Wittes, Kenneth I Berger, Mary S Newman, Ann M Lowe, Emil Kakkis, and Stuart J Swiedler. Enzyme replacement therapy for mucopolysaccharidosis VI: a phase 3, randomized, double-blind, placebo-controlled, multinational study of recombinant human N-acetylgalactosamine 4-sulfatase (recombinant human arylsulfatase B or rhASB) and follow-on, open-label extension study. *J Pediatr*, 148(4):533–539, April 2006.
- [39] Paul Harmatz, David Ketteridge, Roberto Giugliani, Natalie Guffon, Elisa Leão Teles, M Clara Sá Miranda, Zi-Fan Yu, Stuart J Swiedler, and John J Hopwood. Direct comparison of measures of endurance, mobility, and joint function during enzyme-replacement therapy of mucopolysaccharidosis VI (Maroteaux-Lamy syndrome): results after 48 weeks in a phase 2 open-label clinical study of recombinant human N-acetylgalactosamine 4-sulfatase. *Pediatrics*, 115(6):e681–e689, June 2005.
- [40] Paul Harmatz, Chester B Whitley, Lewis Waber, Ray Pais, Robert Steiner, Barbara Plecko, Paige Kaplan, Julie Simon, Ellen Butensky, and John J Hopwood. Enzyme replacement therapy in mucopolysaccharidosis VI (Maroteaux-Lamy syndrome). *J Pediatr*, 144(5):574–580, May 2004.
- [41] Paul Harmatz, Chester B Whitley, Lewis Waber, Ray Pais, Robert Steiner, Barbara Plecko, Paige Kaplan, Julie Simon, Ellen Butensky, and John J Hopwood. Enzyme replacement therapy in mucopolysaccharidosis VI (Maroteaux-Lamy syndrome). *The Journal of Pediatrics*, 144(5):574–580, May 2004.
- [42] E Harms, A Wehner, H P Aung, and K H Röhm. A catalytic role for threonine-12 of E. coli asparaginase II as established by site-directed mutagenesis. *FEBS letters*, 1991.
- [43] J T Harty, A R Tvinnereim, and D W White. CD8(+) T cell effector mechanisms in resistance to infection. *Annual Review of Immunology*, 18(1):275–308, 2000.

- [44] K Haskins and M McDuffie. Acceleration of diabetes in young NOD mice with a CD4+ islet-specific T cell clone. *Science*, 249(4975):1433–1436, September 1990.
- [45] H Hassoun, T Hanada, M Lutchman, K E Sahr, J Palek, M Hanspal, and A H Chishti. Complete deficiency of glycoporphin A in red blood cells from mice with targeted inactivation of the band 3 (AE1) gene. *Blood*, 91(6):2146–2151, March 1998.
- [46] Felix Heymann, Julia Peusquens, Isis Ludwig Portugall, Marlene Kohlhepp, Can Ergen, Patricia Niemietz, Christian Martin, Nico van Rooijen, Jordi C Ochando, Gwendalyn J Randolph, Tom Luedde, Florent Ginhoux, Christian Kurts, Christian Trautwein, and Frank Tacke. Liver inflammation abrogates immunological tolerance induced by Kupffer cells. *Hepatology*, 62(1):279–291, July 2015.
- [47] Andrea Kristina Horst, Katrin Neumann, Linda Diehl, and Gisa Tiegs. Modulation of liver tolerance by conventional and nonconventional antigen-presenting cells and regulatory immune cells. *Cellular and Molecular Immunology*, 13(3):277–292, May 2016.
- [48] Noriko Iikuni, Elaine V Lourenço, Bevra H Hahn, and Antonio La Cava. Cutting edge: Regulatory T cells directly suppress B cells in systemic lupus erythematosus. *J Immunol*, 183(3):1518–1522, August 2009.
- [49] Hirohiko Ise, Mitsuaki Goto, Kenta Komura, and Toshihiro Akaike. Engulfment and clearance of apoptotic cells based on a GlcNAc-binding lectin-like property of surface vimentin. *Glycobiology*, 22(6):788–805, June 2012.
- [50] Birger Jansson, Mathias Uhlén, and Per-Åke Nygren. All individual domains of staphylococcal protein A show Fab binding. *FEMS Immunology & Medical Microbiology*, 20(1):69–78, January 1998.
- [51] Roy Jefferis. Review Article Posttranslational Modifications and the Immunogenicity of Biotherapeutics. *Journal of Immunology Research*, 2016(9):1–15, April 2016.
- [52] Julia Jellusova, Ute Wellmann, Kerstin Amann, Thomas H Winkler, and Lars Nitschke. CD22 x Siglec-G double-deficient mice have massively increased B1 cell numbers and develop systemic autoimmunity. *J Immunol*, 184(7):3618–3627, April 2010.
- [53] Laurent Jaspers, Oliver Schon, Kristoffer Famm, and Greg Winter. Aggregation-resistant domain antibodies selected on phage by heat denaturation. *Nat Biotechnol*, 22(9):1161–1165, August 2004.
- [54] P F Jezyk, M E Haskins, D F Patterson, W J Mellman, and M Greenstein. Mucopolysaccharidosis in a cat with arylsulfatase B deficiency: a model of Maroteaux-Lamy syndrome. *Science*, 198(4319):834–836, November 1977.
- [55] I S Johnson. Human insulin from recombinant DNA technology. *Science*, 219(4585):632–637, February 1983.

Bibliography

- [56] V Judkowski, C Pinilla, K Schroder, L Tucker, N Sarvetnick, and D B Wilson. Identification of MHC class II-restricted peptide ligands, including a glutamic acid decarboxylase 65 sequence, that stimulate diabetogenic T cells from transgenic BDC2.5 nonobese diabetic mice. *J Immunol*, 166(2):908–917, January 2001.
- [57] Valeria Judkowski, Enrique Rodriguez, Clemencia Pinilla, Emma Masteller, Jeffrey A Bluestone, Nora Sarvetnick, and Darcy B Wilson. Peptide specific amelioration of T cell mediated pathogenesis in murine type 1 diabetes. *Clin Immunol*, 113(1):29–37, October 2004.
- [58] Ruba Kado, Georgiana Sanders, and W Joseph McCune. Suppression of normal immune responses after treatment with rituximab. *Current Opinion in Rheumatology*, 28(3):251–258, May 2016.
- [59] L Kappos, G Comi, H Panitch, J Oger, and J Antel. Induction of a non-encephalitogenic type 2 T helper-cell autoimmune response in multiple sclerosis after administration of an altered peptide ligand in a placebo-controlled, randomized phase II trial - ProQuest. *Nature*, 2000.
- [60] L Karageorgos, P Harmatz, J Simon, A Pollard, P R Clements, D A Brooks, and John J Hopwood. Mutational analysis of mucopolysaccharidosis type VI patients undergoing a trial of enzyme replacement therapy. *Hum Mutat*, 23(3):229–233, March 2004.
- [61] Litsa Karageorgos, Doug A Brooks, Anthony Pollard, Elizabeth L Melville, Leanne K Hein, Peter R Clements, David Ketteridge, Stuart J Swiedler, Michael Beck, Roberto Giugliani, Paul Harmatz, James E Wraith, Nathalie Guffon, Elisa Leão Teles, M Clara Sá Miranda, and John J Hopwood. Mutational analysis of 105 mucopolysaccharidosis type VI patients. *Hum Mutat*, 28(9):897–903, September 2007.
- [62] Adam Kaufman and Kevan C Herold. Anti-CD3 mAbs for treatment of type 1 diabetes. *Diabetes/Metabolism Research and Reviews*, 25(4):302–306, May 2009.
- [63] T Kina, K Ikuta, E Takayama, K Wada, A S Majumdar, I L Weissman, and Y Katsura. The monoclonal antibody TER-119 recognizes a molecule associated with glycophorin A and specifically marks the late stages of murine erythroid lineage. *Br J Haematol*, 109(2):280–287, May 2000.
- [64] T Kina, K Ikuta, E Takayama, K Wada, A S Majumdar, I L Weissman, and Y Katsura. The monoclonal antibody TER-119 recognizes a molecule associated with glycophorin A and specifically marks the late stages of murine erythroid lineage. *Br J Haematol*, 109(2):280–287, May 2000.
- [65] P Knolle, J Schlaak, A Uhrig, P Kempf, K H Meyer zum Büschenfelde, and G Gerken. Human Kupffer cells secrete IL-10 in response to lipopolysaccharide (LPS) challenge. *Journal of Hepatology*, 22(2):226–229, February 1995.

- [66] P A Knolle, T Germann, U Treichel, A Uhrig, E Schmitt, S Hegenbarth, A W Lohse, and G Gerken. Endotoxin down-regulates T cell activation by antigen-presenting liver sinusoidal endothelial cells. *The Journal of Immunology*, 162(3):1401–1407, February 1999.
- [67] Stephan Kontos, Alizée J Grimm, and Jeffrey A Hubbell. Engineering antigen-specific immunological tolerance. *Current opinion in immunology*, 35:80–88, August 2015.
- [68] Stephan Kontos and Jeffrey A Hubbell. Drug development: longer-lived proteins. *Chem Soc Rev*, 41(7):2686, 2012.
- [69] Stephan Kontos, Iraklis C Kourtis, Karen Y Dane, and Jeffrey A Hubbell. Engineering antigens for in situ erythrocyte binding induces T-cell deletion. *Proc Natl Acad Sci U S A*, 110(1):E60–8, January 2013.
- [70] K S Lang, C Durantou, H Poehlmann, S Myssina, C Bauer, F Lang, T Wieder, and S M Huber. Cation channels trigger apoptotic death of erythrocytes. *Cell Death Differ*, 10(2):249–256, February 2003.
- [71] Pascal Lapierre, Kathie Béland, Roland Yang, and Fernando Alvarez. Adoptive transfer of ex vivo expanded regulatory T cells in an autoimmune hepatitis murine model restores peripheral tolerance. *Hepatology*, 57(1):217–227, January 2013.
- [72] Carol M Y Lee, Niccolo Iorno, Frederic Sierro, and Daniel Christ. Selection of human antibody fragments by phage display. *Nat Protoc*, 2(11):3001–3008, November 2007.
- [73] Dapeng Li, Gabrielle Romain, Anne-Laure Flamar, Dorothée Duluc, Melissa Dullaers, Xiao-Hua Li, Sandra Zurawski, Nathalie Bosquet, Anna Karolina Palucka, Roger Le Grand, Anne O’Garra, Gerard Zurawski, Jacques Banchereau, and SangKon Oh. Targeting self- and foreign antigens to dendritic cells via DC-ASGPR generates IL-10-producing suppressive CD4+ T cells. *J Exp Med*, 209(1):jem.20110399–121, January 2012.
- [74] H W Lim, P Hillsamer, A H Banham, and C H Kim. Cutting Edge: Direct Suppression of B Cells by CD4+CD25+ Regulatory T Cells. *The Journal of Immunology*, 175(7):4180–4183, September 2005.
- [75] A Limmer, J Ohl, C Kurts, and H G Ljunggren. Efficient presentation of exogenous antigen by liver endothelial cells to CD8+ T cells results in antigen-specific T-cell tolerance. *Nature*, 2000.
- [76] T Litjens, C P Morris, G J Gibson, K R Beckmann, and J J Hopwood. Human N-acetylgalactosamine-4-sulphatase: protein maturation and isolation of genomic clones. *Biochem Int*, 24(2):209–215, May 1991.
- [77] K M Lorentz, S Kontos, G Diaceri, H Henry, and J A Hubbell. Engineered binding to erythrocytes induces immunological tolerance to E. coli asparaginase. *Science Advances*, 1(6):e1500112–e1500112, July 2015.

Bibliography

- [78] H B Lowman, S H Bass, N Simpson, and J A Wells. Selecting high-affinity binding proteins by monovalent phage display. *Biochemistry*, 1991.
- [79] Andreas Lutterotti, Sara Yousef, Andreas Sputtek, Klarissa H Stürner, Jan-Patrick Stellmann, Petra Breiden, Stefanie Reinhardt, Christian Schulze, Maxim Bester, Christoph Heesen, Sven Schippling, Stephen D Miller, Mireia Sospedra, and Roland Martin. Antigen-specific tolerance by autologous myelin peptide-coupled cells: a phase 1 trial in multiple sclerosis. *Sci Transl Med*, 5(188):188ra75, June 2013.
- [80] Matthew S Macauley, Fabian Pfrengle, Christoph Rademacher, Corwin M Nycholat, Andrew J Gale, Annette von Drygalski, and James C Paulson. Antigenic liposomes displaying CD22 ligands induce antigen-specific B cell apoptosis. *J Clin Invest*, 123(7):3074–3083, July 2013.
- [81] Roberto A Maldonado, Robert A LaMothe, Joseph D Ferrari, Ai-Hong Zhang, Robert J Rossi, Pallavi N Kolte, Aaron P Griset, Conlin O’Neil, David H Altreuter, Erica Browning, Lloyd Johnston, Omid C Farokhzad, Robert Langer, David W Scott, Ulrich H von Andrian, and Takashi Kei Kishimoto. Polymeric synthetic nanoparticles for the induction of antigen-specific immunological tolerance. *Proc Natl Acad Sci U S A*, 112(2):E156–65, January 2015.
- [82] Natalia Marek-Trzonkowska, Małgorzata Myśliwiec, Anita Dobyszek, Marcelina Grabowska, Ilona Derkowska, Jolanta Juścińska, Radosław Owczuk, Agnieszka Szadkowska, Piotr Witkowski, Wojciech Młynarski, Przemysław Jarosz-Chobot, Artur Bossowski, Janusz Siebert, and Piotr Trzonkowski. Therapy of type 1 diabetes with CD4(+)CD25(high)CD127-regulatory T cells prolongs survival of pancreatic islets - results of one year follow-up. *Clin Immunol*, 153(1):23–30, July 2014.
- [83] J McCafferty, A D Griffiths, G Winter, and D J Chiswell. Phage antibodies: filamentous phage displaying antibody variable domains. *Nature*, 348(6301):552–554, December 1990.
- [84] Kazuya Michishita, Kimito Kawahata, Takeyuki Kanzaki, Lisa Akahira, Toshiki Eri, and Kazuhiko Yamamoto. Effect of B cell depletion using peptide tetramers in collagen-induced arthritis. *Arthritis Research and Therapy*, 14:33, 2012.
- [85] Stephen D Miller, Danielle M Turley, and Joseph R Podojil. Antigen-specific tolerance strategies for the prevention and treatment of autoimmune disease. *Nat Rev Immunol*, 7(9):665–677, September 2007.
- [86] L Moreland and G Bate. Abatacept. *Nature reviews Drug ...*, 2006.
- [87] Asher Mullard. 2016 FDA drug approvals. *Nat Rev Drug Discov*, 16(2):73–76, February 2017.

- [88] Natalie Muller, Philippe Girard, David L Hacker, Martin Jordan, and Florian M Wurm. Orbital shaker technology for the cultivation of mammalian cells in suspension. *Biotechnology and Bioengineering*, 89(4):400–406, 2005.
- [89] Y Naparstek and P H Plotz. The role of autoantibodies in autoimmune disease. *Annu Rev Immunol*, 11:79–104, 1993.
- [90] E F Muenzer J Neufeld. The mucopolysaccharidoses. *The Metabolic and Molecular Basis of Inherited Disease 7th ed.* C.R. Scriver, A.L. Beaudet, W.S. Sly, and D. Valle, editors. McGraw-Hill Inc., New York, pages 2465–2494, 1995.
- [91] Roza I Nurieva, Shuling Zheng, Wei Jin, Yeonseok Chung, Yongliang Zhang, Gustavo J Martinez, Joseph M Reynolds, Sung-Ling Wang, Xin Lin, Shao-Cong Sun, Guillermina Lozano, and Chen Dong. The E3 ubiquitin ligase GRAIL regulates T cell tolerance and regulatory T cell function by mediating T cell receptor-CD3 degradation. *Immunity*, 32(5):670–680, May 2010.
- [92] T V Obukhanych. T-independent type II immune responses generate memory B cells. *Journal of Experimental Medicine*, 203(2):305–310, February 2006.
- [93] David O’Connell, Baltazar Becerril, Arup Roy-Burman, Mike Daws, and James D Marks. Phage versus Phagemid Libraries for Generation of Human Monoclonal Antibodies. *Journal of Molecular Biology*, 321(1):49–56, August 2002.
- [94] T Okazaki and T Honjo. The PD-1–PD-L pathway in immunological tolerance. *Trends in immunology*, 2006.
- [95] Mark D Pescovitz, Carla J Greenbaum, Heidi Krause-Steinrauf, Dorothy J Becker, Stephen E Gitelman, Robin Goland, Peter A Gottlieb, Jennifer B Marks, Paula F McGee, Antoinette M Moran, Philip Raskin, Henry Rodriguez, Desmond A Schatz, Diane Wherrett, Darrell M Wilson, John M Lachin, and Jay S Skyler. Rituximab, B-Lymphocyte Depletion, and Preservation of Beta-Cell Function. *New England Journal of Medicine*, 361(22):2143–2152, November 2009.
- [96] C Peters, B Schmidt, W Rommerskirch, K Rupp, M Zühlendorf, M Vingron, H E Meyer, R Pohlmann, and K von Figura. Phylogenetic conservation of arylsulfatases. cDNA cloning and expression of human arylsulfatase B. *J Biol Chem*, 265(6):3374–3381, February 1990.
- [97] Cathleen Petzold, Julia Riewaldt, Tina Koenig, Sonja Schallenberg, and Karsten Kretschmer. Dendritic Cell-Targeted Pancreatic β -Cell Antigen Leads to Conversion of Self-Reactive CD4+ T Cells Into Regulatory T Cells and Promotes Immunotolerance in NOD Mice. *The Review of Diabetic Studies : RDS*, 7(1):47–61, 2010.
- [98] Minmin Qin, John M Henstrand, Gary N Zecherle, Dan J Wendt, Wai-Pan Chan, Lin Chen, Paul A Fitzpatrick, and Christophher M Starr. Precursor N-acetylgalactosamine-4-sulfatase, methods of treatment ... US Patent Office.

Bibliography

- [99] Yashas Rajendra, Divor Kiseljak, Lucia Baldi, David L Hacker, and Florian M Wurm. A simple high-yielding process for transient gene expression in CHO cells. *Journal of Biotechnology*, 153(1-2):22–26, April 2011.
- [100] Paul M Ridker, Jean-Claude Tardif, Pierre Amarenco, William Duggan, Robert J Glynn, J Wouter Jukema, John J P Kastelein, Albert M Kim, Wolfgang Koenig, Steven Nissen, James Revkin, Lynda M Rose, Raul D Santos, Pamela F Schwartz, Charles L Shear, and Carla Yunis. Lipid-Reduction Variability and Antidrug-Antibody Formation with Bococizumab. *dx.doi.org*, 376(16):1517–1526, March 2017.
- [101] G Robinson, C Hamers, and E B Songa. Naturally occurring antibodies devoid of light chains - ProQuest. *Nature*, 1993.
- [102] D C Roopenian and S Akilesh. FcRn: the neonatal Fc receptor comes of age. *Nature reviews Immunology*, 2007.
- [103] Romain Rouet, David Lowe, Kip Dudgeon, Brendan Roome, Peter Schofield, David Langley, John Andrews, Peter Whitfeld, Lutz Jermutus, and Daniel Christ. Expression of high-affinity human antibody fragments in bacteria. *Nat Protoc*, 7(2):364–373, February 2012.
- [104] K H Roux, A S Greenberg, L Greene, L Strelets, D Avila, E C McKinney, and M F Flajnik. Structural analysis of the nurse shark (new) antigen receptor (NAR): molecular convergence of NAR and unusual mammalian immunoglobulins. *Proceedings of the National Academy of Sciences*, 95(20):11804–11809, September 1998.
- [105] Kenneth J Scalapino, Qizhi Tang, Jeffrey A Bluestone, Mark L Bonyhadi, and David I Daikh. Suppression of Disease in New Zealand Black/New Zealand White Lupus-Prone Mice by Adoptive Transfer of Ex Vivo Expanded Regulatory T Cells. *The Journal of Immunology*, 177(3):1451–1459, August 2006.
- [106] Ronald H Schwartz. T cell anergy. *Annual Review of Immunology*, 21:305–334, 2003.
- [107] Nicole Sherry, William Hagopian, Johnny Ludvigsson, Sunil M Jain, Jack Wahlen, Robert J Ferry Jr, Bruce Bode, Stephen Aronoff, Christopher Holland, David Carlin, Karen L King, Ronald L Wilder, Stanley Pillemer, Ezio Bonvini, Syd Johnson, Kathryn E Stein, Scott Koenig, Kevan C Herold, and Anastasia G Daifotis. Teplizumab for treatment of type 1 diabetes (Protégé study): 1-year results from a randomised, placebo-controlled trial. *The Lancet*, 378(9790):487–497, August 2011.
- [108] Cassandra E Smith, Todd N Eagar, Jack L Strominger, and Stephen D Miller. Differential induction of IgE-mediated anaphylaxis after soluble vs. cell-bound tolerogenic peptide therapy of autoimmune encephalomyelitis. *Proc Natl Acad Sci U S A*, 102(27):9595–9600, July 2005.
- [109] George P Smith. Filamentous fusion phage: novel expression vectors that display cloned antigens on the virion surface. *Science*, 228:1315–1318, June 1985.

- [110] Michael B Soyka, Willem van de Veen, David Holzmann, Mübeccel Akdis, and Cezmi A Akdis. Scientific foundations of allergen-specific immunotherapy for allergic disease. *Chest*, 146(5):1347–1357, November 2014.
- [111] Joel N H Stern, Derin B Keskin, Zenichiro Kato, Hanspeter Waldner, Sonja Schallenberg, Ana Anderson, Harald von Boehmer, Karsten Kretschmer, and Jack L Strominger. Promoting tolerance to proteolipid protein-induced experimental autoimmune encephalomyelitis through targeting dendritic cells. *Proc Natl Acad Sci U S A*, 107(40):17280–17285, October 2010.
- [112] Qizhi Tang, Kammi J Henriksen, Mingying Bi, Erik B Finger, Greg Szot, Jianqin Ye, Emma L Masteller, Hugh McDevitt, Mark Bonyhadi, and Jeffrey A Bluestone. In Vitro-expanded Antigen-specific Regulatory T Cells Suppress Autoimmune Diabetes. *J Exp Med*, 199(11):1455–1465, June 2004.
- [113] Gisa Tiegs and Ansgar W Lohse. Immune tolerance: What is unique about the liver. *Journal of autoimmunity*, 34(1):1–6, February 2010.
- [114] Daisuke Tokita, George V Mazariegos, Alan F Zahorchak, Nydia Chien, Masanori Abe, Giorgio Raimondi, and Angus W Thomson. High PD-L1/CD86 Ratio on Plasmacytoid Dendritic Cells Correlates With Elevated T-Regulatory Cells in Liver Transplant Tolerance. *Transplantation*, 85(3):369, February 2008.
- [115] Su-Yi Tseng and Michael L Dustin. T-cell activation: a multidimensional signaling network. *Current Opinion in Cell Biology*, 14(5):575–580, 2002.
- [116] Pauline A van Schouwenburg, Simone Kruithof, Christian Votsmeier, Karin van Schie, Margreet H Hart, Rob N de Jong, Esther E L van Buren, Marieke van Ham, Lucien Aarden, Gertjan Wolbink, Diana Wouters, and Theo Rispens. Functional analysis of the anti-adalimumab response using patient-derived monoclonal antibodies. *J Biol Chem*, 289(50):34482–34488, December 2014.
- [117] Flavio Vincenti, Lionel Rostaing, Joseph Grinyo, Kim Rice, Steven Steinberg, Luis Gaite, Marie-Christine Moal, Guillermo A Mondragon-Ramirez, Jatin Kothari, Martin S Polinsky, Herwig-Ulf Meier-Kriesche, Stephane Munier, and Christian P Larsen. Belatacept and Long-Term Outcomes in Kidney Transplantation. *dx.doi.org*, 374(4):333–343, January 2016.
- [118] Gary Walsh. Biopharmaceutical benchmarks 2014. *Nat Biotechnol*, 32(10):992–1000, October 2014.
- [119] Jinhai Wang, Jay Lozier, Gibbes Johnson, Susan Kirshner, Daniela Verthelyi, Anne Pariser, Elizabeth Shores, and Amy Rosenberg. Neutralizing antibodies to therapeutic enzymes: considerations for testing, prevention and treatment. *Nat Biotechnol*, 26(8):901–908, August 2008.

Bibliography

- [120] Jinhai Wang, Jay Lozier, Gibbes Johnson, Susan Kirshner, Daniela Verthelyi, Anne Pariser, Elizabeth Shores, and Amy Rosenberg. Neutralizing antibodies to therapeutic enzymes: considerations for testing, prevention and treatment. *Nat Biotechnol*, 26(8):901–908, August 2008.
- [121] Margreet A Wolfert and Geert-Jan Boons. Adaptive immune activation: glycosylation does matter. *Nature Publishing Group*, 9(12):776–784, December 2013.
- [122] World Health Organization. *The Selection and Use of Essential Medicines*. Report of the WHO Expert Committee, 2015 (including the 19th WHO Model List of Essential Medicines and the 5th WHO Model List of Essential Medicines for Children). World Health Organization, February 2016.
- [123] Ke Wu, Ilona Kryczek, Lieping Chen, Weiping Zou, and Theodore H Welling. Kupffer cell suppression of CD8+ T cells in human hepatocellular carcinoma is mediated by B7-H1/programmed death-1 interactions. *Cancer research*, 69(20):8067–8075, October 2009.
- [124] Sayuri Yamazaki, Diana Dudziak, Gordon F Heidkamp, Christopher Fiorese, Anthony J Bonito, Kayo Inaba, Michel C Nussenzweig, and Ralph M Steinman. CD8+CD205+ Splenic Dendritic Cells Are Specialized to Induce Foxp3+ Regulatory T Cells. *The Journal of Immunology*, 181(10):6923–6933, November 2008.
- [125] Marcel Zocher, Patrick A Baeuerle, Torsten Dreier, and Antonio Iglesias. Specific depletion of autoreactive B lymphocytes by a recombinant fusion protein in vitro and in vivo. *Int Immunol*, 15(7):789–796, July 2003.

Curriculum Vitae

Kym Brünggel

Personal data

Name	Brünggel
First name	Kym
Date of birth	23. 6. 1988
Nationality	Swiss
Home address Switzerland	Seehaldenstrasse 11 5616 Meisterschwanden
Home address USA	5135 South Blackstone Ave. Apt. 305 60615 Chicago
Phone	+41 076 482 22 67 (Switzerland) / +1 773 780 8644 (USA)
E-mail	k.brunggel@gmail.com

Education

2004-2008	School leaving diploma from Kantonsschule Wohlen Core subjects: Mathematics and Physics, Bilingual program french and german
2008-2010	Basic studies in Chemistry, ETH Zürich Department of Chemistry and Applied Biosciences
2010-2011	Bachelor of Science in Biotechnology, ETH Zürich Department of Biosystems Science and Engineering GPA: 5.46/6, performed above standard deviation
2011-2012	Master of Science in Biotechnology, ETH Zürich Department of Biosystems Science and Engineering GPA: 5.54/6

Work

5.9.2011 - 23.12.2012	Research Project in the group of Prof. Daniel J. Müller
21.2.2012 -14.12.2013	Master Thesis in the group of Prof. Jörg Stelling under the supervision of Fabian Rudolf
1.3.2013-present	Doctoral student in the group of Prof. Jeffrey A. Hubbell
3.1.2016-present	Visiting Student University of Chicago

Languages

French: Good, Bilingual Highschool leaving diploma
English: Fluent
German: Native language

Other Information

Hobbies: Rock Climbing, Music (Violin)

